EUROPEAN ORGANISATION FOR NUCLEAR RESEARCH (CERN)

Submitted to: JHEP

CERN-EP-2017-227
20th February 2018

Measurements of differential cross sections of top quark pair production in association with jets in pp collisions at $\sqrt{s} = 13$ TeV using the ATLAS detector

The ATLAS Collaboration

Measurements of differential cross sections of top quark pair production in association with jets by the ATLAS experiment at the LHC are presented. The measurements are performed as functions of the top quark transverse momentum, the transverse momentum of the top quark-antitop quark system and the out-of-plane transverse momentum using data from pp collisions at $\sqrt{s} = 13$ TeV collected by the ATLAS detector at the LHC in 2015 and corresponding to an integrated luminosity of $3.2\,\text{fb}^{-1}$. The top quark pair events are selected in the lepton (electron or muon) + jets channel. The measured cross sections, which are compared to several predictions, allow a detailed study of top quark production.

1 Introduction

The large number of top quark pair ($t\bar{t}$) events produced at the Large Hadron Collider (LHC) allows detailed studies of the characteristics of $t\bar{t}$ production as a function of different kinematic variables. In this paper, the data collected by the ATLAS experiment in 2015 are used to measure differential cross sections for $t\bar{t}$ production in association with jets. The measurement of differential cross sections in different bins of jet multiplicity provides a better understanding of the effect of gluon radiation on $t\bar{t}$ kinematic variables than differential cross sections inclusive in the number of jets previously published by the ATLAS Collaboration at $\sqrt{s} = 13$ TeV [1].

Since the top quark decays almost always to a W boson and a b-quark, the decay of a top quark pair produces six particles in the final state, whose identity depends on the decays of the intermediate W bosons. The channel considered in this analysis is characterised by the leptonic decay of one W boson and the hadronic decay of the other W boson; this is commonly referred to as semileptonic decay mode or ℓ+jets channel. The final-state configuration contains one electron or muon, one neutrino giving rise to missing transverse momentum ($E_{\mathrm{T}}^{\mathrm{miss}}$) and four jets, two of which originate from b-quarks. Events may include additional jets from gluon radiation off initial- or final-state quarks. To study the dependence of this emission on the observables, three configurations are defined depending on the number of additional jets produced within the detector acceptance in association with the top quark pair: the "4-jet exclusive configuration" (no additional jets); the "5-jet exclusive configuration" (only one additional jet); and the "6-jet inclusive configuration" (two or more additional jets). The latter configuration is of particular interest since it provides a similar phase space to the one used by measurements such as Higgs boson production in association with two top quarks and searches with high jet multiplicity.

The three configurations with increasing number of additional jets are expected to provide a better understanding of the effect of gluon radiation on the kinematic variables of top quark pair production. ATLAS already published differential cross section measurements as a function of the number of additional jets [2–4] and of several kinematic variables [1, 5–8]. The results presented in this paper combine the two types of measurements to provide additional information about top quark production and explore the effect of the gluon radiation on $t\bar{t}$ kinematic variables. The CMS Collaboration published similar measurements [9–12].

The observables studied here are the transverse momentum (p_{T})[1] of the top quark-antitop quark system ($p_{\mathrm{T}}^{t\bar{t}}$) and the absolute value of the out-of-plane momentum ($|p_{\mathrm{out}}^{t\bar{t}}|$), defined as the projection of the top quark three-momentum onto the direction perpendicular to a plane defined by the other top quark and the beam axis ($\hat{z}$) in the laboratory frame [13]:

$$\left|p_{\mathrm{out}}^{t\bar{t}}\right| = \left|\vec{p}^{\,t,\mathrm{had}} \cdot \frac{\vec{p}^{\,t,\mathrm{lep}} \times \hat{z}}{|\vec{p}^{\,t,\mathrm{lep}} \times \hat{z}|}\right|,$$

[1] ATLAS uses a right-handed coordinate system with its origin at the nominal interaction point (IP) in the centre of the detector and the z-axis along the beam pipe. The x-axis points from the IP to the centre of the LHC ring, and the y-axis points upward. Cylindrical coordinates (r,ϕ) are used in the transverse plane, ϕ being the azimuthal angle around the beam pipe. The pseudorapidity is defined in terms of the polar angle θ as $\eta = -\ln\tan(\theta/2)$ and the angular separation between particles is defined as $\Delta R = \sqrt{(\Delta\phi)^2 + (\Delta\eta)^2}$. The transverse momentum is the projection of the momentum on the transverse plane.

where $\vec{p}^{\,t,\mathrm{lep}}$ and $\vec{p}^{\,t,\mathrm{had}}$ are the momenta of the semileptonically and hadronically decaying top quarks, respectively. This observable is complementary to $p_{\mathrm{T}}^{t\bar{t}}$ since $p_{\mathrm{out}}^{t\bar{t}}$ is expected to be more sensitive to the direction of gluon radiation; for example the emission of a low p_{T} jet at a large angle with respect to the plane defined by the two top quarks is expected to be better measured with $p_{\mathrm{out}}^{t\bar{t}}$ than $p_{\mathrm{T}}^{t\bar{t}}$. In addition, the differential cross section as a function of the transverse momentum of the hadronic top quark ($p_{\mathrm{T}}^{t,\mathrm{had}}$) is measured. In previous publications [1, 8], differences between the data and the predictions by several Standard Model Monte Carlo (MC) event generators were observed. By measuring the differential cross section of this observable in different jet multiplicities it is possible to identify the regions of phase space in which the discrepancy is largest. The measured differential cross sections as functions of these three observables are compared to predictions from several MC event generators, namely Powheg-Box [14], MadGraph5_aMC@NLO [15] and Sherpa [16].

2 ATLAS detector

ATLAS is a multipurpose detector [17] that provides nearly full solid angle coverage around the interaction point. Charged-particle trajectories with pseudorapidity $|\eta| < 2.5$ are reconstructed in the inner detector, which comprises a silicon pixel detector, a silicon microstrip detector and a transition radiation tracker. The innermost pixel layer, the insertable B-layer [18], was added before the start of 13 TeV LHC operation at an average radius of 33 mm around a new, thinner beam pipe. The inner detector is embedded in a superconducting solenoid generating a 2 T axial magnetic field, allowing precise measurements of charged-particle momenta. Sampling calorimeters with several different designs span the pseudorapidity range up to $|\eta| = 4.9$. High-granularity liquid argon (LAr) electromagnetic (EM) calorimeters are used up to $|\eta| = 3.2$. Hadronic calorimeters based on scintillator-tile active material cover $|\eta| < 1.7$ while LAr technology is used for hadronic calorimetry in the region $1.5 < |\eta| < 4.9$. The calorimeters are surrounded by a muon spectrometer within a magnetic field provided by air-core toroid magnets with a bending integral of about 2.5 Tm in the barrel and up to 6 Tm in the end-caps. Three stations of precision drift tubes and cathode-strip chambers provide an accurate measurement of the muon track curvature in the region $|\eta| < 2.7$. Resistive-plate and thin-gap chambers provide muon triggering capability up to $|\eta| = 2.4$.

Data are selected from inclusive pp interactions using a two-level trigger system [19]. A hardware-based trigger uses custom-made hardware and coarser-granularity detector data to initially reduce the trigger rate to approximately 75 kHz from the original 40 MHz LHC bunch crossing rate. Next, a software-based high-level trigger, which has access to full detector granularity, is applied to further reduce the event rate to 1 kHz.

3 Data and simulation

The differential cross sections are measured using a data set collected during the 2015 LHC pp run at $\sqrt{s} = 13$ TeV and with 25 ns bunch spacing. The average number of pp interactions per bunch crossing ranged from approximately 5 to 25, with a mean of 14. After applying data-quality assessment criteria based

on beam, detector and data-taking quality, the available data correspond to a total integrated luminosity of 3.2 fb^{-1}.

The data were collected using single-muon and single-electron triggers. For each lepton type, multiple trigger conditions are combined to maintain good efficiency in the full momentum range, while controlling the trigger rate. For electrons, the p_{T} thresholds are 24 GeV, 60 GeV and 120 GeV, while for muons the thresholds are 20 GeV and 50 GeV. Isolation requirements are applied to the triggers with the lowest p_{T} thresholds.

The signal and background processes are modelled with various MC event generators described below and summarised in Table 1. Multiple overlaid pp collisions were simulated with the soft QCD processes of Pythia8.186 [20] using parameter values from tune A2 [21] and the MSTW2008LO [22] set of parton distribution functions (PDFs). The EvtGen v1.2.0 program [23] was used to simulate the decay of bottom and charm hadrons, except for the Sherpa event generator. The detector response was simulated [24] in GEANT4 [25]. The data and MC events were reconstructed with the same software algorithms.

3.1 Signal simulation samples

In this section the MC samples used for the generation of $t\bar{t}$ events are described for the nominal sample, the alternative samples used to estimate systematic uncertainties and the other samples used in the post-unfolding comparison. The top quark mass (m_t) was set to 172.5 GeV in all MC event generators.

For the generation of $t\bar{t}$ events [26], the Powheg-Box v2 event generator with the CT10 PDF set [27] was used for the matrix element calculations. Events in which both W bosons decay hadronically were not included. The Powheg-Box event generator, from now on called Powheg, uses the four-flavour scheme for the next-to-leading-order (NLO) matrix element calculations together with the fixed four-flavour PDF set CT10f4. For this process, the top quarks were decayed using MadSpin [28] to preserve all spin correlations, while parton shower, hadronisation, and the underlying event were simulated using Pythia6.428 [29] with the CTEQ6L1 PDF set [30] and the Perugia2012 tune [31]. The h_{damp} parameter, which controls the p_{T} of the first gluon or quark emission beyond the Born configuration in Powheg, was set to the mass of the top quark. The main effect of this parameter is to regulate the high-p_{T} emission against which the $t\bar{t}$ system recoils. Signal $t\bar{t}$ events generated with those settings are referred to as the nominal signal sample.

To estimate the effect of the parton shower algorithm, a Powheg+Herwig++ sample was generated with the same Powheg settings as for the nominal sample. The parton shower, hadronisation and underlying event simulation were produced with Herwig++ [32] (version 2.7.1) using the UE-EE-5 tune [33] and the CTEQ6L1 PDF set.

The impact of the matrix element (ME) event generator choice is evaluated using events generated with MadGraph5_aMC@NLO+Herwig++ with the UE-EE-5 tune. The events were generated with version 2.1.1 of MadGraph5_aMC@NLO. NLO matrix elements and the CT10 PDF set were used for the $t\bar{t}$ hard-scattering process. These events were passed through a fast simulation using a parametrisation of the performance of the ATLAS electromagnetic and hadronic calorimeters [34] and full simulation of the response in the inner detector and muon spectrometer.

The effects of different levels of gluon radiation are evaluated using two samples with different factorisation and hadronisation scales relative to the nominal sample, as well as a different h_{damp} parameter value. Specifically, in one sample the factorisation and hadronisation scales were reduced by a factor of two, the h_{damp} parameter was increased to $2m_t$ and the 'radHi' tune variation from the Perugia2012 tune set is used. In the second sample, the factorisation and hadronisation scales were increased by a factor of two, the h_{damp} parameter was unchanged and the 'radLo' tune variation from the Perugia2012 tune set was used.

The measured differential cross sections are compared to several additional $t\bar{t}$ samples [26, 35, 36].

- Two MadGraph5_aMC@NLO+Pythia8 samples having two different hard-scattering scales, $H_{\text{T}}/2$ [2] and $\sqrt{m_t^2 + p_{\text{T,t}}^2}$ and using the same A14 tune.
- Two Powheg+Pythia8 samples simulated with different values of the h_{damp} parameter ($h_{\text{damp}} = m_t$ and $h_{\text{damp}} = 1.5m_t$) also using the A14 tune.
- Two additional Powheg+Pythia8 samples with alternative radiation settings (similar to those described above for Powheg+Pythia6).
- A Powheg+Herwig7 sample generated with the h_{damp} parameter set to $1.5m_t$ and using the H7-UE-MMHT tune which use the NNPDF3.0 PDF [37] for the ME.
- A Sherpa 2.2.1 sample in which events were generated with a $t\bar{t}$ matrix element and up to one additional parton simulated at NLO and two, three and four partons at LO. The CT10 PDF set was used.

The $t\bar{t}$ samples are normalised using $\sigma_{t\bar{t}} = 832^{+20}_{-29}(\text{scale}) \pm 35\ (\text{PDF})$ pb as calculated with the Top++2.0 program to next-to-next-to-leading order (NNLO) in perturbative QCD, including soft-gluon resummation to next-to-next-to-leading-log order (NNLL) (see Ref. [38] and references therein), and assuming a top quark mass $m_t = 172.5$ GeV. The first uncertainty comes from the independent variation of the factorisation and renormalisation scales, μ_{F} and μ_{R}, while the second one is associated with variations in the PDF and α_{S}, following the PDF4LHC prescription with the MSTW2008 68% CL NNLO, CT10 NNLO and NNPDF2.3 5f FFN PDF sets see Refs. [27, 39–41].

3.2 Background simulation samples

Several processes can produce the same final state as the $t\bar{t}$ semileptonic channel. The events produced by these backgrounds need to be estimated and subtracted from data to calculate the top quark pair cross sections. They are fully estimated using MC simulation with the exception of the W+jets background, for which data-driven techniques complement the MC simulation prediction. The processes considered are single-top quark production, W+jets and Z+jets production, diboson final states and top quark pairs produced in association with weak bosons ($t\bar{t} + W/Z/WW$, denoted by $t\bar{t}V$).

The simulation of single-top quark events from Wt and s-channel production was performed using the configuration described above for the nominal $t\bar{t}$ sample. The overlap between the Wt and $t\bar{t}$ samples was handled using the diagram-removal scheme [42]. Electroweak t-channel single-top quark events were

[2] H_{T} is defined as the scalar sum of the transverse momenta of the two top quarks.

Table 1: Summary of MC samples, showing the event generator for the hard-scattering process, cross section normalisation precision, PDF choice, as well as the parton shower generator and the corresponding tune used in the analysis.

Physics process	Generator	PDF set for hard process	Parton shower	Tune	Cross section normalisation
$t\bar{t}$ signal	Powheg-Box v2	CT10	Pythia 6.428	Perugia2012	NNLO +NNLL
$t\bar{t}$ PS syst.	Powheg-Box v2	CTEQ6L1	Herwig++2.7.1	UE-EE-5	NNLO +NNLL
$t\bar{t}$ ME syst.	MadGraph5_aMC@NLO	CT10	Herwig++2.7.1	UE-EE-5	NLO
$t\bar{t}$ rad. syst.	Powheg-Box v2	CT10	Pythia 6.428	'radHi/Lo'	NNLO +NNLL
Single top: t-channel	Powheg-Box v1	CT10f4	Pythia 6.428	Perugia2012	NLO
Single top: s-channel	Powheg-Box v2	CT10	Pythia 6.428	Perugia2012	NLO
Single top: Wt-channel	Powheg-Box v2	CT10	Pythia 6.428	Perugia2012	NLO +NNLL
$t\bar{t}+W/Z/WW$	MadGraph5_aMC@NLO	NNPDF2.3LO	Pythia 8.186	A14	NLO
$W(\rightarrow \ell\nu)$+ jets	Sherpa 2.1.1	CT10	Sherpa	Sherpa	NNLO
$Z(\rightarrow \ell\bar{\ell})$+ jets	Sherpa 2.1.1	CT10	Sherpa	Sherpa	NNLO
WW, WZ, ZZ	Sherpa 2.1.1	CT10	Sherpa	Sherpa	NLO

generated using the Powheg-Box v1 event generator. The single-top quark cross sections for the t- and s-channels are normalised using their NLO predictions, while for the Wt channel it is normalised using its NLO +NNLL prediction [43–45].

Inclusive samples containing single W or Z bosons in association with jets were simulated using the Sherpa 2.1.1 event generator [16]. Matrix elements were calculated with up to two partons at NLO and four partons at leading-order (LO) using the Comix [46] and OpenLoop [47] matrix element event generators and merged with the Sherpa parton shower [48] using the ME+PS@NLO prescription [49]. The CT10 PDF sets were used in conjunction with dedicated parton shower tuning developed by the authors of Sherpa. The Z+jets events are normalised using the NNLO cross sections [50] while the normalisation for the W+jets events is obtained with a data-driven method described in Section 5.

Diboson processes, with one of the bosons decaying hadronically and the other leptonically, were simulated using the Sherpa 2.1.1 event generator [16, 51]. They are calculated for up to one (ZZ) or zero (WW, WZ) additional partons at NLO and up to three additional partons at LO using the Comix and OpenLoops matrix element event generators and merged with the Sherpa parton shower using the ME+PS@NLO prescription. The CT10 PDF sets were used in conjunction with dedicated parton shower tuning developed by the authors of Sherpa. The event generator cross sections, which are already at the NLO accuracy, are used in this case.

The $t\bar{t}V$ events were simulated using the MadGraph5_aMC@NLO event generator at LO interfaced to the Pythia 8.186 parton shower model [52]. The matrix elements were simulated with up to two ($t\bar{t}+W$), one ($t\bar{t}+Z$) or no ($t\bar{t}+WW$) extra partons. The ATLAS underlying-event tune A14 was used together with the NNPDF2.3LO PDF sets. The events are normalised using their respective NLO cross sections [15].

4 Object reconstruction and event selection

The following sections describe the reconstruction- and particle-level objects used to characterise the final-state event topology and to define the fiducial phase space regions for the measurements.

4.1 Detector-level object reconstruction

Primary vertices are formed from reconstructed tracks which are spatially compatible with the interaction region. The hard-scatter primary vertex is chosen to be the one with at least two associated tracks and the highest $\sum p_{\mathrm{T}}^2$, where the sum extends over all tracks with $p_{\mathrm{T}} > 0.4\,\mathrm{GeV}$ matched to the vertex.

Electron candidates are reconstructed by matching tracks in the inner detector to energy deposits in the EM calorimeter. They must satisfy a "tight" likelihood-based identification criterion based on shower shapes in the EM calorimeter, track quality and detection of transition radiation produced in the transition radiation tracker detector [53]. The reconstructed EM clusters are required to have a transverse energy $E_{\mathrm{T}} > 25$ GeV and a pseudorapidity $|\eta| < 2.47$, excluding the transition region between the barrel and the end-cap calorimeters ($1.37 < |\eta| < 1.52$). The associated track must have a longitudinal impact parameter $|z_0 \sin\theta| < 0.5$ mm and a transverse impact parameter significance $|d_0|/\sigma(d_0) < 5$, where d_0 is measured with respect to the beam line. Isolation requirements based on calorimeter and tracking quantities are used to reduce the background from non-prompt and fake electrons [54]. The isolation criteria are p_{T}- and η-dependent, and ensure an efficiency of 90% for electrons with p_{T} of 25 GeV and 99% efficiency for electrons with p_{T} of 60 GeV. The identification, isolation and trigger efficiencies are measured using electrons from Z boson decays [55].

Muon candidates are identified by matching tracks in the muon spectrometer to tracks in the inner detector [56]. The track p_{T} is determined through a global fit of the hits which takes into account the energy loss in the calorimeters. Muons are required to have $p_{\mathrm{T}} > 25$ GeV and $|\eta| < 2.5$. To reduce the background from muons originating from heavy-flavour decays inside jets, muons are required to be isolated using track quality and isolation criteria similar to those applied to electrons. If a muon shares a track with an electron, it is likely to have undergone bremsstrahlung and hence the electron is not selected.

Jets are reconstructed using the anti-k_t algorithm [57] with radius parameter $R = 0.4$ as implemented in the FastJet package [58]. Jet reconstruction in the calorimeter starts from topological clustering of individual calorimeter cell signals calibrated to be consistent with electromagnetic or hadronic cluster shapes using corrections determined in simulation and inferred from test-beam data [59]. Jet four-momenta are then corrected for pile-up effects using the jet-area method [60]. To reduce the number of jets originating from pile-up, an additional selection criterion based on a jet-vertex tagging technique is applied. The jet-vertex tagging is a likelihood discriminant that combines information from several track-based variables [61] and the criterion is only applied to jets with $p_{\mathrm{T}} < 60$GeV and $|\eta| < 2.4$. Jets are calibrated using an energy- and η-dependent simulation-based calibration scheme with *in situ* corrections based on data [62, 63], and are accepted if they have $p_{\mathrm{T}} > 25$ GeV and $|\eta| < 2.5$.

For objects satisfying both the jet and lepton selection criteria, a procedure called "overlap removal" is applied to assign objects to a unique hypothesis. To prevent double-counting of electron energy deposits

as jets, the jet closest to a reconstructed electron is discarded if they are $\Delta R < 0.2$ apart. Subsequently, to reduce the impact of non-prompt electrons, if an electron is $\Delta R < 0.4$ from a jet, then that electron is removed. If a jet has fewer than three tracks and is $\Delta R < 0.4$ from a muon, the jet is removed. Finally, the muon is removed if it is $\Delta R < 0.4$ from a jet with at least three tracks.

The purity of the selected $t\bar{t}$ sample is improved by identifying jets containing b-hadrons, so called b-tagged jets. This identification exploits the long lifetime of b-hadrons and the invariant mass of tracks from the corresponding reconstructed secondary vertex, which is on average several GeV larger than that in jets originating from gluons or light-flavour quarks. Information from the track impact parameters, secondary-vertex location and decay topology are combined in a multivariate algorithm (MV2c20) [64]. The operating point corresponds to an overall 77% b-tagging efficiency in $t\bar{t}$ events, with a corresponding rejection of charm-quark jets (light-flavour and gluon jets) by a factor of 4.5 (140) [64]. Jets that pass this selection are identified as b-tagged jets.

The $E_{\mathrm{T}}^{\mathrm{miss}}$ vector is computed from the sum of the transverse momenta of the reconstructed calibrated physics objects (electrons, photons, hadronically decaying τ-leptons, jets and muons) together with the transverse energy deposited in the calorimeter cells, calibrated using tracking information, not associated with these objects [65]. To avoid double-counting of energy, the muon energy loss in the calorimeters is subtracted in the $E_{\mathrm{T}}^{\mathrm{miss}}$ calculation. This variable is not used in the selection but is used in the top quark reconstruction described below.

4.2 Particle-level object definition

Particle-level objects are defined in simulated events using only stable particles, i.e. particles with a mean lifetime $\tau > 30$ ps. The fiducial phase space for the measurements presented in this paper is defined using a series of requirements applied to particle-level objects analogous to those used in the selection of the reconstruction-level objects, described above.

Electrons and muons must not originate, either directly or through a τ decay, from a hadron in the MC event record. This ensures that the lepton is from the decay of a real W boson without requiring a direct match to it. The four-momenta of leptons are modified by adding the four-momenta of all photons within $\Delta R = 0.1$ and not originating from hadron decays, to take into account final-state photon radiation. Such leptons are then required to have $p_{\mathrm{T}} > 25$ GeV and $|\eta| < 2.5$.

Particle-level jets are reconstructed using the same anti-k_t algorithm used at reconstruction level. The jet-reconstruction procedure takes as input all stable particles, except for leptons not from hadron decay as described above, inside a radius $R = 0.4$. Particle level jets are required to have $p_{\mathrm{T}} > 25$ GeV and $|\eta| < 2.5$. A jet is identified as a b-jet if a hadron containing a b-quark is matched to the jet through a ghost-matching technique described in Ref. [60]; the hadron must have $p_{\mathrm{T}} > 5$ GeV. No overlap removal criteria are applied to particle-level objects. Neutrinos and charged leptons from hadron decays are included in particle-level jets.

4.3 Event selection and fiducial phase space definition

Events at both reconstruction and particle levels are required to contain exactly one electron or muon and at least four jets, with at least two tagged as b-jets. Each event is then unequivocally assigned to the 4-jet, 5-jet or 6-jet-inclusive configurations, depending on the number of reconstructed jets.

Dilepton $t\bar{t}$ events, where only one lepton satisfies the fiducial selection, are included by definition in the fiducial measurement. In the fiducial phase space definition, semileptonic $t\bar{t}$ decays into τ-leptons are considered as signal only if the τ-lepton decays leptonically.

5 Background determination and event yields

After the event selection, various backgrounds still contribute to the event yields. The different background contributions are estimated by using MC simulations or data-driven techniques as detailed below for each source. The latter are used when the accuracy of the MC simulation is not adequate, as in the case of W boson production in association with multiple jets and the background originating from jets mimicking the signature of charged leptons.

The single-top quark background is the largest background contribution in all considered regions, amounting to 5% of the total event yield and 30% of the total background estimate. This background is modelled with a MC simulation, and the event yields are normalised using calculations of their cross sections, as described in Section 3.

Multijet production processes, including $t\bar{t}$ production with all hadronic decay and $t\bar{t}$ decays into τ-leptons which then decay hadronically, have a large cross section and can mimic the lepton+jets signature due to hadrons misidentified as prompt leptons (fake leptons), conversion of photons for the electron channel or semileptonic decays of heavy-flavour hadrons (non-prompt real leptons). The multijet background is estimated directly from data by using a matrix method [66] in which signal and control regions are defined using lepton identification criteria. The method depends on the probability of a real (fake) lepton to pass the tight selection criteria, which is referred to as the real (fake) efficiency. These efficiencies are measured in data control regions dominated by real or fake lepton events. In the e+jets channel, the fake efficiency is parametrised as a function of p_{T} and η, as well as the azimuthal angle difference between the lepton and the $E_{\mathrm{T}}^{\mathrm{miss}}$ vector, $\Delta\phi$. In the μ+jets channel, the fake efficiency is calculated for low and high lepton p_{T}. The low p_{T} parametrisation depends on $\Delta\phi$, p_{T} and $E_{\mathrm{T}}^{\mathrm{miss}}$, whereas the high p_{T} parametrisation only uses p_{T}. The real efficiencies are measured with the $Z \to \ell\ell$ events using the tag-and-probe method. In the e+jets channel, the efficiency is parametrised as a function of p_{T}, whereas in the μ+jets channel the parametrisation depends on $\Delta\phi$ and p_{T}. The multijet background contributes to the total event yield at the level of approximately 4% and 30% of the total background estimate.

The W+jets background represents the third largest background, amounting to 2–3% of the total event yield and 20% of the total background estimate. The estimation of this background is performed using a combination of MC simulations and data-driven techniques; the Sherpa MC event generator is used to estimate the contribution from the W+jets process. The normalisation and the heavy-flavour fractions of this process, which are affected by large theoretical uncertainties, are determined from data. The overall

W+jets normalisation is obtained by exploiting the expected charge asymmetry in the production of W^+ and W^- bosons in pp collisions. This asymmetry is predicted by theory [67] and evaluated using MC simulations, assuming other processes are symmetric in charge except for a small contamination from single-top quark, $t\bar{t}V$ and WZ events, which is subtracted using MC simulations. The total number of W+jets events with a positively or negatively charged W boson ($N_{W^+} + N_{W^-}$) in the sample is thus estimated using the following equation:

$$N_{W^+} + N_{W^-} = \left(\frac{r_{\mathrm{MC}} + 1}{r_{\mathrm{MC}} - 1}\right)(D_+ - D_-), \tag{1}$$

where r_{MC} is the ratio of the number of events with positively charged leptons to the number of events with negatively charged leptons in the MC simulations, and D_+ and D_- are the numbers of events with positive and negative leptons in the data, respectively, corrected for the aforementioned non-W+jets charge-asymmetric contributions using simulation. The corrections due to event generator mis-modelling of W boson production in association with jets of different flavour (W+$b\bar{b}$, W+$c\bar{c}$, W+c, W+light flavours) are estimated using a dedicated control sample in data which uses the same lepton as for the signal but requiring exactly two jets. In their determination, the overall normalisation scaling factor obtained using Eq. (1) is applied first. Then heavy-flavour scaling factors obtained in the two-jet control region are extrapolated to the signal region using MC simulations, assuming constant relative rates for the signal and control regions. Taking into account the heavy-flavour scale factors, the overall normalisation factor is calculated again using Eq. (1). This iterative procedure is repeated until the total predicted W+jets yield in the two-jet control configuration agrees with the data yield. The procedure is explained in detail in Ref. [68].

The background contributions from Z+jets, $t\bar{t}V$ and diboson events are obtained from MC simulation, and the event yields are normalised using the theoretical calculations of their cross sections, as described in Section 3. The total contribution from these processes is 1–2% of the total event yield or 11–14% of the total background.

Dilepton top quark pair events can satisfy the event selection if one lepton does not satisfy the requirements listed above and at least two additional jets are produced. Events with at least a top quark decaying to a τ-lepton which subsequently decays leptonically, can also pass the event selection. These events contribute 3-5% to the total event yield, and are considered in the analysis at both reconstruction and particle levels. Cases where both top quarks decay semileptonically into τ-leptons, and where both τ-leptons decay hadronically, are accounted for in the multijet background.

The event yields in the three configurations are displayed in Table 2 for data, simulated signal, and backgrounds. Figure 1 shows[3] the comparison between data and predictions for the 4-jet configuration for different distributions. All of the distributions are shown for the combined ℓ+jets channel (combining electron and muon channels). The background contributions in the other configurations are similar, as shown in Figure 2. The event selection results in a total background contamination of 10–15%, depending on the configuration. A constant difference between data and prediction is observed in Figures 2(b) and 2(c), the same effect is also seen in the distribution of the number of jets, shown in Figure 3. This discrepancy has also been observed in studies of associated production of jets with top quark pairs [4]. Nevertheless, the predictions are compatible with the data within the total uncertainties.

[3] All data as well as theory points are plotted at the graphical bin centre on the x-axis throughout this paper.

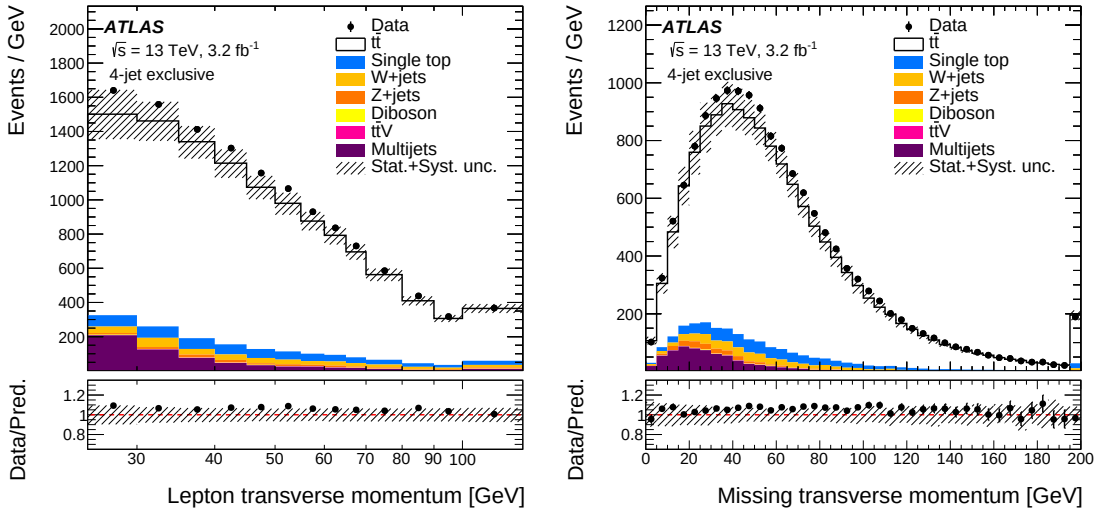

(a) (b)

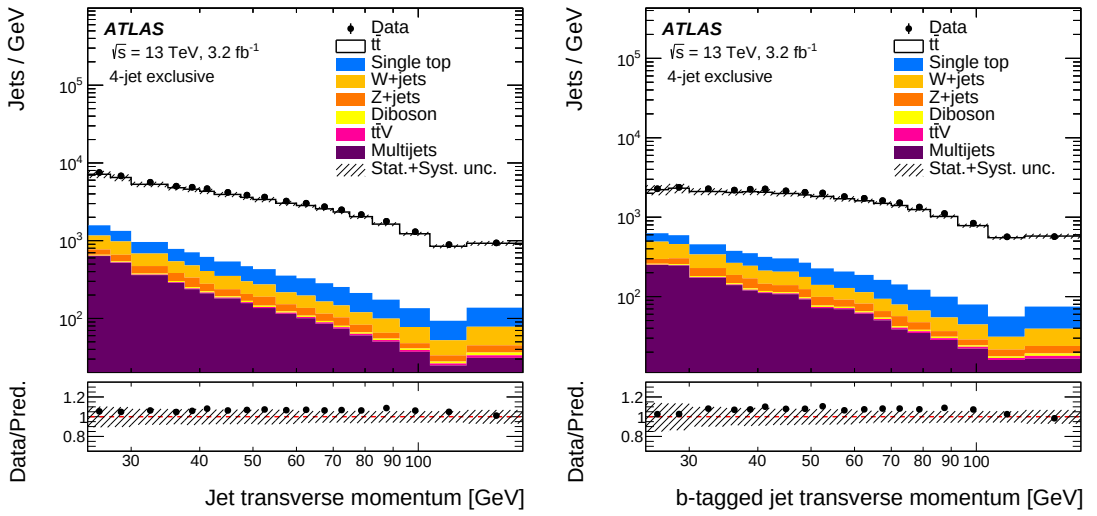

(c) (d)

Figure 1: Kinematic distributions in the 4-jet exclusive configuration at reconstruction level: (a) lepton transverse momentum, (b) missing transverse momentum, transverse momentum of (c) the selected jets and (d) of the selected b-tagged jets. Data distributions are compared to predictions using the nominal sample as the $t\bar{t}$ signal model. The hatched area indicates the combined statistical and systematic uncertainties in the total prediction, excluding systematic uncertainties related to the modelling of the $t\bar{t}$ production. Events beyond the range of the horizontal axis are included in the last bin.

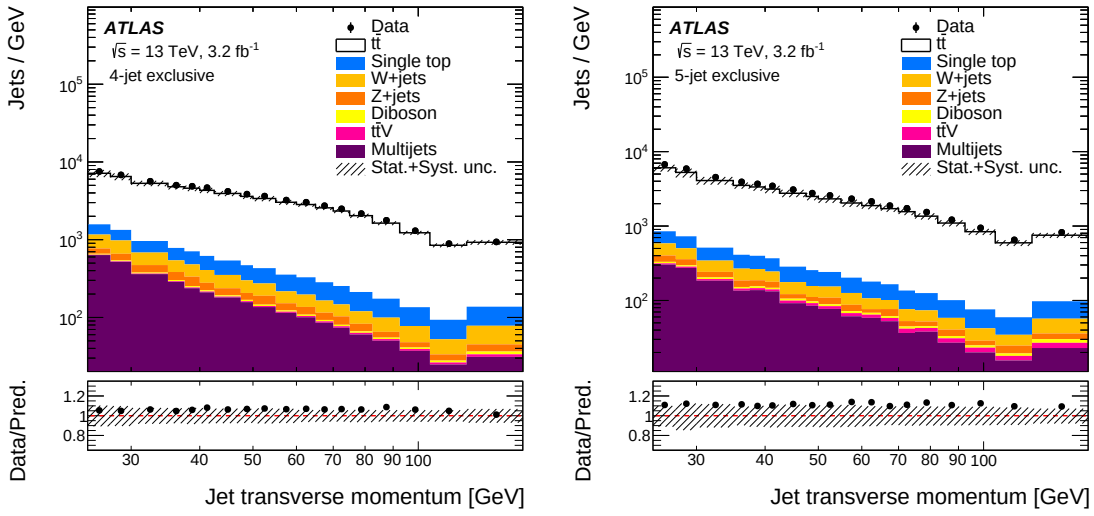

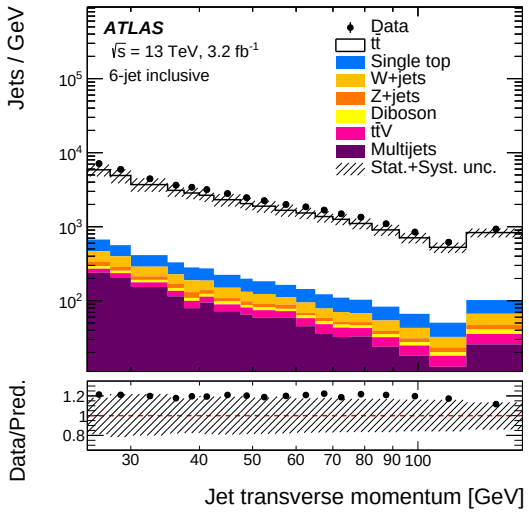

Figure 2: Distribution of the transverse momentum of selected jets in the (a) 4-jet exclusive, (b) 5-jet exclusive and (c) 6-jet inclusive configurations at reconstruction level. Data distributions are compared to predictions using the nominal sample as the $t\bar{t}$ signal model. The hatched area indicates the combined statistical and systematic uncertainties in the total prediction, excluding systematic uncertainties related to the modelling of the $t\bar{t}$ production. Events beyond the range of the horizontal axis are included in the last bin.

Table 2: Event yields in the 4-jet exclusive (left), 5-jet exclusive (centre) and 6-jet inclusive (right) configurations. The uncertainties include the combined statistical and systematic uncertainties, excluding the systematic uncertainties related to the modelling of the $t\bar{t}$ system.

4-jet exclusive	
Sample	Yield
$t\bar{t}$	61400^{+3300}_{-3400}
W+jets	2200^{+1400}_{-1600}
Z+jets	840^{+630}_{-620}
Diboson	140^{+100}_{-100}
Single top	3600^{+360}_{-360}
Multijet	3300^{+1700}_{-1800}
$t\bar{t}\,V$	103^{+17}_{-17}
Total prediction	71600^{+4800}_{-5000}
Data	75768
Data/prediction	1.06 ± 0.07

5-jet exclusive	
Sample	Yield
$t\bar{t}$	36900^{+3700}_{-3700}
W+jets	890^{+600}_{-680}
Z+jets	340^{+330}_{-330}
Diboson	100^{+100}_{-100}
Single top	1730^{+240}_{-240}
Multijet	1460^{+770}_{-780}
$t\bar{t}\,V$	132^{+21}_{-21}
Total prediction	41600^{+4000}_{-4300}
Data	46243
Data/prediction	1.11 ± 0.11

6-jet inclusive	
Sample	Yield
$t\bar{t}$	25400^{+4700}_{-4400}
W+jets	540^{+400}_{-450}
Z+jets	160^{+100}_{-100}
Diboson	110^{+57}_{-57}
Single top	980^{+210}_{-200}
Multijet	920^{+500}_{-500}
$t\bar{t}\,V$	224^{+40}_{-40}
Total prediction	28400^{+4900}_{-4900}
Data	33582
Data/prediction	1.2 ± 0.2

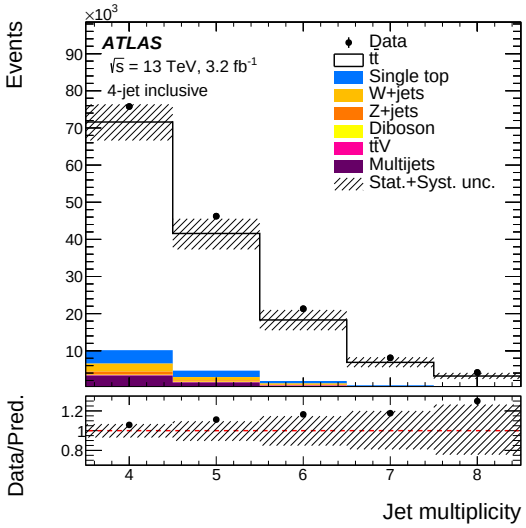

Figure 3: Distribution of the jet multiplicity in the 4-jet inclusive configuration. Data distributions are compared to predictions. The hatched area indicates the combined statistical and systematic uncertainties in the total prediction, excluding systematic uncertainties related to the modelling of the $t\bar{t}$ production. Events beyond the range of the horizontal axis are included in the last bin.

6 Reconstruction of top quark kinematic properties

The two top quarks are reconstructed from their decay products so that the differential cross sections can be measured as functions of observables involving the top quark and the $t\bar{t}$ system. In the following, the leptonic (hadronic) top quark refers to the one that decays into a leptonically (hadronically) decaying W boson.

The pseudo-top algorithm [7] reconstructs the four-momenta of the top quarks and their complete decay chain from final-state objects, namely the charged lepton (electron or muon), missing transverse momentum, and four jets, two of which are b-tagged. Only about 14% of the selected events contain more than two b-tagged jets, in which case the two with the highest transverse momentum are considered as coming from the top quarks, while the others are considered for the W reconstruction. The same algorithm is used to reconstruct the kinematic properties of top quarks at reconstruction level and particle level in the three configurations.

The algorithm starts with the reconstruction of the neutrino four-momentum. While the x and y components of the neutrino momentum are set to the corresponding components of the missing transverse momentum, the z component is calculated by imposing a W boson mass constraint on the invariant mass of the charged-lepton–neutrino system. If the resulting quadratic equation has two real solutions, the one with the smaller value of $|p_z|$ is chosen. If the discriminant of the equation is negative, only the real part is considered.

The leptonically decaying W boson is reconstructed from the charged lepton and the reconstructed neutrino. The leptonic top quark is reconstructed from the leptonic W boson and the b-tagged jet closest in ΔR to the charged lepton. The hadronic W boson is reconstructed from the two jets whose invariant mass is closest to the mass of the W boson; only jets that do not pass the b-tagging requirements are considered. Finally, the hadronic top quark is reconstructed from the hadronic W boson and the other b-jet. This choice yields the best performance of the algorithm in terms of the correspondence between the reconstruction level and particle level.

The performance of the algorithm was studied in each of the three configurations. The algorithm reconstructs the masses of the hadronic W boson and the top quark with similar performances in all three configurations. Hence, the presence of additional jets in the 5- and 6-jet configurations, where different combinations in the jet assignment to the W boson are possible, does not impact the reconstruction significantly.

7 Measured observables

The goal of this analysis is to measure differential cross sections for observables in regions of phase space sensitive to gluon radiation. Three observables are chosen because they are shown to be sensitive to radiation or other effects correlated with the number of jets: $p_{\mathrm{T}}^{t,\mathrm{had}}$, $p_{\mathrm{T}}^{t\bar{t}}$ and $\left|p_{\mathrm{out}}^{t\bar{t}}\right|$.

Figure 4 shows the $p_{\mathrm{T}}^{t\bar{t}}$ distributions for the three configurations. The $p_{\mathrm{T}}^{t\bar{t}}$ distribution is expected to depend strongly on gluon radiation; if no additional jets beyond those of the $t\bar{t}$ decay are produced, the $t\bar{t}$ system should have small $p_{\mathrm{T}}^{t\bar{t}}$. If an additional jet is produced, the $t\bar{t}$ system recoils against it, hence it should take

larger p_{T} values. This effect is more pronounced with more additional jets, as observed in Figure 4. The $p_{\mathrm{T}}^{t,\mathrm{had}}$ distributions for the three configurations are shown in Figure 5. The predictions tend to underestimate (overestimate) the data at low (high) $p_{\mathrm{T}}^{t,\mathrm{had}}$. This effect is most clearly observed in the 4-jet configuration; a stress test performed on the unfolding (described in Section 8) demonstrated that the difference between data and prediction does not affect the results. The $\left|p_{\mathrm{out}}^{t\bar{t}}\right|$ distributions are shown in Figure 6; the shape of the measured distribution displays a small dependence on the number of additional jets.

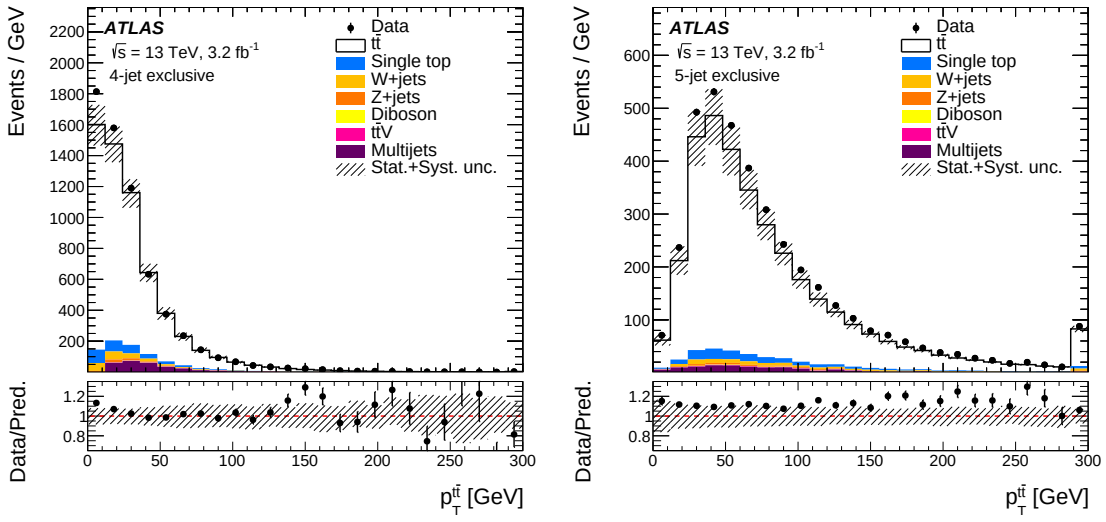

(a)

(b)

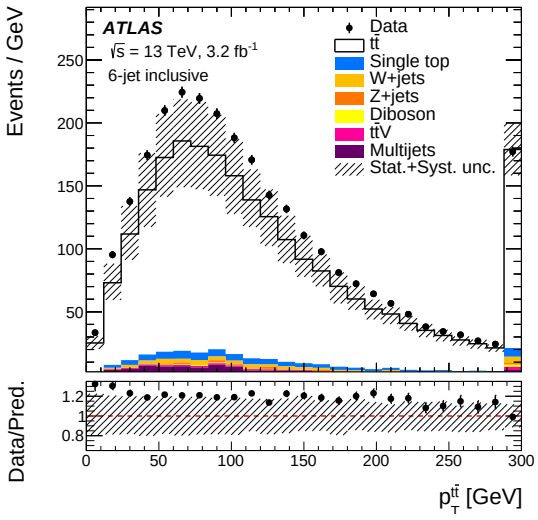

(c)

Figure 4: Distributions of $p_{\mathrm{T}}^{t\bar{t}}$ at reconstruction level: (a) 4-jet exclusive, (b) 5-jet exclusive and (c) 6-jet inclusive configurations. Data distributions are compared to predictions. The hatched area indicates the combined statistical and systematic uncertainties in the total prediction, excluding systematic uncertainties related to the modelling of the $t\bar{t}$ production. Events beyond the range of the horizontal axis are included in the last bin.

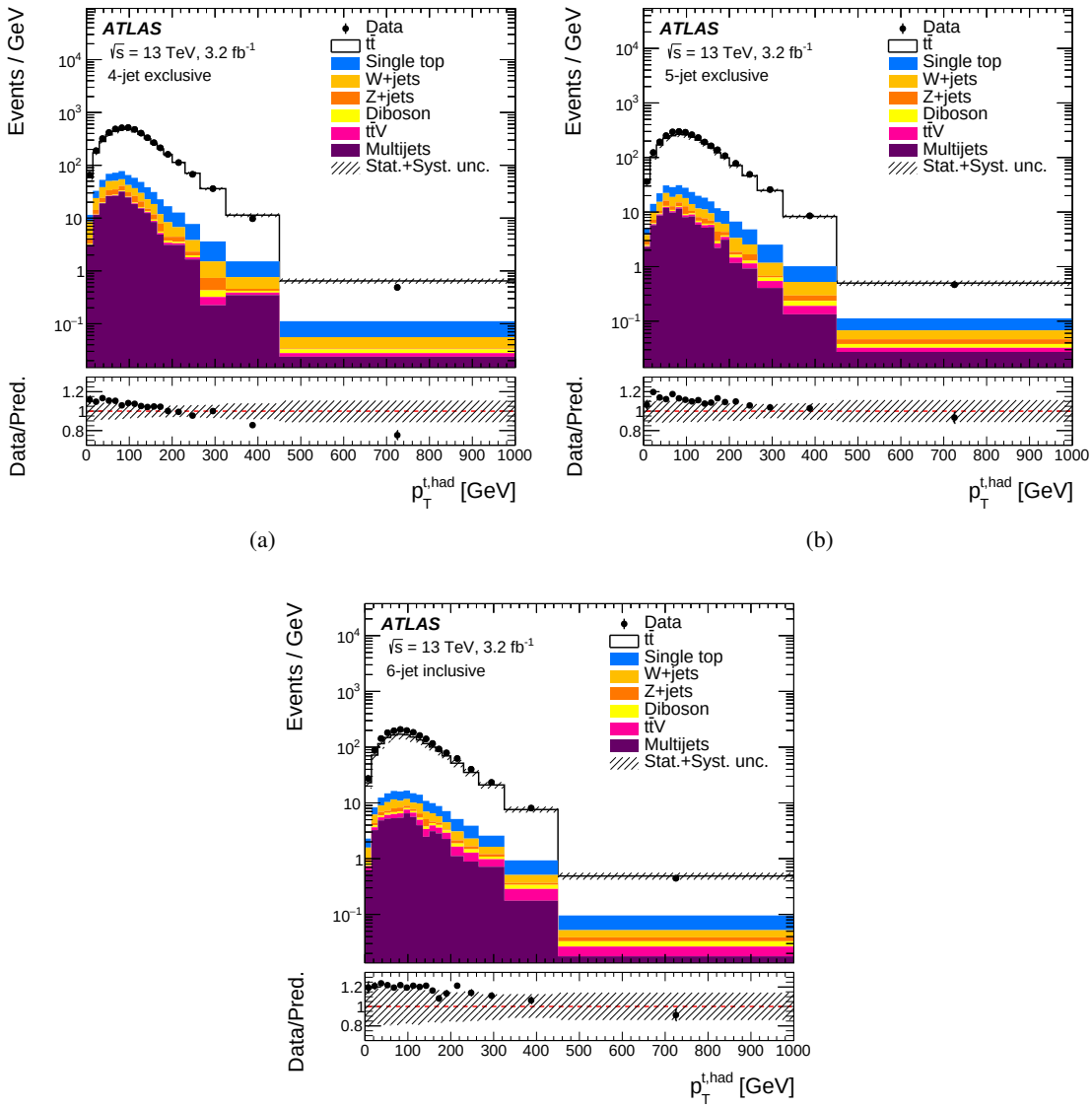

(a) (b)

(c)

Figure 5: Distributions of $p_{\mathrm{T}}^{t,\mathrm{had}}$ at reconstruction level: (a) 4-jet exclusive, (b) 5-jet exclusive and (c) 6-jet inclusive configurations. Data distributions are compared to predictions. The hatched area indicates the combined statistical and systematic uncertainties in the total prediction, excluding systematic uncertainties related to the modelling of the $t\bar{t}$ production. Events beyond the range of the horizontal axis are included in the last bin.

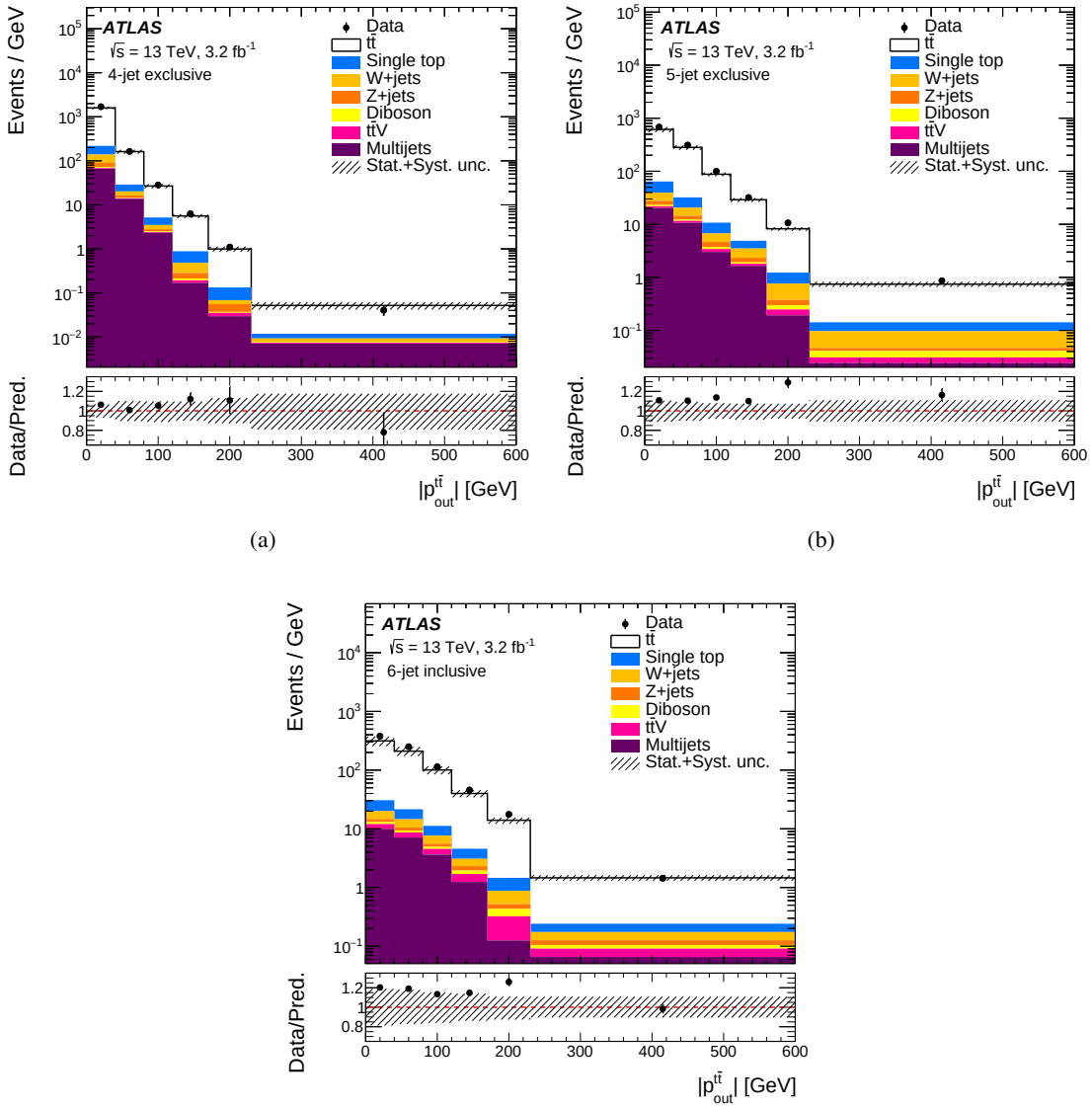

(a) (b)

(c)

Figure 6: Distributions of $\left|p_{\text{out}}^{t\bar{t}}\right|$ at reconstruction level: (a) 4-jet exclusive, (b) 5-jet exclusive and (c) 6-jet inclusive configurations. Data distributions are compared to predictions. The hatched area indicates the combined statistical and systematic uncertainties in the total prediction, excluding systematic uncertainties related to the modelling of the $t\bar{t}$ production. Events beyond the range of the horizontal axis are included in the last bin.

8 Unfolding procedure

The measured differential cross sections are obtained from the reconstruction-level distributions using an unfolding technique which corrects for detector and reconstruction effects. The iterative Bayesian method [69] as implemented in RooUnfold [70] is used.

The individual electron and muon channels have very similar corrections and give compatible results at reconstruction level. They are therefore combined by summing the distributions before the unfolding procedure.

For each observable, the unfolding procedure starts from the number of events at reconstruction level in bin j of the distribution (N^j_{reco}), after subtracting the background events estimated as described in Section 5 (N^j_{bg}). Next, the acceptance correction f^j_{acc} is defined as the ratio of the number of events passing both the particle- and reconstruction-level selections to the number of events passing the reconstruction-level selection. This factor corrects for events that are generated outside the fiducial phase space region but pass the reconstruction-level selection.

The reconstruction-level objects used to reconstruct the top quarks are required to be angularly matched to the corresponding particle-level object as assigned by the pseudo-top algorithm. The jets assigned to the W boson can be swapped. This requirement leads to a better correspondence between the particle and reconstruction levels. The matching requirement for the lepton, using the direction given by its associated track, is $\Delta R < 0.02$ while jets are required to be within $\Delta R < 0.35$. The matching correction f^j_{match} is defined as the ratio of events matched among the events passing both the particle-level and reconstruction-level selections for the same number of jets; it corrects for events in which a match is not found.

The unfolding step uses a migration matrix ($\mathcal{M}$) derived from simulated $t\bar{t}$ events which maps the binned particle-level events to the binned reconstruction-level events. The probability for particle-level events to be reconstructed in the same bin is therefore represented by the elements on the diagonal, and the off-diagonal elements describe the fraction of particle-level events that migrate into other bins. Therefore, the elements of each row add up to unity (within rounding). The number of bins is optimised for maximum information extraction under stable unfolding conditions. This is achieved by requiring that closure and stress tests are satisfied without introducing any bias. The unfolding is performed using four iterations to balance the unfolding stability with respect to the previous iteration (below 0.1%) and the growth of the statistical uncertainty. The effect of varying the number of iterations by one was found to be negligible. Finally, the efficiency ϵ is defined as the ratio of the number of matched events to the number of events passing the particle-level selection. This factor corrects for the inefficiency of the reconstruction.

The unfolding procedure for an observable X at particle level is summarised by the following expression for the absolute differential cross section:

$$\frac{\mathrm{d}\sigma^{\text{fid}}}{\mathrm{d}X^i} \equiv \frac{1}{\mathcal{L}\cdot\Delta X^i}\cdot\frac{1}{\epsilon^i}\cdot\sum_j \mathcal{M}^{-1}_{ij}\cdot f^j_{\text{match}}\cdot f^j_{\text{acc}}\cdot\left(N^j_{\text{reco}}-N^j_{\text{bg}}\right),$$

where the index j labels bins at reconstruction level while the i index labels bins at particle level; ΔX^i is the bin width while $\mathcal{L}$ is the integrated luminosity, and the Bayesian unfolding is symbolised by $\mathcal{M}_{ij}^{-1}$. The integrated fiducial cross section is obtained by integrating the unfolded cross section over the bins, and its value is used to compute the normalised differential cross section:

$$\frac{1}{\sigma^{\text{fid}}} \cdot \frac{\mathrm{d}\sigma^{\text{fid}}}{\mathrm{d}X^i}.$$

The unfolding of the observables is carried out independently in each configuration taking into account the bin-to-bin correlations within the distributions but not across jet multiplicity bins or among different observables within one jet multiplicity. Events that have a different number of jets at particle level and reconstruction level do not enter any migration matrix but are considered by the acceptance correction.

9 Systematic uncertainties

This section describes the estimation of systematic uncertainties related to object reconstruction and calibration, MC event generator modelling and background estimation. The uncertainty in the unfolded distribution is evaluated as follows. The considered distribution is varied at reconstruction level, unfolded using corrections from the nominal $t\bar{t}$ signal sample, and the unfolded distribution is compared to the particle-level distribution. All reconstruction- and background-related systematic uncertainties are evaluated using the nominal event generator, while alternative event generators are employed to assess uncertainties in the $t\bar{t}$ system modelling as discussed in Sec. 9.2. In these cases, the corrections derived from the event generator are used to unfold the reconstruction-level spectra of the alternative event generator.

The covariance matrix incorporating statistical and systematic uncertainties is obtained for each observable by summing two covariance matrices. The first covariance matrix includes statistical and systematic uncertainties from detector effects and background estimation by using pseudo-experiments to combine the sources. The second covariance matrix is derived by adding four separate covariance matrices corresponding to the effects of the signal modelling: event generator, parton shower and hadronisation, initial- and final-state radiation (ISR/FSR) and PDF uncertainties. The bin-to-bin correlation values are set to unity for all these matrices.

The covariance matrices due to the statistical and systematic uncertainties are obtained for each observable by evaluating the covariance between the kinematic bins using pseudo-experiments. In particular, the correlations due to statistical fluctuations from the size of both the data sample and the simulated signal samples are evaluated by varying the event counts independently in every bin before unfolding, and then propagating the resulting variations through the unfolding. The full description of the method is provided in Ref. [71].

9.1 Experimental uncertainties

The jet energy scale (JES) uncertainty is estimated using a combination of simulations, test-beam data and *in situ* measurements [62, 72, 73]. Additional contributions from jet-flavour composition, η-intercalibration, hadrons passing through the calorimeter without interacting (punch-through), single-particle response, calorimeter response to different jet flavours, and pile-up are considered, resulting in 19 eigenvector uncertainty components. The uncertainty in the jet energy resolution (JER) is obtained with an *in situ* measurement of the jet response in dijet events [74].

The efficiency to tag jets containing b-hadrons is corrected in simulated events by applying scale factors, extracted from a $t\bar{t}$ dilepton sample, to account for the residual difference between data and simulation. Scale factors are also applied for jets originating from light or charm quarks that are misidentified as b-jets. The associated flavour-tagging uncertainties, split into eigenvector components, are computed by varying the scale factors within their uncertainties [75–77].

The lepton reconstruction efficiency in simulated events is corrected by scale factors derived from measurements of these efficiencies in data using a control region enriched in $Z \to \ell^+\ell^-$ events. The lepton-trigger and reconstruction-efficiency scale factors, energy scale and resolution are varied within their uncertainties [56, 65].

The uncertainty associated with $E_{\mathrm{T}}^{\mathrm{miss}}$ is calculated by propagating the energy scale and resolution uncertainties to all jets and leptons in the $E_{\mathrm{T}}^{\mathrm{miss}}$ calculation. Additional $E_{\mathrm{T}}^{\mathrm{miss}}$ uncertainties arising from energy deposits not associated with any reconstructed objects are also included [65].

9.2 Signal modelling uncertainties

Uncertainties in the signal modelling affect the kinematic properties of simulated $t\bar{t}$ events as well as reconstruction- and particle-level efficiencies. To assess the uncertainty related to the matrix-element model and matching algorithm used in the MC event generator for the $t\bar{t}$ signal process, events simulated with MadGraph5_aMC@NLO + Herwig++ are unfolded using the migration matrix and correction factors derived from an alternative Powheg+Herwig++ sample. The difference between the unfolded distribution and the known particle level distribution of the MadGraph5_aMC@NLO+Herwig++ sample is assigned as the uncertainty, which is then symmetrised.

To assess the impact of different parton-shower models, events simulated with Powheg interfaced to Herwig++ are unfolded using the migration matrix and correction factors derived with the nominal sample. The difference between the unfolded distribution and the known particle-level distribution of the Powheg +Herwig++ sample is assigned as the relative uncertainty, which is then symmetrised.

To evaluate the uncertainties related to the modelling of the initial- and final-state gluon radiation (ISR/FSR), $t\bar{t}$ MC samples with modified ISR/FSR modelling are used. The MC samples used for the evaluation of this uncertainty are generated using the Powheg event generator interfaced to the Pythia shower model, where the parameters are varied as described in Section 3. The impact of the uncertainty related to the PDF is assessed using the $t\bar{t}$ sample generated with a MadGraph5_aMC@NLO interfaced to Herwig++. PDF-varied corrections and response matrix for the unfolding procedure are obtained by

reweighting the central PDF4LHC15 PDF set to the full set of its 30 eigenvectors as described in Ref. [40]. Using these corrections, the central MadGraph5_aMC@NLO+Herwig++ distribution is unfolded, the relative difference is computed with respect to the expected central particle-level spectrum, and the total uncertainty is obtained by adding these relative differences in quadrature. In addition, the difference between the central PDF4LHC15 and CT10 is evaluated in a similar way and added in quadrature to the PDF uncertainty.

9.3 Background modelling uncertainties

Systematic uncertainties affecting the backgrounds evaluated with MC simulation are estimated using an alternative background MC sample produced by rescaling the nominal background sample. The alternative sample, instead of the nominal one, is subtracted from data. The uncertainty is evaluated as the difference between the unfolded distribution using the alternative background MC sample and the nominal one.

A 15% normalisation uncertainty is applied to the single-top quark background. This includes the uncertainty associated with the emission of additional radiation which is evaluated to be smaller than 15%. The 5% theoretical uncertainty in the normalisation is also included.

In the case of the Z+jets and diboson backgrounds, the uncertainties include a contribution from the overall cross section normalisation as well as an additional 24% uncertainty per additional jet [78]: 48%, 72% and 96% in the 4-jet, 5-jet and 6-jet configurations, respectively.

The systematic uncertainties due to the overall normalisation and the heavy-flavour fractions of W+jets events are obtained by varying the data-driven scale factors. The overall impact of these uncertainties is less than 2%. Each detector systematic uncertainty includes the impact of those on the W+jets estimate. In addition, a 24% uncertainty per radiated jet, as described for the Z+jets and diboson samples, is applied to the W+jets background uncertainty.

The uncertainty in the background from non-prompt and fake leptons is evaluated by changing the selection used to define the control region and propagating the statistical uncertainty of the parametrisations of the efficiency to pass the tighter lepton requirements for real and fake leptons.

In addition, an extra 50% normalisation uncertainty is applied to this background to account for the remaining mis-modelling observed in various control regions. This systematic uncertainty also includes the impact of the normalisation on the estimation of the W+jets background.

9.4 Size of the simulated samples and luminosity uncertainty

Test distributions, created with independent Poisson fluctuations of the event count in each bin, are unfolded to account for the size of the simulated samples. The uncertainty is the standard deviation given by all unfolded distributions.

The uncertainty in the integrated luminosity is 2.1% and is derived, following techniques similar to those described in Ref. [79], from the luminosity scale calibration using a pair of x–y beam-separation scans performed in August 2015.

9.5 Summary plots of systematic uncertainties

Figure 7 presents the uncertainties as a function of $p_{\mathrm{T}}^{t,\mathrm{had}}$ in the $t\bar{t}$ fiducial phase space differential cross sections. The uncertainties are between 8% and 25% for the absolute cross sections and between 4% and 9% in almost the full range of the normalised cross sections. In all configurations the uncertainties are larger at the low and high ends of the spectrum. Comparing Figures 7(b), 7(c) and 7(d) shows that the JES uncertainty increases with the number of jets and is the dominant uncertainty in the 6-jet configuration. The uncertainties for the other observables have similar values and behaviour. In the 4-jet configuration, the dominant uncertainty is due to flavour-tagging. The total uncertainties are reduced for the normalised cross sections because of the cancelling out of correlated uncertainties, such as the flavour-tagging and the JES uncertainties as seen by comparing Figures 7(a) and 7(b).

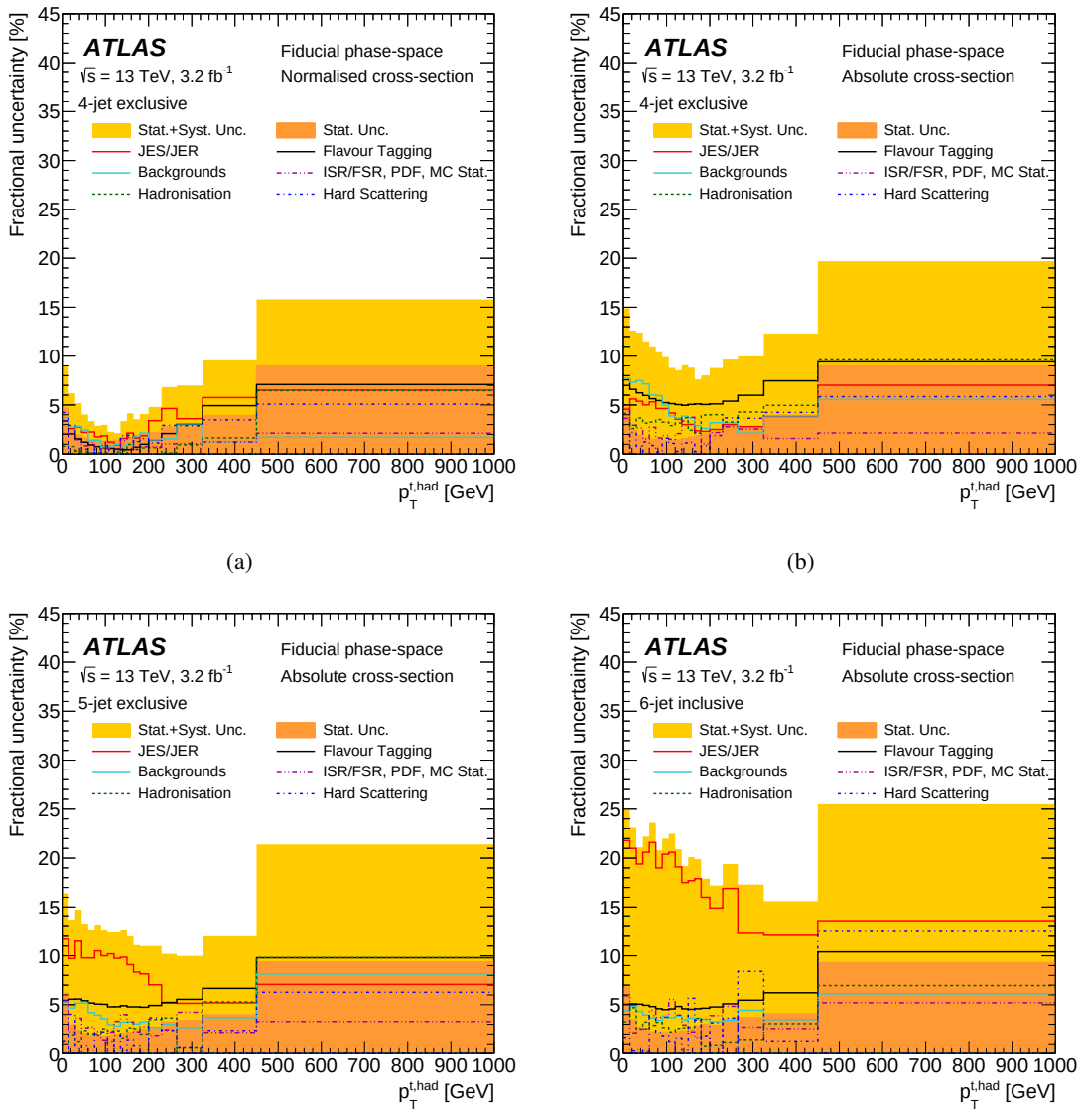

Figure 7: Uncertainties in the fiducial phase space differential cross sections as a function of $p_{\mathrm{T}}^{t,\mathrm{had}}$: normalised (a) in the 4-jet exclusive configuration; absolute (b) in the 4-jet exclusive, (c) 5-jet exclusive, and (d) 6-jet inclusive configurations. The yellow bands indicate the total uncertainty in each bin.

10 Results and comparisons with predictions

The measured differential cross sections as functions of $p_{\mathrm{T}}^{t,\mathrm{had}}$, $p_{\mathrm{T}}^{t\bar{t}}$ and $|p_{\mathrm{out}}^{t\bar{t}}|$ are shown in Figures 8–10 for the three configurations. All absolute differential cross sections are presented while only a selection of the normalised results is presented in which shape effects are more visible (this includes the $p_{\mathrm{T}}^{t,\mathrm{had}}$ results in the 4-jet configuration and the $p_{\mathrm{T}}^{t\bar{t}}$ and $|p_{\mathrm{out}}^{t\bar{t}}|$ results in the 6-jet configuration). Several MC predictions are compared to data; a subset of the most relevant predictions is shown in the figures while the compatibility to data is tested for a comprehensive list of MC predictions and shown in Tables 3–8.

The level of agreement between the measured differential cross sections and the predictions is quantified using χ^2 values which are evaluated employing the full covariance matrices of the uncertainties; the uncertainties in the theoretical predictions are not included in this evaluation. The p-values (probabilities that the χ^2 is larger than or equal to the observed value) are then evaluated from the χ^2 and the number of degrees of freedom (NDF). The detailed procedure for the calculation of the χ^2 and p-values is described in Ref. [1].

The differential cross section as a function of $p_{\mathrm{T}}^{t,\mathrm{had}}$ is shown in Figure 8. All MC predictions underestimate (overestimate) the data at low (high) values of $p_{\mathrm{T}}^{t,\mathrm{had}}$; this tendency is reduced at higher jet multiplicity. This is consistent with the CMS results for the same observable and various jet multiplicities [12]. In addition, these results obtained here improve the understanding of similar effects observed in previous ATLAS analyses [1, 8]; the effect is mainly due to events with exactly four jets. The χ^2 values for all predictions and all configurations are shown in Tables 3 and 4 for the absolute and normalised differential cross sections, respectively. In general, all predictions are compatible with the data in the 5- and 6-jet configurations for both the absolute and normalised differential cross sections while there is tension for the 4-jet configuration, especially for the absolute differential cross section. The main exception is the prediction obtained from the Powheg+Herwig++ calculation, which is inconsistent with the measured differential cross sections for the 4- and 6-jet configurations.

The differential cross sections as a function of $p_{\mathrm{T}}^{t\bar{t}}$ for different jet multiplicities are shown in Figure 9 and the χ^2 values are presented in Tables 5 and 6. In general, good agreement is observed in the 4- and 5-jet configurations while there is some tension in the 6-jet configuration. However, the χ^2 values show that the MadGraph5_aMC@NLO event generator is not compatible with data in the 4- and 5-jet configurations in both the absolute and normalised differential cross sections. This was not observed in the measurement inclusive in the number of jets [1] because different configurations are dominant at different values of $p_{\mathrm{T}}^{t\bar{t}}$. Indeed, the absolute cross section in the first two bins of the 4-jet configuration is larger than in the other configurations while the cross section in the last two bins is largest in the 6-jet configuration. Since the mis-modelling is observed in regions of p_{T} in which the cross section in that configuration is subdominant, it could not be observed in the previous measurement. The Powheg+Herwig++ prediction does not model the data well in all configurations. Furthermore, both 'radHi' calculations are not compatible with the data for the 4- and 6-jet configurations for the absolute differential cross sections.

The differential cross sections as functions of $|p_{\mathrm{out}}^{t\bar{t}}|$ are shown in Figure 10 and confirm the mis-modelling of the MadGraph5_aMC@NLO prediction for the 4- and 5-jet configurations observed for $p_{\mathrm{T}}^{t\bar{t}}$. The p-values shown in Tables 7 and 8 drop significantly at higher jet multiplicity for all predictions. Several predictions are not compatible with the absolute cross sections in the 6-jet configuration but have better

agreement with the normalised cross sections; nevertheless, some discrimination is still observed with the normalised cross sections. As before, the POWHEG+HERWIG++ prediction is not compatible with data in the 5-jet configuration.

An example of the discriminating power of the analysis is given in Figure 11; several predictions with different values of the fragmentation and renormalisation scales and of the h_{damp} parameter are compared to the measured differential cross sections for the 6-jet configuration. From the comparison shown in Figure 11(a), it can be seen that among the three PYTHIA6 predictions the best agreement is obtained by the 'radLo' calculation which is tuned to yield a lower amount of gluon radiation. This sample has an $h_{\text{damp}} = m_t$ and the factorisation and renormalisation scales increased by a factor of two compared to their nominal value. Since the h_{damp} parameter in the 'radLo' calculation is the same as the one in the nominal sample, it is possible to conclude that the reason for the different behaviour is due to the scale variation. A similar conclusion can be drawn for the comparison of the POWHEG+PYTHIA8 sample in Figure 11(c) where the 'radLo' calculation shows the best agreement. Changing h_{damp} has a small impact as shown in the comparison of the two POWHEG+PYTHIA8 predictions with different h_{damp} presented in Figure 11(b). The relative levels of agreement between data and the 'radHi' and 'radLo' predictions in the 6-jet configuration is opposite to what was observed in Ref. [4] where the 'radHi' prediction was observed to have a better agreement with data, e.g. for the jet multiplicity spectrum. This is not the only difference between the results of the two analyses; for example, in Ref. [4] MADGRAPH5_aMC@NLO+HERWIG++ was compatible with data while it is not compatible in some of the combinations of variables and jet multiplicity considered in this paper. It is clear that MC models have difficulty describing the sets of observables listed in the two papers simultaneously.

Figure 12 shows the ratio of the data to the nominal prediction for the normalised $p_{\text{T}}^{t,\text{had}}$ and $p_{\text{T}}^{t\bar{t}}$ differential cross sections for the three configurations. It can be seen that the differences between the data and the prediction are largest for the 4-jet configuration. The description of the 5- and 6-jet configurations by the prediction is slightly better. For $p_{\text{T}}^{t\bar{t}}$, the conclusions are less clear, and a reduction of the uncertainties would help to discriminate between the different predictions.

Table 3: Comparison of the measured fiducial phase space absolute differential cross sections as a function of $p_{\mathrm{T}}^{t,\mathrm{had}}$ and the predictions from several MC generators in different n-jet configurations. For each prediction a χ^2 and a p-value are calculated using the covariance matrix of the measured spectrum. The number of degrees of freedom (NDF) is equal to the number of bins in the distribution.

	4-jet exclusive		5-jet exclusive		6-jet inclusive	
	χ^2/NDF	p-value	χ^2/NDF	p-value	χ^2/NDF	p-value
Powheg+Pythia6	28.9/18	0.05	13.0/18	0.79	13.0/18	0.79
Powheg+Pythia6 (radHi)	29.2/18	0.05	14.7/18	0.68	17.2/18	0.51
Powheg+Pythia6 (radLo)	32.5/18	0.02	14.3/18	0.71	13.9/18	0.74
Powheg+Pythia8 ($h_{\mathrm{damp}} = m_t$)	25.2/18	0.12	14.7/18	0.68	15.7/18	0.61
Powheg+Pythia8 ($h_{\mathrm{damp}} = 1.5\,m_t$)	22.7/18	0.20	13.3/18	0.77	16.3/18	0.57
Powheg+Pythia8 (radHi) ($h_{\mathrm{damp}} = 3\,m_t$)	20.0/18	0.33	14.5/18	0.70	23.9/18	0.16
Powheg+Pythia8 (radLo) ($h_{\mathrm{damp}} = 1.5\,m_t$)	24.7/18	0.13	14.7/18	0.68	13.1/18	0.79
Powheg+Herwig7	20.8/18	0.29	12.0/18	0.85	12.4/18	0.82
Powheg+Herwig++	37.1/18	<0.01	27.7/18	0.07	38.7/18	<0.01
MadGraph5_aMC@NLO+Herwig++	25.7/18	0.11	11.1/18	0.89	20.3/18	0.32
MadGraph5_aMC@NLO+Pythia8 ($H_{\mathrm{T}}/2$)	22.9/18	0.19	21.2/18	0.27	17.7/18	0.47
MadGraph5_aMC@NLO+Pythia8 ($\sqrt{m_t^2 + p_{\mathrm{T}}^2}$)	25.4/18	0.11	19.3/18	0.37	23.1/18	0.18
Sherpa 2.2.1	24.7/18	0.14	18.3/18	0.43	18.3/18	0.44

Table 4: Comparison of the measured fiducial phase space normalised differential cross sections as a function of $p_{\mathrm{T}}^{t,\mathrm{had}}$ and the predictions from several MC generators in different n-jet configurations. For each prediction a χ^2 and a p-value are calculated using the covariance matrix of the measured spectrum. The number of degrees of freedom (NDF) is equal to the number of bins in the distribution minus one.

	4-jet exclusive		5-jet exclusive		6-jet inclusive	
	χ^2/NDF	p-value	χ^2/NDF	p-value	χ^2/NDF	p-value
Powheg+Pythia6	23.4/17	0.14	14.1/17	0.66	14.8/17	0.61
Powheg+Pythia6 (radHi)	23.4/17	0.14	14.9/17	0.60	15.9/17	0.53
Powheg+Pythia6 (radLo)	25.6/17	0.08	16.5/17	0.49	16.5/17	0.49
Powheg+Pythia8 ($h_{\mathrm{damp}} = m_t$)	22.7/17	0.16	16.9/17	0.46	18.3/17	0.37
Powheg+Pythia8 ($h_{\mathrm{damp}} = 1.5\,m_t$)	20.4/17	0.25	15.6/17	0.56	18.8/17	0.34
Powheg+Pythia8 (radHi) ($h_{\mathrm{damp}} = 3\,m_t$)	17.8/17	0.40	16.3/17	0.50	19.3/17	0.31
Powheg+Pythia8 (radLo) ($h_{\mathrm{damp}} = 1.5\,m_t$)	21.1/17	0.22	17.8/17	0.40	17.5/17	0.42
Powheg+Herwig7	16.6/17	0.48	12.1/17	0.80	12.8/17	0.75
Powheg+Herwig++	19.1/17	0.33	20.7/17	0.24	28.1/17	0.04
MadGraph5_aMC@NLO+Herwig++	16.3/17	0.50	11.5/17	0.83	23.9/17	0.12
MadGraph5_aMC@NLO+Pythia8 ($H_{\mathrm{T}}/2$)	20.3/17	0.26	21.9/17	0.19	22.5/17	0.17
MadGraph5_aMC@NLO+Pythia8 ($\sqrt{m_t^2 + p_{\mathrm{T}}^2}$)	20.7/17	0.24	18.1/17	0.38	28.5/17	0.04
Sherpa 2.2.1	21.8/17	0.19	20.0/17	0.28	17.5/17	0.42

Table 5: Comparison of the measured fiducial phase space absolute differential cross sections as a function of $p_{\mathrm{T}}^{t\bar{t}}$ and the predictions from several MC generators in different n-jet configurations. For each prediction a χ^2 and a p-value are calculated using the covariance matrix of the measured spectrum. The number of degrees of freedom (NDF) is equal to the number of bins in the distribution.

	4-jet exclusive		5-jet exclusive		6-jet inclusive	
	χ^2/NDF	p-value	χ^2/NDF	p-value	χ^2/NDF	p-value
Powheg+Pythia6	7.9/6	0.25	6.0/6	0.43	6.4/6	0.38
Powheg+Pythia6 (radHi)	15.9/6	0.01	5.8/6	0.45	36.2/6	<0.01
Powheg+Pythia6 (radLo)	4.9/6	0.56	5.8/6	0.45	6.5/6	0.37
Powheg+Pythia8 ($h_{\mathrm{damp}} = m_t$)	7.3/6	0.29	5.7/6	0.45	8.0/6	0.24
Powheg+Pythia8 ($h_{\mathrm{damp}} = 1.5\,m_t$)	7.6/6	0.27	3.3/6	0.77	12.3/6	0.06
Powheg+Pythia8 (radHi) ($h_{\mathrm{damp}} = 3\,m_t$)	13.9/6	0.03	3.2/6	0.78	54.8/6	<0.01
Powheg+Pythia8 (radLo) ($h_{\mathrm{damp}} = 1.5\,m_t$)	5.5/6	0.49	5.0/6	0.55	6.6/6	0.36
Powheg+Herwig7	10.2/6	0.12	5.1/6	0.53	5.0/6	0.54
Powheg+Herwig++	8.2/6	0.23	25.8/6	<0.01	20.8/6	<0.01
MadGraph5_aMC@NLO+Herwig++	98.3/6	<0.01	8.6/6	0.20	12.4/6	0.05
MadGraph5_aMC@NLO+Pythia8 ($H_{\mathrm{T}}/2$)	41.2/6	<0.01	34.5/6	<0.01	22.8/6	<0.01
MadGraph5_aMC@NLO+Pythia8 ($\sqrt{m_t^2 + p_{\mathrm{T}}^2}$)	46.7/6	<0.01	31.4/6	<0.01	18.6/6	<0.01
Sherpa 2.2.1	13.3/6	0.04	1.8/6	0.94	21.7/6	<0.01

Table 6: Comparison of the measured fiducial phase space normalised differential cross sections as a function of $p_{\mathrm{T}}^{t\bar{t}}$ and the predictions from several MC generators in different n-jet configurations. For each prediction a χ^2 and a p-value are calculated using the covariance matrix of the measured spectrum. The number of degrees of freedom (NDF) is equal to the number of bins in the distribution minus one.

	4-jet exclusive		5-jet exclusive		6-jet inclusive	
	χ^2/NDF	p-value	χ^2/NDF	p-value	χ^2/NDF	p-value
Powheg+Pythia6	4.3/5	0.51	3.0/5	0.70	3.9/5	0.56
Powheg+Pythia6 (radHi)	5.2/5	0.40	6.3/5	0.28	9.8/5	0.08
Powheg+Pythia6 (radLo)	6.2/5	0.29	3.5/5	0.62	5.2/5	0.39
Powheg+Pythia8 ($h_{\mathrm{damp}} = m_t$)	7.6/5	0.18	4.5/5	0.48	4.7/5	0.46
Powheg+Pythia8 ($h_{\mathrm{damp}} = 1.5\,m_t$)	5.5/5	0.36	3.9/5	0.57	6.2/5	0.28
Powheg+Pythia8 (radHi) ($h_{\mathrm{damp}} = 3\,m_t$)	6.5/5	0.26	4.0/5	0.55	10.5/5	0.06
Powheg+Pythia8 (radLo) ($h_{\mathrm{damp}} = 1.5\,m_t$)	5.2/5	0.39	5.6/5	0.35	7.6/5	0.18
Powheg+Herwig7	10.5/5	0.06	5.1/5	0.41	3.1/5	0.68
Powheg+Herwig++	18.6/5	<0.01	16.2/5	<0.01	19.4/5	<0.01
MadGraph5_aMC@NLO+Herwig++	12.8/5	0.03	10.0/5	0.07	9.3/5	0.10
MadGraph5_aMC@NLO+Pythia8 ($H_{\mathrm{T}}/2$)	26.8/5	<0.01	10.2/5	0.07	8.2/5	0.14
MadGraph5_aMC@NLO+Pythia8 ($\sqrt{m_t^2 + p_{\mathrm{T}}^2}$)	17.3/5	<0.01	10.0/5	0.07	7.8/5	0.17
Sherpa 2.2.1	7.5/5	0.19	1.7/5	0.89	2.2/5	0.82

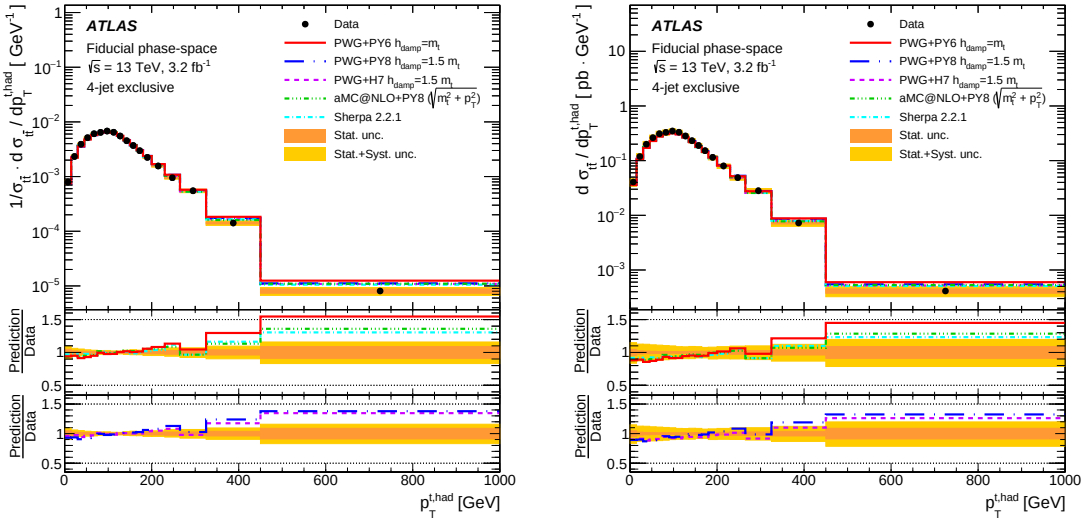

(a)

(b)

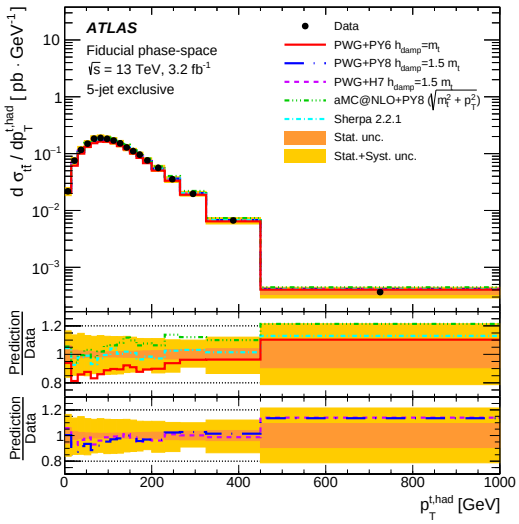

(c)

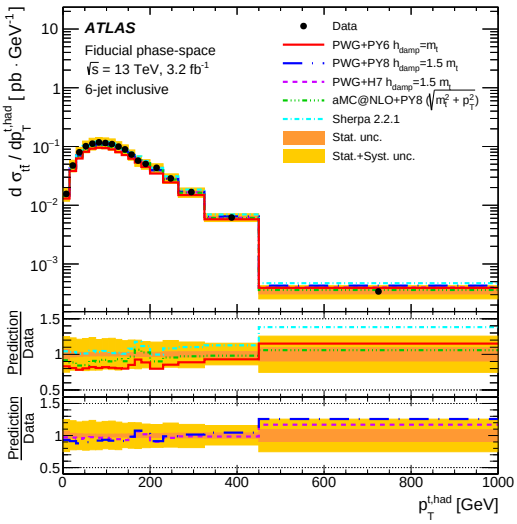

(d)

Figure 8: Differential cross sections in the fiducial phase space as a function of $p_{\mathrm{T}}^{t,\mathrm{had}}$: normalised (a) in the 4-jet exclusive configuration, absolute (b) in the 4-jet exclusive, (c) 5-jet exclusive and (d) 6-jet inclusive configurations. The shaded area represents the total statistical and systematic uncertainties.

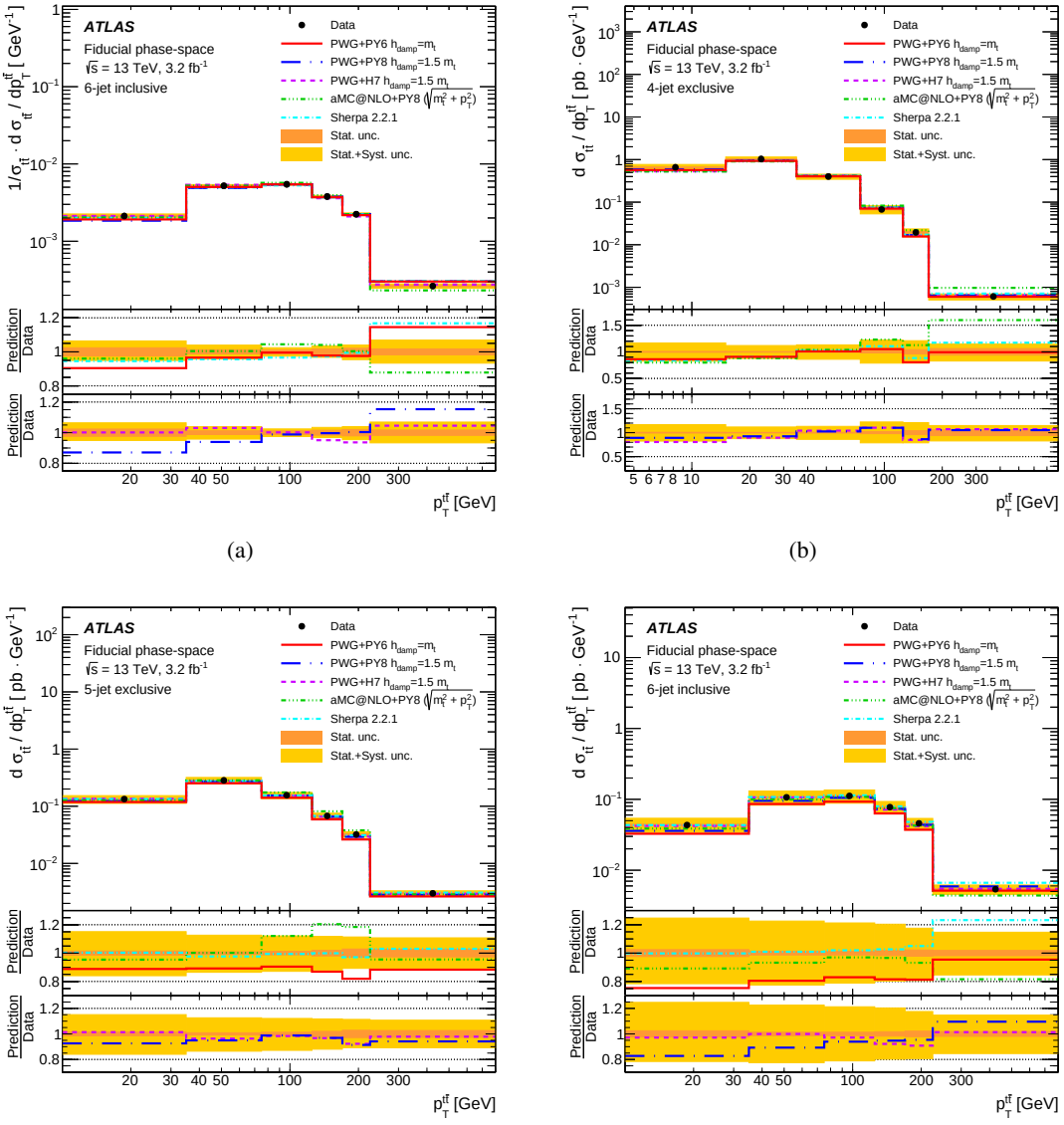

Figure 9: Differential cross sections in the fiducial phase space as a function of $p_{\mathrm{T}}^{t\bar{t}}$: normalised (a) in the 6-jet inclusive configuration, absolute (b) in the 4-jet exclusive, (c) 5-jet exclusive and (d) 6-jet inclusive configurations. The shaded area represents the total statistical and systematic uncertainties.

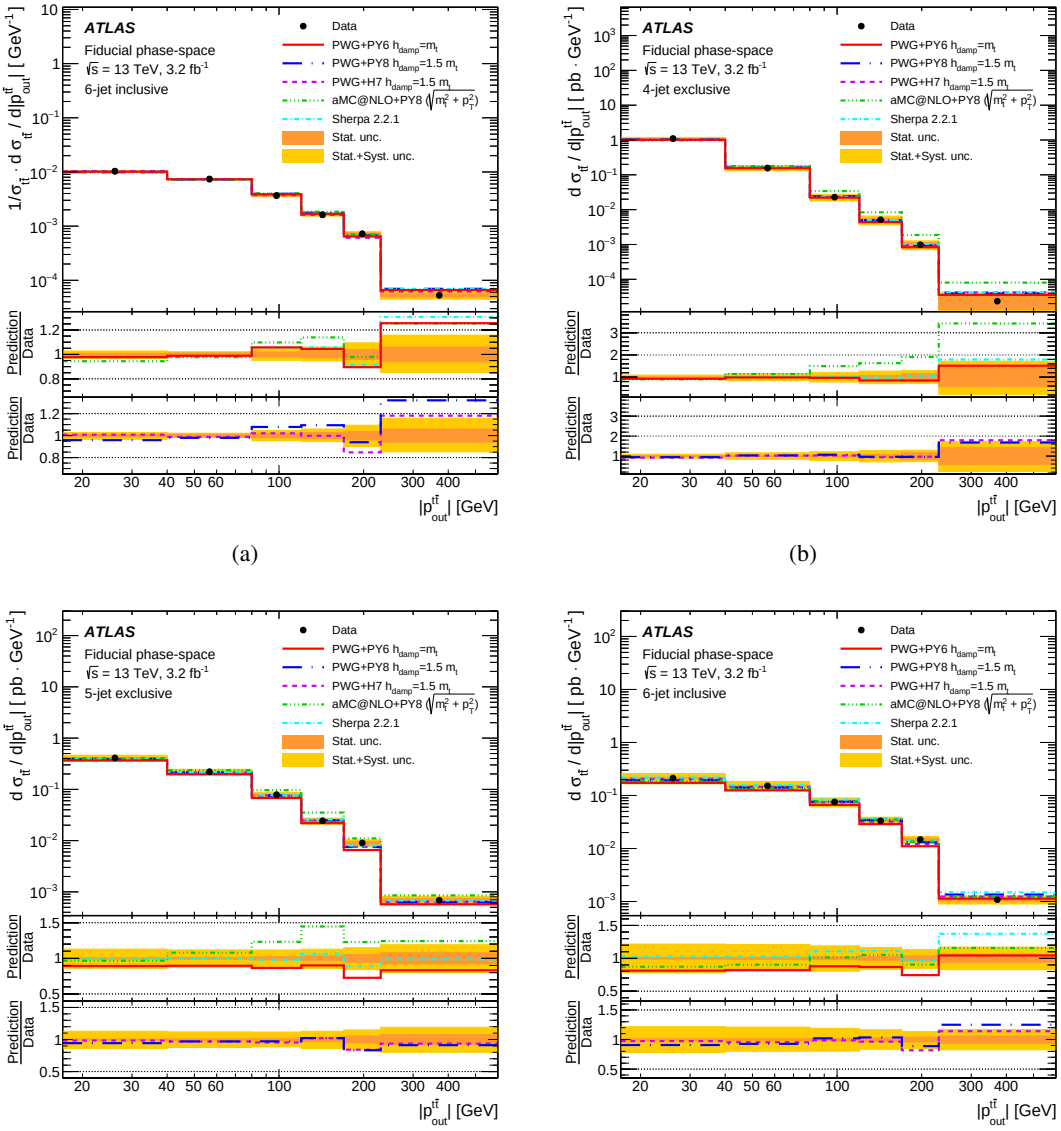

Figure 10: Differential cross sections in the fiducial phase space as a function of $\left|p_{\text{out}}^{t\bar{t}}\right|$: normalised (a) in the 6-jet inclusive configuration, absolute (b) in the 4-jet exclusive, (c) 5-jet exclusive and (d) 6-jet inclusive configurations. The shaded area represents the total statistical and systematic uncertainties.

Table 7: Comparison of the measured fiducial phase space absolute differential cross sections as a function of $\left|p_{\text{out}}^{t\bar{t}}\right|$ and the predictions from several MC generators in different n-jet configurations. For each prediction a χ^2 and a p-value are calculated using the covariance matrix of the measured spectrum. The number of degrees of freedom (NDF) is equal to the number of bins in the distribution.

	4-jet exclusive		5-jet exclusive		6-jet inclusive	
	χ^2/NDF	p-value	χ^2/NDF	p-value	χ^2/NDF	p-value
Powheg+Pythia6	4.1/6	0.67	10.0/6	0.12	10.2/6	0.12
Powheg+Pythia6 (radHi)	7.1/6	0.32	7.4/6	0.28	14.4/6	0.03
Powheg+Pythia6 (radLo)	2.5/6	0.87	10.2/6	0.12	14.8/6	0.02
Powheg+Pythia8 ($h_{\text{damp}} = m_t$)	3.0/6	0.81	9.7/6	0.14	10.1/6	0.12
Powheg+Pythia8 ($h_{\text{damp}} = 1.5\,m_t$)	3.1/6	0.80	7.3/6	0.29	10.7/6	0.10
Powheg+Pythia8 (radHi) ($h_{\text{damp}} = 3\,m_t$)	5.4/6	0.49	7.4/6	0.29	24.8/6	<0.01
Powheg+Pythia8 (radLo) ($h_{\text{damp}} = 1.5\,m_t$)	2.4/6	0.88	8.2/6	0.22	9.2/6	0.16
Powheg+Herwig7	4.6/6	0.59	6.4/6	0.38	12.3/6	0.06
Powheg+Herwig++	8.0/6	0.24	28.7/6	<0.01	37.6/6	<0.01
MadGraph5_aMC@NLO+Herwig++	59.9/6	<0.01	10.0/6	0.12	22.1/6	<0.01
MadGraph5_aMC@NLO+Pythia8 ($H_{\text{T}}/2$)	41.0/6	<0.01	38.1/6	<0.01	10.3/6	0.11
MadGraph5_aMC@NLO+Pythia8 ($\sqrt{m_t^2 + p_{\text{T}}^2}$)	41.0/6	<0.01	40.9/6	<0.01	10.5/6	0.10
Sherpa 2.2.1	3.5/6	0.74	5.7/6	0.46	12.8/6	0.05

Table 8: Comparison of the measured fiducial phase space normalised differential cross sections as a function of $\left|p_{\text{out}}^{t\bar{t}}\right|$ and the predictions from several MC generators in different n-jet configurations. For each prediction a χ^2 and a p-value are calculated using the covariance matrix of the measured spectrum. The number of degrees of freedom (NDF) is equal to the number of bins in the distribution minus one.

	4-jet exclusive		5-jet exclusive		6-jet inclusive	
	χ^2/NDF	p-value	χ^2/NDF	p-value	χ^2/NDF	p-value
Powheg+Pythia6	2.1/5	0.84	5.1/5	0.41	8.0/5	0.15
Powheg+Pythia6 (radHi)	5.2/5	0.40	5.7/5	0.34	11.6/5	0.04
Powheg+Pythia6 (radLo)	1.2/5	0.95	5.1/5	0.40	8.6/5	0.13
Powheg+Pythia8 ($h_{\text{damp}} = m_t$)	1.4/5	0.93	6.7/5	0.25	9.0/5	0.11
Powheg+Pythia8 ($h_{\text{damp}} = 1.5\,m_t$)	1.0/5	0.96	6.2/5	0.29	11.9/5	0.04
Powheg+Pythia8 (radHi) ($h_{\text{damp}} = 3\,m_t$)	2.9/5	0.71	7.5/5	0.18	14.3/5	0.01
Powheg+Pythia8 (radLo) ($h_{\text{damp}} = 1.5\,m_t$)	0.5/5	0.99	6.6/5	0.26	10.5/5	0.06
Powheg+Herwig7	2.3/5	0.80	4.6/5	0.46	5.3/5	0.38
Powheg+Herwig++	7.3/5	0.20	15.0/5	0.01	10.4/5	0.07
MadGraph5_aMC@NLO+Herwig++	36.3/5	<0.01	10.2/5	0.07	6.7/5	0.24
MadGraph5_aMC@NLO+Pythia8 ($H_{\text{T}}/2$)	47.9/5	<0.01	28.9/5	<0.01	16.2/5	<0.01
MadGraph5_aMC@NLO+Pythia8 ($\sqrt{m_t^2 + p_{\text{T}}^2}$)	46.5/5	<0.01	30.7/5	<0.01	15.7/5	<0.01
Sherpa 2.2.1	1.5/5	0.92	4.6/5	0.46	8.2/5	0.15

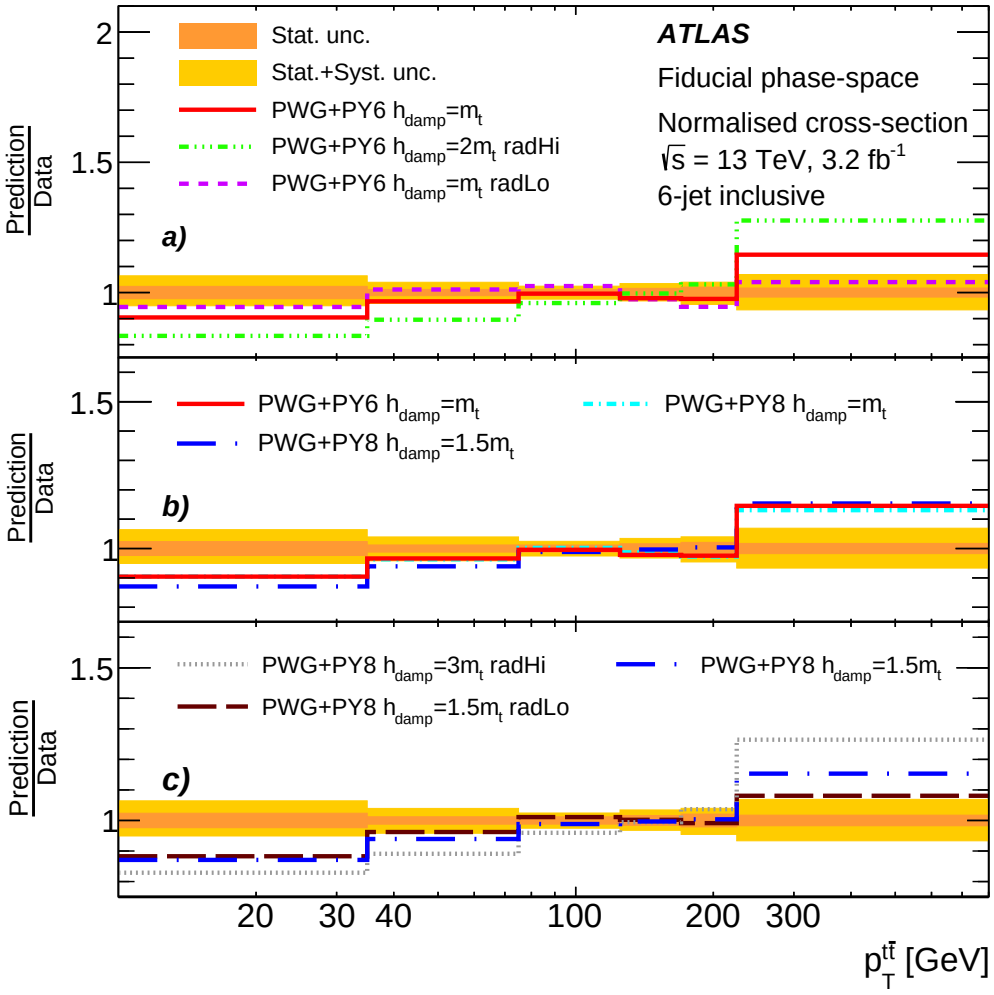

Figure 11: Normalised differential cross sections as a function of $p_{\mathrm{T}}^{t\bar{t}}$ in the 6-jet inclusive configuration in the fiducial phase space. The dark shaded area is the statistical uncertainty and the light shaded area represents the total uncertainty.

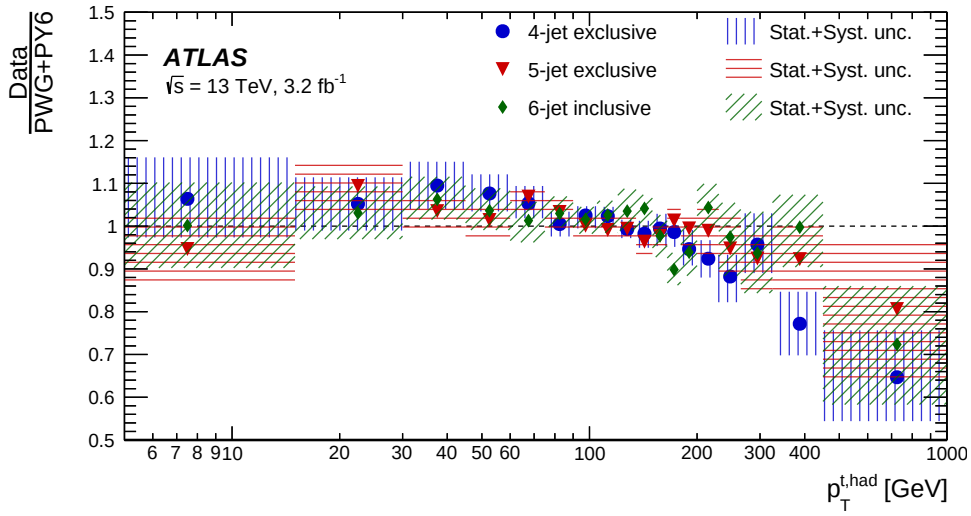

(a)

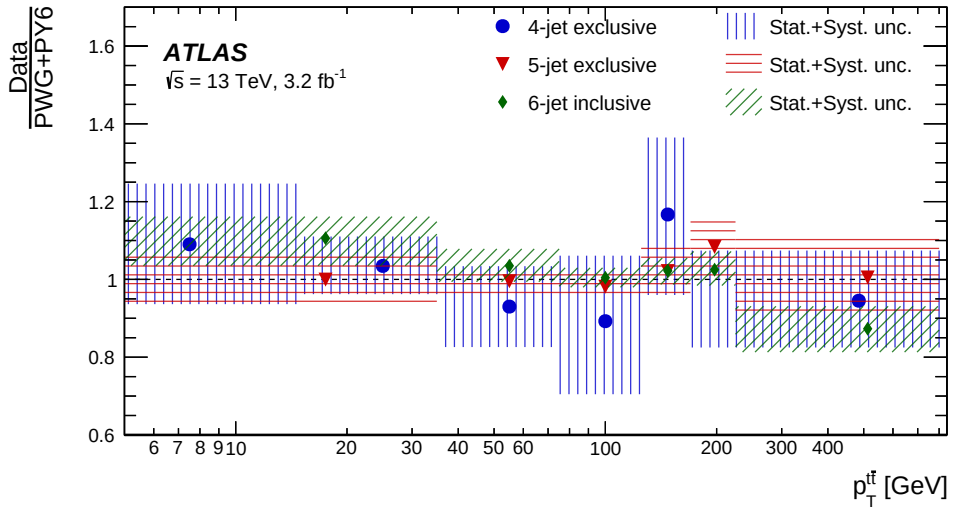

(b)

Figure 12: Normalised (a) ratio of data to the nominal prediction as a function of $p_{\mathrm{T}}^{t,\mathrm{had}}$ and (b) as a function of $p_{\mathrm{T}}^{t\bar{t}}$ in the 4-jet exclusive, 5-jet exclusive and 6-jet inclusive configurations.

11 Conclusions

Measurements of differential cross sections for top quark pair production in association with jets are presented using data from the 13 TeV pp collisions collected by the ATLAS detector at the LHC in 2015, corresponding to an integrated luminosity of 3.2 fb^{-1}. Both the absolute and normalised differential cross sections are measured as functions of the top quark transverse momentum, the transverse momentum of the top quark pair system and the out-of-plane transverse momentum. The top quark pair events are selected in the lepton (electron or muon) + jets channel and three mutually exclusive configurations are defined according to the number of additional jets reconstructed in each event. Regions of phase space sensitive to the effects of gluon radiation are identified. The predictions of several Monte Carlo calculations are compared to the measurements. Differences between the data and some of the predictions are observed. The measured $\left|p_{\text{out}}^{t\bar{t}}\right|$ and $p_{\text{T}}^{t\bar{t}}$ distributions in the 6-jet configuration disfavour several predictions. The measured $p_{\text{T}}^{t,\text{had}}$ distribution in the 4-jet configuration is underestimated by the predictions at low values and overestimated at high values; this tendency of the predictions is reduced at higher jet multiplicity. Overall, the measurements presented here improve the discriminating power of previous ATLAS results and the data have the potential to further constrain the MC models used to describe the top quark pair production.

Acknowledgements

We thank CERN for the very successful operation of the LHC, as well as the support staff from our institutions without whom ATLAS could not be operated efficiently.

We acknowledge the support of ANPCyT, Argentina; YerPhI, Armenia; ARC, Australia; BMWFW and FWF, Austria; ANAS, Azerbaijan; SSTC, Belarus; CNPq and FAPESP, Brazil; NSERC, NRC and CFI, Canada; CERN; CONICYT, Chile; CAS, MOST and NSFC, China; COLCIENCIAS, Colombia; MSMT CR, MPO CR and VSC CR, Czech Republic; DNRF and DNSRC, Denmark; IN2P3-CNRS, CEA-DRF/IRFU, France; SRNSFG, Georgia; BMBF, HGF, and MPG, Germany; GSRT, Greece; RGC, Hong Kong SAR, China; ISF, I-CORE and Benoziyo Center, Israel; INFN, Italy; MEXT and JSPS, Japan; CNRST, Morocco; NWO, Netherlands; RCN, Norway; MNiSW and NCN, Poland; FCT, Portugal; MNE/IFA, Romania; MES of Russia and NRC KI, Russian Federation; JINR; MESTD, Serbia; MSSR, Slovakia; ARRS and MIZŠ, Slovenia; DST/NRF, South Africa; MINECO, Spain; SRC and Wallenberg Foundation, Sweden; SERI, SNSF and Cantons of Bern and Geneva, Switzerland; MOST, Taiwan; TAEK, Turkey; STFC, United Kingdom; DOE and NSF, United States of America. In addition, individual groups and members have received support from BCKDF, the Canada Council, CANARIE, CRC, Compute Canada, FQRNT, and the Ontario Innovation Trust, Canada; EPLANET, ERC, ERDF, FP7, Horizon 2020 and Marie Skłodowska-Curie Actions, European Union; Investissements d'Avenir Labex and Idex, ANR, Région Auvergne and Fondation Partager le Savoir, France; DFG and AvH Foundation, Germany; Herakleitos, Thales and Aristeia programmes co-financed by EU-ESF and the Greek NSRF; BSF, GIF and Minerva, Israel; BRF, Norway; CERCA Programme Generalitat de Catalunya, Generalitat Valenciana, Spain; the Royal Society and Leverhulme Trust, United Kingdom.

The crucial computing support from all WLCG partners is acknowledged gratefully, in particular from CERN, the ATLAS Tier-1 facilities at TRIUMF (Canada), NDGF (Denmark, Norway, Sweden), CC-IN2P3 (France), KIT/GridKA (Germany), INFN-CNAF (Italy), NL-T1 (Netherlands), PIC (Spain), ASGC (Taiwan), RAL (UK) and BNL (USA), the Tier-2 facilities worldwide and large non-WLCG resource providers. Major contributors of computing resources are listed in Ref. [80].

References

[1] ATLAS Collaboration, *Measurements of top-quark pair differential cross-sections in the lepton+jets channel in pp collisions at $\sqrt{s}$ = 13 TeV using the ATLAS detector*, JHEP **11** (2017) 191, arXiv: 1708.00727 [hep-ex].

[2] ATLAS Collaboration, *Measurement of $t\bar{t}$ production with a veto on additional central jet activity in pp collisions at $\sqrt{s}$ = 7 TeV using the ATLAS detector*, Eur. Phys. J. C **72** (2012) 2043, arXiv: 1203.5015 [hep-ex].

[3] ATLAS Collaboration, *Measurement of jet activity in top quark events using the $e\mu$ final state with two b-tagged jets in pp collisions at $\sqrt{s}$ = 8 TeV with the ATLAS detector*, JHEP **09** (2016) 074, arXiv: 1606.09490 [hep-ex].

[4] ATLAS Collaboration, *Measurement of jet activity produced in top-quark events with an electron, a muon and two b-tagged jets in the final state in pp collisions at $\sqrt{s}$ = 13 TeV with the ATLAS detector*, Eur. Phys. J. C **77** (2017) 220, arXiv: 1610.09978 [hep-ex].

[5] ATLAS Collaboration, *Measurements of top quark pair relative differential cross-sections with ATLAS in pp collisions at $\sqrt{s}$ = 7 TeV*, Eur. Phys. J. C **73** (2013) 2261, arXiv: 1207.5644 [hep-ex].

[6] ATLAS Collaboration, *Measurements of normalized differential cross-sections for $t\bar{t}$ production in pp collisions at $\sqrt{s}$ = 7 TeV using the ATLAS detector*, Phys. Rev. D **90** (2014) 072004, arXiv: 1407.0371 [hep-ex].

[7] ATLAS Collaboration, *Differential top-antitop cross-section measurements as a function of observables constructed from final-state particles using pp collisions at $\sqrt{s}$ = 7 TeV in the ATLAS detector*, JHEP **06** (2015) 100, arXiv: 1502.05923 [hep-ex].

[8] ATLAS Collaboration, *Measurements of top-quark pair differential cross-sections in the lepton+jets channel in pp collisions at $\sqrt{s}$ = 8 TeV using the ATLAS detector*, Eur. Phys. J. C **76** (2016) 538, arXiv: 1511.04716 [hep-ex].

[9] CMS Collaboration, *Measurement of differential top-quark-pair production cross sections in pp colisions at $\sqrt{s}$ = 7 TeV*, Eur. Phys. J. C **73** (2013) 2339, arXiv: 1211.2220 [hep-ex].

[10] CMS Collaboration, *Measurement of the differential cross section for top quark pair production in pp collisions at $\sqrt{s}$ = 8 TeV*, Eur. Phys. J. C **75** (2015) 542, arXiv: 1505.04480 [hep-ex].

[11] CMS Collaboration, *Measurement of $t\bar{t}$ production with additional jet activity, including b quark jets, in the dilepton decay channel using pp collisions at $\sqrt{s}$ = 8 TeV*, Eur. Phys. J. C **76** (2016) 379, arXiv: 1510.03072 [hep-ex].

[12] CMS Collaboration, *Measurement of differential cross sections for top quark pair production using the lepton+jets final state in proton–proton collisions at* 13 *TeV*, Phys. Rev. D **95** (2017) 092001, arXiv: 1610.04191 [hep-ex].

[13] L. Apanasevich et al., *Evidence for Parton k_T Effects in High- p_T Particle Production*, Phys. Rev. Lett. **81** (1998) 2642.

[14] S. Frixione, P. Nason and C. Oleari, *Matching NLO QCD computations with parton shower simulations: the POWHEG method*, JHEP **11** (2007) 070, arXiv: 0709.2092 [hep-ph].

[15] J. Alwall et al., *The automated computation of tree-level and next-to-leading order differential cross sections, and their matching to parton shower simulations*, JHEP **07** (2014) 079, arXiv: 1405.0301 [hep-ph].

[16] T. Gleisberg et al., *Event generation with SHERPA 1.1*, JHEP **02** (2009) 007, arXiv: 0811.4622 [hep-ph].

[17] ATLAS Collaboration, *The ATLAS Experiment at the CERN Large Hadron Collider*, JINST **3** (2008) S08003.

[18] ATLAS Collaboration, *ATLAS Insertable B-Layer Technical Design Report*, ATLAS-TDR-19, 2010, URL: https://cds.cern.ch/record/1291633, *ATLAS Insertable B-Layer Technical Design Report Addendum*, ATLAS-TDR-19-ADD-1, 2012, URL: https://cds.cern.ch/record/1451888.

[19] ATLAS Collaboration, *Performance of the ATLAS Trigger System in 2015*, Eur. Phys. J. C **77** (2017) 317, arXiv: 1611.09661 [hep-ex].

[20] T. Sjöstrand, S. Mrenna and P. Z. Skands, *A brief introduction to PYTHIA 8.1*, Comput. Phys. Commun. **178** (2008) 852, arXiv: 0710.3820 [hep-ph].

[21] ATLAS Collaboration, *Summary of ATLAS Pythia 8 tunes*, ATL-PHYS-PUB-2012-003, 2012, URL: https://cds.cern.ch/record/1474107.

[22] A. D. Martin, W. J. Stirling, R. S. Thorne and G. Watt, *Parton distributions for the LHC*, Eur. Phys. J. C **63** (2009) 189, arXiv: 0901.0002 [hep-ph].

[23] D. J. Lange, *The EvtGen particle decay simulation package*, Nucl. Instrum. Meth. A **462** (2001) 152.

[24] ATLAS Collaboration, *The ATLAS Simulation Infrastructure*, Eur. Phys. J. C **70** (2010) 823, arXiv: 1005.4568 [physics.ins-det].

[25] S. Agostinelli et al., *GEANT4: a simulation toolkit*, Nucl. Instrum. Methods Phys. A **506** (2003) 250.

[26] ATLAS Collaboration, *Simulation of top-quark production for the ATLAS experiment at* $\sqrt{s}$ = 13 *TeV*, ATL-PHYS-PUB-2016-004, 2016, URL: https://cds.cern.ch/record/2120417.

[27] H.-L. Lai, M. Guzzi, J. Huston, Z. Li, P. M. Nadolsky et al., *New parton distributions for collider physics*, Phys. Rev. D **82** (2010) 074024, arXiv: 1007.2241 [hep-ph].

[28] P. Artoisenet, R. Frederix, O. Mattelaer and R. Rietkerk, *Automatic spin-entangled decays of heavy resonances in Monte Carlo simulations*, JHEP **03** (2013) 015, arXiv: 1212.3460 [hep-ph].

[29] T. Sjöstrand, S. Mrenna and P. Z. Skands, *PYTHIA 6.4 physics and manual*, JHEP **05** (2006) 026, arXiv: hep-ph/0603175.

[30] D. Stump et al., *Inclusive jet production, parton distributions, and the search for new physics*, JHEP **10** (2003) 046, arXiv: hep-ph/0303013.

[31] P. Z. Skands, *Tuning Monte Carlo generators: The Perugia tunes*, Phys. Rev. D **82** (2010) 074018, arXiv: 1005.3457 [hep-ph].

[32] M. Bahr et al., *Herwig++ physics and manual*, Eur. Phys. J. C **58** (2008) 639, arXiv: 0803.0883 [hep-ph].

[33] ATLAS Collaboration, *ATLAS Pythia 8 tunes to 7 TeV data*, ATL-PHYS-PUB-2014-021, 2014, URL: https://cds.cern.ch/record/1966419.

[34] ATLAS Collaboration, *Performance of the Fast ATLAS Tracking Simulation (FATRAS) and the ATLAS Fast Calorimeter Simulation (FastCaloSim) with single particles*, ATL-SOFT-PUB-2014-01, 2014, URL: https://cds.cern.ch/record/1669341.

[35] ATLAS Collaboration, *Studies on top-quark Monte Carlo modelling for Top2016*, ATL-PHYS-PUB-2016-020, 2016, URL: https://cds.cern.ch/record/2216168.

[36] ATLAS Collaboration, *Studies on top-quark Monte Carlo modelling with Sherpa and MG5_aMC@NLO*, ATL-PHYS-PUB-2017-007, 2017, URL: https://cds.cern.ch/record/2261938.

[37] R. D. Ball et al., *Parton distributions for the LHC Run II*, JHEP **04** (2015) 040, arXiv: 1410.8849 [hep-ph].

[38] M. Czakon and A. Mitov, *Top++: A program for the calculation of the top-pair cross-section at hadron colliders*, Comput. Phys. Commun. **185** (2014) 2930, arXiv: 1112.5675 [hep-ph].

[39] A. D. Martin, W. J. Stirling, R. S. Thorne and G. Watt, *Uncertainties on α_S in global PDF analyses and implications for predicted hadronic cross sections*, Eur. Phys. J. C **64** (2009) 653, arXiv: 0905.3531 [hep-ph].

[40] M. Botje et al., *The PDF4LHC Working Group Interim Recommendations*, (2011), arXiv: 1101.0538 [hep-ph].

[41] R. D. Ball et al., *Parton distributions with LHC data*, Nucl. Phys. B **867** (2013) 244, arXiv: 1207.1303 [hep-ex].

[42] S. Frixione, E. Laenen, P. Motylinski, B. Webber and C. D. White, *Single-top hadroproduction in association with a W boson*, JHEP **07** (2008) 029, arXiv: 0805.3067 [hep-ph].

[43] N. Kidonakis, *Next-to-next-to-leading-order collinear and soft gluon corrections for t-channel single top quark production*, Phys. Rev. D **83** (2011) 091503, arXiv: 1103.2792 [hep-ph].

[44] M. Aliev, H. Lacker, U. Langenfeld, S. Moch, P. Uwer et al., *HATHOR: HAdronic Top and Heavy quarks crOss section calculatoR*, Comput. Phys. Commun. **182** (2011) 1034, arXiv: 1007.1327 [hep-ph].

[45] P. Kant et al., *HatHor for single top-quark production: Updated predictions and uncertainty estimates for single top-quark production in hadronic collisions*, Comput. Phys. Commun. **191** (2015) 74, arXiv: 1406.4403 [hep-ph].

[46] T. Gleisberg and S. Höche, *Comix, a new matrix element generator*, JHEP **12** (2008) 039, arXiv: 0808.3674 [hep-ph].

[47] F. Cascioli, P. Maierhofer and S. Pozzorini, *Scattering Amplitudes with Open Loops*, Phys. Rev. Lett. **108** (2012) 111601, arXiv: 1111.5206 [hep-ph].

[48] S. Schumann and F. Krauss, *A Parton shower algorithm based on Catani-Seymour dipole factorisation*, JHEP **03** (2008) 038, arXiv: 0709.1027 [hep-ph].

[49] S. Hoeche, F. Krauss, M. Schonherr, F. Siegert, *QCD matrix elements + parton showers: The NLO case*, JHEP **04** (2013) 027, arXiv: 1207.5030 [hep-ph].

[50] ATLAS Collaboration, *Monte Carlo Generators for the Production of a W or Z/γ^* Boson in Association with Jets at ATLAS in Run 2*, ATL-PHYS-PUB-2016-003, 2016, URL: https://cds.cern.ch/record/2120133.

[51] ATLAS Collaboration, *Multi-boson simulation for 13 TeV ATLAS analyses*, ATL-PHYS-PUB-2016-002, 2016, URL: https://cds.cern.ch/record/2119986.

[52] ATLAS Collaboration, *Modelling of the $t\bar{t}H$ and $t\bar{t}V(V = W, Z)$ processes for $\sqrt{s} = 13$ TeV ATLAS analyses*, ATL-PHYS-PUB-2016-005, 2016, URL: https://cds.cern.ch/record/2120826.

[53] ATLAS Collaboration, *Expected electron performance in the ATLAS experiment*, ATL-PHYS-PUB-2011-006, 2011, URL: https://cds.cern.ch/record/1345327.

[54] ATLAS Collaboration, *Measurement of the $t\bar{t}$ production cross-section using $e\mu$ events with b-tagged jets in pp collisions at $\sqrt{s} = 13$ TeV with the ATLAS detector*, Phys. Lett. B **761** (2016) 136, arXiv: 1606.02699 [hep-ex].

[55] ATLAS Collaboration, *Electron efficiency measurements with the ATLAS detector using 2012 LHC proton–proton collision data*, Eur. Phys. J. C **77** (2017) 195, arXiv: 1612.01456 [hep-ex].

[56] ATLAS Collaboration, *Muon reconstruction performance of the ATLAS detector in proton–proton collision data at $\sqrt{s} = 13$ TeV*, Eur. Phys. J. C **76** (2016) 292, arXiv: 1603.05598 [hep-ex].

[57] M. Cacciari, G. P. Salam and G. Soyez, *The anti-k_t jet clustering algorithm*, JHEP **04** (2008) 063, arXiv: 0802.1189 [hep-ph].

[58] M. Cacciari, G. P. Salam and G. Soyez, *FastJet user manual*, Eur. Phys. J. C **72** (2012) 1896, arXiv: 1111.6097 [hep-ph].

[59] ATLAS Collaboration, *Topological cell clustering in the ATLAS calorimeters and its performance in LHC Run 1*, Eur. Phys. J. C **77** (2017) 490, arXiv: 1603.02934 [hep-ex].

[60] M. Cacciari, G. P. Salam and G. Soyez, *The catchment area of jets*, JHEP **04** (2008) 005, arXiv: 0802.1188 [hep-ph].

[61] ATLAS Collaboration, *Performance of pile-up mitigation techniques for jets in pp collisions at $\sqrt{s} = 8$ TeV using the ATLAS detector*, Eur. Phys. J. C **76** (2016) 581, arXiv: 1510.03823 [hep-ex].

[62] ATLAS Collaboration, *Jet energy measurement and its systematic uncertainty in proton–proton collisions at $\sqrt{s} = 7$ TeV with the ATLAS detector*, Eur. Phys. J. C **75** (2015) 17, arXiv: 1406.0076 [hep-ex].

[63] ATLAS Collaboration, *Jet energy scale measurements and their systematic uncertainties in proton–proton collisions at $\sqrt{s} = 13$ TeV with the ATLAS detector*, Phys. Rev. D **96** (2017) 072002, arXiv: 1703.09665 [hep-ex].

[64] ATLAS Collaboration, *Expected performance of the ATLAS b-tagging algorithms in Run-2*, ATL-PHYS-PUB-2015-022, 2015, URL: https://cds.cern.ch/record/2037697.

[65] ATLAS Collaboration, *Performance of algorithms that reconstruct missing transverse momentum in $\sqrt{s} = 8$ TeV proton–proton collisions in the ATLAS detector*, Eur. Phys. J. C **77** (2017) 241, arXiv: 1609.09324 [hep-ex].

[66] ATLAS Collaboration, *Measurement of the top quark pair production cross-section with ATLAS in the single lepton channel*, Phys. Lett. B **711** (2012) 244, arXiv: 1201.1889 [hep-ex].

[67] F. Halzen, Y. S. Jeong and C. S. Kim, *Charge asymmetry of weak boson production at the LHC and the charm content of the proton*, Phys. Rev. D **88** (2013) 073013, arXiv: 1304.0322 [hep-ph].

[68] ATLAS Collaboration, *A search for $t\bar{t}$ resonances using lepton-plus-jets events in proton–proton collisions at $\sqrt{s}$ = 8 TeV with the ATLAS detector*, JHEP **08** (2015) 148, arXiv: 1505.07018 [hep-ex].

[69] G. D'Agostini, *A multidimensional unfolding method based on Bayes' theorem*, Nucl. Instrum. Meth. A **362** (1995) 487.

[70] T. Adye, *Unfolding algorithms and tests using RooUnfold*, 2011, arXiv: 1105.1160 [physics.data-an].

[71] ATLAS Collaboration, *Measurement of the differential cross-section of highly boosted top quarks as a function of their transverse momentum in $\sqrt{s}$ = 8 TeV proton–proton collisions using the ATLAS detector*, Phys. Rev. D **93** (2016) 032009, arXiv: 1510.03818 [hep-ex].

[72] ATLAS Collaboration, *Jet energy measurement with the ATLAS detector in proton–proton collisions at $\sqrt{s}$ = 7 TeV*, Eur. Phys. J. C **73** (2013) 2304, arXiv: 1112.6426 [hep-ex].

[73] ATLAS Collaboration, *Single hadron response measurement and calorimeter jet energy scale uncertainty with the ATLAS detector at the LHC*, Eur. Phys. J. C **73** (2013) 2305, arXiv: 1203.1302 [hep-ex].

[74] ATLAS Collaboration, *Jet energy resolution in proton–proton collisions at $\sqrt{s}$ = 7 TeV recorded in 2010 with the ATLAS detector*, Eur. Phys. J. C **73** (2013) 2306, arXiv: 1210.6210 [hep-ex].

[75] ATLAS Collaboration, *Calibration of b-tagging using dileptonic top pair events in a combinatorial likelihood approach with the ATLAS experiment*, ATLAS-CONF-2014-004, 2014, URL: https://cds.cern.ch/record/1664335.

[76] ATLAS Collaboration, *Measurement of the b-tag Efficiency in a Sample of Jets Containing Muons with 5 fb^{-1} of data from the ATLAS detector*, ATLAS-CONF-2012-043, 2012, URL: https://cds.cern.ch/record/1435197.

[77] ATLAS Collaboration, *Measurement of the Mistag Rate of b-tagging algorithms with 5 fb^{-1} of Data Collected by the ATLAS Detector*, ATLAS-CONF-2012-040, 2012, URL: https://cds.cern.ch/record/1435194.

[78] J. Alwall, S. Hoche, F. Krauss, N. Lavesson, L. Lonnblad et al., *Comparative study of various algorithms for the merging of parton showers and matrix elements in hadronic collisions*, Eur. Phys. J. C **53** (2008) 473, arXiv: 0706.2569 [hep-ph].

[79] ATLAS Collaboration, *Luminosity determination in pp collisions at $\sqrt{s}$ = 8 TeV using the ATLAS detector at the LHC*, Eur. Phys. J. C **76** (2016) 653, arXiv: 1608.03953 [hep-ex].

[80] ATLAS Collaboration, *ATLAS Computing Acknowledgements 2016–2017*, ATL-GEN-PUB-2016-002, URL: https://cds.cern.ch/record/2202407.

The ATLAS Collaboration

M. Aaboud[137d], G. Aad[88], B. Abbott[115], O. Abdinov[12,*], B. Abeloos[119], S.H. Abidi[161], O.S. AbouZeid[139], N.L. Abraham[151], H. Abramowicz[155], H. Abreu[154], Y. Abulaiti[148a,148b], B.S. Acharya[167a,167b,a], S. Adachi[157], L. Adamczyk[41a], J. Adelman[110], M. Adersberger[102], T. Adye[133], A.A. Affolder[139], Y. Afik[154], C. Agheorghiesei[28c], J.A. Aguilar-Saavedra[128a,128f], S.P. Ahlen[24], F. Ahmadov[68,b], G. Aielli[135a,135b], S. Akatsuka[71], H. Akerstedt[148a,148b], T.P.A. Åkesson[84], E. Akilli[52], A.V. Akimov[98], G.L. Alberghi[22a,22b], J. Albert[172], P. Albicocco[50], M.J. Alconada Verzini[74], S.C. Alderweireldt[108], M. Aleksa[32], I.N. Aleksandrov[68], C. Alexa[28b], G. Alexander[155], T. Alexopoulos[10], M. Alhroob[115], B. Ali[130], M. Aliev[76a,76b], G. Alimonti[94a], J. Alison[33], S.P. Alkire[38], B.M.M. Allbrooke[151], B.W. Allen[118], P.P. Allport[19], A. Aloisio[106a,106b], A. Alonso[39], F. Alonso[74], C. Alpigiani[140], A.A. Alshehri[56], M.I. Alstaty[88], B. Alvarez Gonzalez[32], D. Álvarez Piqueras[170], M.G. Alviggi[106a,106b], B.T. Amadio[16], Y. Amaral Coutinho[26a], C. Amelung[25], D. Amidei[92], S.P. Amor Dos Santos[128a,128c], S. Amoroso[32], C. Anastopoulos[141], L.S. Ancu[52], N. Andari[19], T. Andeen[11], C.F. Anders[60b], J.K. Anders[77], K.J. Anderson[33], A. Andreazza[94a,94b], V. Andrei[60a], S. Angelidakis[37], I. Angelozzi[109], A. Angerami[38], A.V. Anisenkov[111,c], N. Anjos[13], A. Annovi[126a], C. Antel[60a], M. Antonelli[50], A. Antonov[100,*], D.J. Antrim[166], F. Anulli[134a], M. Aoki[69], L. Aperio Bella[32], G. Arabidze[93], Y. Arai[69], J.P. Araque[128a], V. Araujo Ferraz[26a], A.T.H. Arce[48], R.E. Ardell[80], F.A. Arduh[74], J-F. Arguin[97], S. Argyropoulos[66], M. Arik[20a], A.J. Armbruster[32], L.J. Armitage[79], O. Arnaez[161], H. Arnold[51], M. Arratia[30], O. Arslan[23], A. Artamonov[99,*], G. Artoni[122], S. Artz[86], S. Asai[157], N. Asbah[45], A. Ashkenazi[155], L. Asquith[151], K. Assamagan[27], R. Astalos[146a], M. Atkinson[169], N.B. Atlay[143], K. Augsten[130], G. Avolio[32], B. Axen[16], M.K. Ayoub[35a], G. Azuelos[97,d], A.E. Baas[60a], M.J. Baca[19], H. Bachacou[138], K. Bachas[76a,76b], M. Backes[122], P. Bagnaia[134a,134b], M. Bahmani[42], H. Bahrasemani[144], J.T. Baines[133], M. Bajic[39], O.K. Baker[179], P.J. Bakker[109], E.M. Baldin[111,c], P. Balek[175], F. Balli[138], W.K. Balunas[124], E. Banas[42], A. Bandyopadhyay[23], Sw. Banerjee[176,e], A.A.E. Bannoura[178], L. Barak[155], E.L. Barberio[91], D. Barberis[53a,53b], M. Barbero[88], T. Barillari[103], M-S Barisits[65], J.T. Barkeloo[118], T. Barklow[145], N. Barlow[30], S.L. Barnes[36c], B.M. Barnett[133], R.M. Barnett[16], Z. Barnovska-Blenessy[36a], A. Baroncelli[136a], G. Barone[25], A.J. Barr[122], L. Barranco Navarro[170], F. Barreiro[85], J. Barreiro Guimarães da Costa[35a], R. Bartoldus[145], A.E. Barton[75], P. Bartos[146a], A. Basalaev[125], A. Bassalat[119,f], R.L. Bates[56], S.J. Batista[161], J.R. Batley[30], M. Battaglia[139], M. Bauce[134a,134b], F. Bauer[138], K.T. Bauer[166], H.S. Bawa[145,g], J.B. Beacham[113], M.D. Beattie[75], T. Beau[83], P.H. Beauchemin[165], P. Bechtle[23], H.P. Beck[18,h], H.C. Beck[57], K. Becker[122], M. Becker[86], C. Becot[112], A.J. Beddall[20e], A. Beddall[20b], V.A. Bednyakov[68], M. Bedognetti[109], C.P. Bee[150], T.A. Beermann[32], M. Begalli[26a], M. Begel[27], J.K. Behr[45], A.S. Bell[81], G. Bella[155], L. Bellagamba[22a], A. Bellerive[31], M. Bellomo[154], K. Belotskiy[100], O. Beltramello[32], N.L. Belyaev[100], O. Benary[155,*], D. Benchekroun[137a], M. Bender[102], N. Benekos[10], Y. Benhammou[155], E. Benhar Noccioli[179], J. Benitez[66], D.P. Benjamin[48], M. Benoit[52], J.R. Bensinger[25], S. Bentvelsen[109], L. Beresford[122], M. Beretta[50], D. Berge[109], E. Bergeaas Kuutmann[168], N. Berger[5], L.J. Bergsten[25], J. Beringer[16], S. Berlendis[58], N.R. Bernard[89], G. Bernardi[83], C. Bernius[145], F.U. Bernlochner[23], T. Berry[80], P. Berta[86], C. Bertella[35a], G. Bertoli[148a,148b], I.A. Bertram[75], C. Bertsche[45], G.J. Besjes[39], O. Bessidskaia Bylund[148a,148b], M. Bessner[45], N. Besson[138], A. Bethani[87], S. Bethke[103], A. Betti[23], A.J. Bevan[79], J. Beyer[103], R.M. Bianchi[127], O. Biebel[102], D. Biedermann[17], R. Bielski[87], K. Bierwagen[86], N.V. Biesuz[126a,126b], M. Biglietti[136a], T.R.V. Billoud[97], H. Bilokon[50], M. Bindi[57], A. Bingul[20b], C. Bini[134a,134b],

S. Biondi[22a,22b], T. Bisanz[57], C. Bittrich[47], D.M. Bjergaard[48], J.E. Black[145], K.M. Black[24], R.E. Blair[6], T. Blazek[146a], I. Bloch[45], C. Blocker[25], A. Blue[56], U. Blumenschein[79], S. Blunier[34a], G.J. Bobbink[109], V.S. Bobrovnikov[111,c], S.S. Bocchetta[84], A. Bocci[48], C. Bock[102], M. Boehler[51], D. Boerner[178], D. Bogavac[102], A.G. Bogdanchikov[111], C. Bohm[148a], V. Boisvert[80], P. Bokan[168,i], T. Bold[41a], A.S. Boldyrev[101], A.E. Bolz[60b], M. Bomben[83], M. Bona[79], M. Boonekamp[138], A. Borisov[132], G. Borissov[75], J. Bortfeldt[32], D. Bortoletto[122], V. Bortolotto[62a], D. Boscherini[22a], M. Bosman[13], J.D. Bossio Sola[29], J. Boudreau[127], E.V. Bouhova-Thacker[75], D. Boumediene[37], C. Bourdarios[119], S.K. Boutle[56], A. Boveia[113], J. Boyd[32], I.R. Boyko[68], A.J. Bozson[80], J. Bracinik[19], A. Brandt[8], G. Brandt[178], O. Brandt[60a], F. Braren[45], U. Bratzler[158], B. Brau[89], J.E. Brau[118], W.D. Breaden Madden[56], K. Brendlinger[45], A.J. Brennan[91], L. Brenner[109], R. Brenner[168], S. Bressler[175], D.L. Briglin[19], T.M. Bristow[49], D. Britton[56], D. Britzger[60b], F.M. Brochu[30], I. Brock[23], R. Brock[93], G. Brooijmans[38], T. Brooks[80], W.K. Brooks[34b], E. Brost[110], J.H Broughton[19], P.A. Bruckman de Renstrom[42], D. Bruncko[146b], A. Bruni[22a], G. Bruni[22a], L.S. Bruni[109], S. Bruno[135a,135b], BH Brunt[30], M. Bruschi[22a], N. Bruscino[127], P. Bryant[33], L. Bryngemark[45], T. Buanes[15], Q. Buat[144], P. Buchholz[143], A.G. Buckley[56], I.A. Budagov[68], F. Buehrer[51], M.K. Bugge[121], O. Bulekov[100], D. Bullock[8], T.J. Burch[110], S. Burdin[77], C.D. Burgard[109], A.M. Burger[5], B. Burghgrave[110], K. Burka[42], S. Burke[133], I. Burmeister[46], J.T.P. Burr[122], D. Büscher[51], V. Büscher[86], E. Buschmann[57], P. Bussey[56], J.M. Butler[24], C.M. Buttar[56], J.M. Butterworth[81], P. Butti[32], W. Buttinger[27], A. Buzatu[153], A.R. Buzykaev[111,c], Changqiao C.-Q.[36a], S. Cabrera Urbán[170], D. Caforio[130], H. Cai[169], V.M. Cairo[2], O. Cakir[4a], N. Calace[52], P. Calafiura[16], A. Calandri[88], G. Calderini[83], P. Calfayan[64], G. Callea[40a,40b], L.P. Caloba[26a], S. Calvente Lopez[85], D. Calvet[37], S. Calvet[37], T.P. Calvet[88], R. Camacho Toro[33], S. Camarda[32], P. Camarri[135a,135b], D. Cameron[121], R. Caminal Armadans[169], C. Camincher[58], S. Campana[32], M. Campanelli[81], A. Camplani[94a,94b], A. Campoverde[143], V. Canale[106a,106b], M. Cano Bret[36c], J. Cantero[116], T. Cao[155], M.D.M. Capeans Garrido[32], I. Caprini[28b], M. Caprini[28b], M. Capua[40a,40b], R.M. Carbone[38], R. Cardarelli[135a], F. Cardillo[51], I. Carli[131], T. Carli[32], G. Carlino[106a], B.T. Carlson[127], L. Carminati[94a,94b], R.M.D. Carney[148a,148b], S. Caron[108], E. Carquin[34b], S. Carrá[94a,94b], G.D. Carrillo-Montoya[32], D. Casadei[19], M.P. Casado[13,j], A.F. Casha[161], M. Casolino[13], D.W. Casper[166], R. Castelijn[109], V. Castillo Gimenez[170], N.F. Castro[128a,k], A. Catinaccio[32], J.R. Catmore[121], A. Cattai[32], J. Caudron[23], V. Cavaliere[169], E. Cavallaro[13], D. Cavalli[94a], M. Cavalli-Sforza[13], V. Cavasinni[126a,126b], E. Celebi[20d], F. Ceradini[136a,136b], L. Cerda Alberich[170], A.S. Cerqueira[26b], A. Cerri[151], L. Cerrito[135a,135b], F. Cerutti[16], A. Cervelli[22a,22b], S.A. Cetin[20d], A. Chafaq[137a], D. Chakraborty[110], S.K. Chan[59], W.S. Chan[109], Y.L. Chan[62a], P. Chang[169], J.D. Chapman[30], D.G. Charlton[19], C.C. Chau[31], C.A. Chavez Barajas[151], S. Che[113], S. Cheatham[167a,167c], A. Chegwidden[93], S. Chekanov[6], S.V. Chekulaev[163a], G.A. Chelkov[68,l], M.A. Chelstowska[32], C. Chen[36a], C. Chen[67], H. Chen[27], J. Chen[36a], S. Chen[35b], S. Chen[157], X. Chen[35c,m], Y. Chen[70], H.C. Cheng[92], H.J. Cheng[35a,35d], A. Cheplakov[68], E. Cheremushkina[132], R. Cherkaoui El Moursli[137e], E. Cheu[7], K. Cheung[63], L. Chevalier[138], V. Chiarella[50], G. Chiarelli[126a], G. Chiodini[76a], A.S. Chisholm[32], A. Chitan[28b], Y.H. Chiu[172], M.V. Chizhov[68], K. Choi[64], A.R. Chomont[37], S. Chouridou[156], Y.S. Chow[62a], V. Christodoulou[81], M.C. Chu[62a], J. Chudoba[129], A.J. Chuinard[90], J.J. Chwastowski[42], L. Chytka[117], A.K. Ciftci[4a], D. Cinca[46], V. Cindro[78], I.A. Cioara[23], A. Ciocio[16], F. Cirotto[106a,106b], Z.H. Citron[175], M. Citterio[94a], M. Ciubancan[28b], A. Clark[52], M.R. Clark[38], P.J. Clark[49], R.N. Clarke[16], C. Clement[148a,148b], Y. Coadou[88], M. Cobal[167a,167c], A. Coccaro[52], J. Cochran[67], L. Colasurdo[108], B. Cole[38], A.P. Colijn[109], J. Collot[58], T. Colombo[166], P. Conde Muiño[128a,128b], E. Coniavitis[51], S.H. Connell[147b], I.A. Connelly[87], S. Constantinescu[28b], G. Conti[32], F. Conventi[106a,n], A.M. Cooper-Sarkar[122], F. Cormier[171], K.J.R. Cormier[161],

M. Corradi[134a,134b], E.E. Corrigan[84], F. Corriveau[90,o], A. Cortes-Gonzalez[32], G. Costa[94a], M.J. Costa[170], D. Costanzo[141], G. Cottin[30], G. Cowan[80], B.E. Cox[87], K. Cranmer[112], S.J. Crawley[56], R.A. Creager[124], G. Cree[31], S. Crépé-Renaudin[58], F. Crescioli[83], W.A. Cribbs[148a,148b], M. Cristinziani[23], V. Croft[112], G. Crosetti[40a,40b], A. Cueto[85], T. Cuhadar Donszelmann[141], A.R. Cukierman[145], J. Cummings[179], M. Curatolo[50], J. Cúth[86], S. Czekierda[42], P. Czodrowski[32], G. D'amen[22a,22b], S. D'Auria[56], L. D'eramo[83], M. D'Onofrio[77], M.J. Da Cunha Sargedas De Sousa[128a,128b], C. Da Via[87], W. Dabrowski[41a], T. Dado[146a], T. Dai[92], O. Dale[15], F. Dallaire[97], C. Dallapiccola[89], M. Dam[39], J.R. Dandoy[124], M.F. Daneri[29], N.P. Dang[176], N.S. Dann[87], M. Danninger[171], M. Dano Hoffmann[138], V. Dao[150], G. Darbo[53a], S. Darmora[8], J. Dassoulas[3], A. Dattagupta[118], T. Daubney[45], W. Davey[23], C. David[45], T. Davidek[131], D.R. Davis[48], P. Davison[81], E. Dawe[91], I. Dawson[141], K. De[8], R. de Asmundis[106a], A. De Benedetti[115], S. De Castro[22a,22b], S. De Cecco[83], N. De Groot[108], P. de Jong[109], H. De la Torre[93], F. De Lorenzi[67], A. De Maria[57], D. De Pedis[134a], A. De Salvo[134a], U. De Sanctis[135a,135b], A. De Santo[151], K. De Vasconcelos Corga[88], J.B. De Vivie De Regie[119], R. Debbe[27], C. Debenedetti[139], D.V. Dedovich[68], N. Dehghanian[3], I. Deigaard[109], M. Del Gaudio[40a,40b], J. Del Peso[85], D. Delgove[119], F. Deliot[138], C.M. Delitzsch[7], A. Dell'Acqua[32], L. Dell'Asta[24], M. Della Pietra[106a,106b], D. della Volpe[52], M. Delmastro[5], C. Delporte[119], P.A. Delsart[58], D.A. DeMarco[161], S. Demers[179], M. Demichev[68], A. Demilly[83], S.P. Denisov[132], D. Denysiuk[138], D. Derendarz[42], J.E. Derkaoui[137d], F. Derue[83], P. Dervan[77], K. Desch[23], C. Deterre[45], K. Dette[161], M.R. Devesa[29], P.O. Deviveiros[32], A. Dewhurst[133], S. Dhaliwal[25], F.A. Di Bello[52], A. Di Ciaccio[135a,135b], L. Di Ciaccio[5], W.K. Di Clemente[124], C. Di Donato[106a,106b], A. Di Girolamo[32], B. Di Girolamo[32], B. Di Micco[136a,136b], R. Di Nardo[32], K.F. Di Petrillo[59], A. Di Simone[51], R. Di Sipio[161], D. Di Valentino[31], C. Diaconu[88], M. Diamond[161], F.A. Dias[39], M.A. Diaz[34a], J. Dickinson[16], E.B. Diehl[92], J. Dietrich[17], S. Díez Cornell[45], A. Dimitrievska[16], J. Dingfelder[23], P. Dita[28b], S. Dita[28b], F. Dittus[32], F. Djama[88], T. Djobava[54b], J.I. Djuvsland[60a], M.A.B. do Vale[26c], M. Dobre[28b], D. Dodsworth[25], C. Doglioni[84], J. Dolejsi[131], Z. Dolezal[131], M. Donadelli[26d], S. Donati[126a,126b], J. Donini[37], J. Dopke[133], A. Doria[106a], M.T. Dova[74], A.T. Doyle[56], E. Drechsler[57], M. Dris[10], Y. Du[36b], J. Duarte-Campderros[155], F. Dubinin[98], A. Dubreuil[52], E. Duchovni[175], G. Duckeck[102], A. Ducourthial[83], O.A. Ducu[97,p], D. Duda[109], A. Dudarev[32], A.Chr. Dudder[86], E.M. Duffield[16], L. Duflot[119], M. Dührssen[32], C. Dulsen[178], M. Dumancic[175], A.E. Dumitriu[28b], A.K. Duncan[56], M. Dunford[60a], A. Duperrin[88], H. Duran Yildiz[4a], M. Düren[55], A. Durglishvili[54b], D. Duschinger[47], B. Dutta[45], D. Duvnjak[1], M. Dyndal[45], B.S. Dziedzic[42], C. Eckardt[45], K.M. Ecker[103], R.C. Edgar[92], T. Eifert[32], G. Eigen[15], K. Einsweiler[16], T. Ekelof[168], M. El Kacimi[137c], R. El Kosseifi[88], V. Ellajosyula[88], M. Ellert[168], S. Elles[5], F. Ellinghaus[178], A.A. Elliot[172], N. Ellis[32], J. Elmsheuser[27], M. Elsing[32], D. Emeliyanov[133], Y. Enari[157], J.S. Ennis[173], M.B. Epland[48], J. Erdmann[46], A. Ereditato[18], M. Ernst[27], S. Errede[169], M. Escalier[119], C. Escobar[170], B. Esposito[50], O. Estrada Pastor[170], A.I. Etienvre[138], E. Etzion[155], H. Evans[64], A. Ezhilov[125], M. Ezzi[137e], F. Fabbri[22a,22b], L. Fabbri[22a,22b], V. Fabiani[108], G. Facini[81], R.M. Fakhrutdinov[132], S. Falciano[134a], R.J. Falla[81], J. Faltova[32], Y. Fang[35a], M. Fanti[94a,94b], A. Farbin[8], A. Farilla[136a], E.M. Farina[123a,123b], T. Farooque[93], S. Farrell[16], S.M. Farrington[173], P. Farthouat[32], F. Fassi[137e], P. Fassnacht[32], D. Fassouliotis[9], M. Faucci Giannelli[49], A. Favareto[53a,53b], W.J. Fawcett[122], L. Fayard[119], O.L. Fedin[125,q], W. Fedorko[171], S. Feigl[121], L. Feligioni[88], C. Feng[36b], E.J. Feng[32], M. Feng[48], M.J. Fenton[56], A.B. Fenyuk[132], L. Feremenga[8], P. Fernandez Martinez[170], J. Ferrando[45], A. Ferrari[168], P. Ferrari[109], R. Ferrari[123a], D.E. Ferreira de Lima[60b], A. Ferrer[170], D. Ferrere[52], C. Ferretti[92], F. Fiedler[86], A. Filipčič[78], M. Filipuzzi[45], F. Filthaut[108], M. Fincke-Keeler[172], K.D. Finelli[24], M.C.N. Fiolhais[128a,128c,r], L. Fiorini[170], C. Fischer[13], J. Fischer[178], W.C. Fisher[93], N. Flaschel[45],

I. Fleck[143], P. Fleischmann[92], R.R.M. Fletcher[124], T. Flick[178], B.M. Flierl[102], L.R. Flores Castillo[62a], G.T. Forcolin[87], A. Formica[138], F.A. Förster[13], A. Forti[87], A.G. Foster[19], D. Fournier[119], H. Fox[75], S. Fracchia[141], P. Francavilla[126a,126b], M. Franchini[22a,22b], S. Franchino[60a], D. Francis[32], L. Franconi[121], M. Franklin[59], M. Frate[166], M. Fraternali[123a,123b], D. Freeborn[81], S.M. Fressard-Batraneanu[32], B. Freund[97], D. Froidevaux[32], J.A. Frost[122], C. Fukunaga[158], T. Fusayasu[104], J. Fuster[170], O. Gabizon[154], A. Gabrielli[22a,22b], A. Gabrielli[16], G.P. Gach[41a], S. Gadatsch[32], S. Gadomski[80], G. Gagliardi[53a,53b], L.G. Gagnon[97], C. Galea[108], B. Galhardo[128a,128c], E.J. Gallas[122], B.J. Gallop[133], P. Gallus[130], G. Galster[39], K.K. Gan[113], S. Ganguly[175], Y. Gao[77], Y.S. Gao[145,g], F.M. Garay Walls[34a], C. García[170], J.E. García Navarro[170], J.A. García Pascual[35a], M. Garcia-Sciveres[16], R.W. Gardner[33], N. Garelli[145], V. Garonne[121], A. Gascon Bravo[45], K. Gasnikova[45], C. Gatti[50], A. Gaudiello[53a,53b], G. Gaudio[123a], I.L. Gavrilenko[98], C. Gay[171], G. Gaycken[23], E.N. Gazis[10], C.N.P. Gee[133], J. Geisen[57], M. Geisen[86], M.P. Geisler[60a], K. Gellerstedt[148a,148b], C. Gemme[53a], M.H. Genest[58], C. Geng[92], S. Gentile[134a,134b], C. Gentsos[156], S. George[80], D. Gerbaudo[13], G. Geßner[46], S. Ghasemi[143], M. Ghneimat[23], B. Giacobbe[22a], S. Giagu[134a,134b], N. Giangiacomi[22a,22b], P. Giannetti[126a], S.M. Gibson[80], M. Gignac[171], M. Gilchriese[16], D. Gillberg[31], G. Gilles[178], D.M. Gingrich[3,d], M.P. Giordani[167a,167c], F.M. Giorgi[22a], P.F. Giraud[138], P. Giromini[59], G. Giugliarelli[167a,167c], D. Giugni[94a], F. Giuli[122], M. Giulini[60b], B.K. Gjelsten[121], S. Gkaitatzis[156], I. Gkialas[9,s], E.L. Gkougkousis[13], P. Gkountoumis[10], L.K. Gladilin[101], C. Glasman[85], J. Glatzer[13], P.C.F. Glaysher[45], A. Glazov[45], M. Goblirsch-Kolb[25], J. Godlewski[42], S. Goldfarb[91], T. Golling[52], D. Golubkov[132], A. Gomes[128a,128b,128d], R. Gonçalo[128a], R. Goncalves Gama[26a], J. Goncalves Pinto Firmino Da Costa[138], G. Gonella[51], L. Gonella[19], A. Gongadze[68], F. Gonnella[19], J.L. Gonski[59], S. González de la Hoz[170], S. Gonzalez-Sevilla[52], L. Goossens[32], P.A. Gorbounov[99], H.A. Gordon[27], B. Gorini[32], E. Gorini[76a,76b], A. Gorišek[78], A.T. Goshaw[48], C. Gössling[46], M.I. Gostkin[68], C.A. Gottardo[23], C.R. Goudet[119], D. Goujdami[137c], A.G. Goussiou[140], N. Govender[147b,t], E. Gozani[154], I. Grabowska-Bold[41a], P.O.J. Gradin[168], E.C. Graham[77], J. Gramling[166], E. Gramstad[121], S. Grancagnolo[17], V. Gratchev[125], P.M. Gravila[28f], C. Gray[56], H.M. Gray[16], Z.D. Greenwood[82,u], C. Grefe[23], K. Gregersen[81], I.M. Gregor[45], P. Grenier[145], K. Grevtsov[5], J. Griffiths[8], A.A. Grillo[139], K. Grimm[75], S. Grinstein[13,v], Ph. Gris[37], J.-F. Grivaz[119], S. Groh[86], E. Gross[175], J. Grosse-Knetter[57], G.C. Grossi[82], Z.J. Grout[81], A. Grummer[107], L. Guan[92], W. Guan[176], J. Guenther[32], F. Guescini[163a], D. Guest[166], O. Gueta[155], B. Gui[113], E. Guido[53a,53b], T. Guillemin[5], S. Guindon[32], U. Gul[56], C. Gumpert[32], J. Guo[36c], W. Guo[92], Y. Guo[36a,w], R. Gupta[43], S. Gurbuz[20a], G. Gustavino[115], B.J. Gutelman[154], P. Gutierrez[115], N.G. Gutierrez Ortiz[81], C. Gutschow[81], C. Guyot[138], M.P. Guzik[41a], C. Gwenlan[122], C.B. Gwilliam[77], A. Haas[112], C. Haber[16], H.K. Hadavand[8], N. Haddad[137e], A. Hadef[88], S. Hageböck[23], M. Hagihara[164], H. Hakobyan[180,*], M. Haleem[45], J. Haley[116], G. Halladjian[93], G.D. Hallewell[88], K. Hamacher[178], P. Hamal[117], K. Hamano[172], A. Hamilton[147a], G.N. Hamity[141], P.G. Hamnett[45], K. Han[36a,x], L. Han[36a], S. Han[35a,35d], K. Hanagaki[69,y], K. Hanawa[157], M. Hance[139], D.M. Handl[102], B. Haney[124], P. Hanke[60a], J.B. Hansen[39], J.D. Hansen[39], M.C. Hansen[23], P.H. Hansen[39], K. Hara[164], A.S. Hard[176], T. Harenberg[178], F. Hariri[119], S. Harkusha[95], P.F. Harrison[173], N.M. Hartmann[102], Y. Hasegawa[142], A. Hasib[49], S. Hassani[138], S. Haug[18], R. Hauser[93], L. Hauswald[47], L.B. Havener[38], M. Havranek[130], C.M. Hawkes[19], R.J. Hawkings[32], D. Hayden[93], C.P. Hays[122], J.M. Hays[79], H.S. Hayward[77], S.J. Haywood[133], T. Heck[86], V. Hedberg[84], L. Heelan[8], S. Heer[23], K.K. Heidegger[51], S. Heim[45], T. Heim[16], B. Heinemann[45,z], J.J. Heinrich[102], L. Heinrich[112], C. Heinz[55], J. Hejbal[129], L. Helary[32], A. Held[171], S. Hellman[148a,148b], C. Helsens[32], R.C.W. Henderson[75], Y. Heng[176], S. Henkelmann[171], A.M. Henriques Correia[32], S. Henrot-Versille[119], G.H. Herbert[17], H. Herde[25], V. Herget[177], Y. Hernández Jiménez[147c], H. Herr[86], G. Herten[51], R. Hertenberger[102],

L. Hervas[32], T.C. Herwig[124], G.G. Hesketh[81], N.P. Hessey[163a], J.W. Hetherly[43], S. Higashino[69], E. Higón-Rodriguez[170], K. Hildebrand[33], E. Hill[172], J.C. Hill[30], K.H. Hiller[45], S.J. Hillier[19], M. Hils[47], I. Hinchliffe[16], M. Hirose[51], D. Hirschbuehl[178], B. Hiti[78], O. Hladik[129], D.R. Hlaluku[147c], X. Hoad[49], J. Hobbs[150], N. Hod[163a], M.C. Hodgkinson[141], P. Hodgson[141], A. Hoecker[32], M.R. Hoeferkamp[107], F. Hoenig[102], D. Hohn[23], T.R. Holmes[33], M. Holzbock[102], M. Homann[46], S. Honda[164], T. Honda[69], T.M. Hong[127], B.H. Hooberman[169], W.H. Hopkins[118], Y. Horii[105], A.J. Horton[144], J-Y. Hostachy[58], A. Hostiuc[140], S. Hou[153], A. Hoummada[137a], J. Howarth[87], J. Hoya[74], M. Hrabovsky[117], J. Hrdinka[32], I. Hristova[17], J. Hrivnac[119], T. Hryn'ova[5], A. Hrynevich[96], P.J. Hsu[63], S.-C. Hsu[140], Q. Hu[27], S. Hu[36c], Y. Huang[35a], Z. Hubacek[130], F. Hubaut[88], F. Huegging[23], T.B. Huffman[122], E.W. Hughes[38], M. Huhtinen[32], R.F.H. Hunter[31], P. Huo[150], N. Huseynov[68,b], J. Huston[93], J. Huth[59], R. Hyneman[92], G. Iacobucci[52], G. Iakovidis[27], I. Ibragimov[143], L. Iconomidou-Fayard[119], Z. Idrissi[137e], P. Iengo[32], O. Igonkina[109,aa], T. Iizawa[174], Y. Ikegami[69], M. Ikeno[69], Y. Ilchenko[11,ab], D. Iliadis[156], N. Ilic[145], F. Iltzsche[47], G. Introzzi[123a,123b], P. Ioannou[9,*], M. Iodice[136a], K. Iordanidou[38], V. Ippolito[59], M.F. Isacson[168], N. Ishijima[120], M. Ishino[157], M. Ishitsuka[159], C. Issever[122], S. Istin[20a], F. Ito[164], J.M. Iturbe Ponce[62a], R. Iuppa[162a,162b], H. Iwasaki[69], J.M. Izen[44], V. Izzo[106a], S. Jabbar[3], P. Jackson[1], R.M. Jacobs[23], V. Jain[2], K.B. Jakobi[86], K. Jakobs[51], S. Jakobsen[65], T. Jakoubek[129], D.O. Jamin[116], D.K. Jana[82], R. Jansky[52], J. Janssen[23], M. Janus[57], P.A. Janus[41a], G. Jarlskog[84], N. Javadov[68,b], T. Javůrek[51], M. Javurkova[51], F. Jeanneau[138], L. Jeanty[16], J. Jejelava[54a,ac], A. Jelinskas[173], P. Jenni[51,ad], C. Jeske[173], S. Jézéquel[5], H. Ji[176], J. Jia[150], H. Jiang[67], Y. Jiang[36a], Z. Jiang[145], S. Jiggins[81], J. Jimenez Pena[170], S. Jin[35b], A. Jinaru[28b], O. Jinnouchi[159], H. Jivan[147c], P. Johansson[141], K.A. Johns[7], C.A. Johnson[64], W.J. Johnson[140], K. Jon-And[148a,148b], R.W.L. Jones[75], S.D. Jones[151], S. Jones[7], T.J. Jones[77], J. Jongmanns[60a], P.M. Jorge[128a,128b], J. Jovicevic[163a], X. Ju[176], A. Juste Rozas[13,v], M.K. Köhler[175], A. Kaczmarska[42], M. Kado[119], H. Kagan[113], M. Kagan[145], S.J. Kahn[88], T. Kaji[174], E. Kajomovitz[154], C.W. Kalderon[84], A. Kaluza[86], S. Kama[43], A. Kamenshchikov[132], N. Kanaya[157], L. Kanjir[78], V.A. Kantserov[100], J. Kanzaki[69], B. Kaplan[112], L.S. Kaplan[176], D. Kar[147c], K. Karakostas[10], N. Karastathis[10], M.J. Kareem[163b], E. Karentzos[10], S.N. Karpov[68], Z.M. Karpova[68], V. Kartvelishvili[75], A.N. Karyukhin[132], K. Kasahara[164], L. Kashif[176], R.D. Kass[113], A. Kastanas[149], Y. Kataoka[157], C. Kato[157], A. Katre[52], J. Katzy[45], K. Kawade[70], K. Kawagoe[73], T. Kawamoto[157], G. Kawamura[57], E.F. Kay[77], V.F. Kazanin[111,c], R. Keeler[172], R. Kehoe[43], J.S. Keller[31], E. Kellermann[84], J.J. Kempster[80], J Kendrick[19], H. Keoshkerian[161], O. Kepka[129], B.P. Kerševan[78], S. Kersten[178], R.A. Keyes[90], M. Khader[169], F. Khalil-zada[12], A. Khanov[116], A.G. Kharlamov[111,c], T. Kharlamova[111,c], A. Khodinov[160], T.J. Khoo[52], V. Khovanskiy[99,*], E. Khramov[68], J. Khubua[54b,ae], S. Kido[70], M. Kiehn[52], C.R. Kilby[80], H.Y. Kim[8], S.H. Kim[164], Y.K. Kim[33], N. Kimura[156], O.M. Kind[17], B.T. King[77], D. Kirchmeier[47], J. Kirk[133], A.E. Kiryunin[103], T. Kishimoto[157], D. Kisielewska[41a], V. Kitali[45], O. Kivernyk[5], E. Kladiva[146b], T. Klapdor-Kleingrothaus[51], M.H. Klein[92], M. Klein[77], U. Klein[77], K. Kleinknecht[86], P. Klimek[110], A. Klimentov[27], R. Klingenberg[46,*], T. Klingl[23], T. Klioutchnikova[32], F.F. Klitzner[102], E.-E. Kluge[60a], P. Kluit[109], S. Kluth[103], E. Kneringer[65], E.B.F.G. Knoops[88], A. Knue[51], A. Kobayashi[157], D. Kobayashi[73], T. Kobayashi[157], M. Kobel[47], M. Kocian[145], P. Kodys[131], T. Koffas[31], E. Koffeman[109], N.M. Köhler[103], T. Koi[145], M. Kolb[60b], I. Koletsou[5], T. Kondo[69], N. Kondrashova[36c], K. Köneke[51], A.C. König[108], T. Kono[69,af], R. Konoplich[112,ag], N. Konstantinidis[81], B. Konya[84], R. Kopeliansky[64], S. Koperny[41a], K. Korcyl[42], K. Kordas[156], A. Korn[81], I. Korolkov[13], E.V. Korolkova[141], O. Kortner[103], S. Kortner[103], T. Kosek[131], V.V. Kostyukhin[23], A. Kotwal[48], A. Koulouris[10], A. Kourkoumeli-Charalampidi[123a,123b], C. Kourkoumelis[9], E. Kourlitis[141], V. Kouskoura[27], A.B. Kowalewska[42], R. Kowalewski[172], T.Z. Kowalski[41a], C. Kozakai[157],

W. Kozanecki[138], A.S. Kozhin[132], V.A. Kramarenko[101], G. Kramberger[78], D. Krasnopevtsev[100], M.W. Krasny[83], A. Krasznahorkay[32], D. Krauss[103], J.A. Kremer[41a], J. Kretzschmar[77], K. Kreutzfeldt[55], P. Krieger[161], K. Krizka[16], K. Kroeninger[46], H. Kroha[103], J. Kroll[129], J. Kroll[124], J. Kroseberg[23], J. Krstic[14], U. Kruchonak[68], H. Krüger[23], N. Krumnack[67], M.C. Kruse[48], T. Kubota[91], H. Kucuk[81], S. Kuday[4b], J.T. Kuechler[178], S. Kuehn[32], A. Kugel[60a], F. Kuger[177], T. Kuhl[45], V. Kukhtin[68], R. Kukla[88], Y. Kulchitsky[95], S. Kuleshov[34b], Y.P. Kulinich[169], M. Kuna[11], T. Kunigo[71], A. Kupco[129], T. Kupfer[46], O. Kuprash[155], H. Kurashige[70], L.L. Kurchaninov[163a], Y.A. Kurochkin[95], M.G. Kurth[35a,35d], E.S. Kuwertz[172], M. Kuze[159], J. Kvita[117], T. Kwan[172], D. Kyriazopoulos[141], A. La Rosa[103], J.L. La Rosa Navarro[26d], L. La Rotonda[40a,40b], F. La Ruffa[40a,40b], C. Lacasta[170], F. Lacava[134a,134b], J. Lacey[45], D.P.J. Lack[87], H. Lacker[17], D. Lacour[83], E. Ladygin[68], R. Lafaye[5], B. Laforge[83], S. Lai[57], S. Lammers[64], W. Lampl[7], E. Lançon[27], U. Landgraf[51], M.P.J. Landon[79], M.C. Lanfermann[52], V.S. Lang[45], J.C. Lange[13], R.J. Langenberg[32], A.J. Lankford[166], F. Lanni[27], K. Lantzsch[23], A. Lanza[123a], A. Lapertosa[53a,53b], S. Laplace[83], J.F. Laporte[138], T. Lari[94a], F. Lasagni Manghi[22a,22b], M. Lassnig[32], T.S. Lau[62a], P. Laurelli[50], W. Lavrijsen[16], A.T. Law[139], P. Laycock[77], T. Lazovich[59], M. Lazzaroni[94a,94b], B. Le[91], O. Le Dortz[83], E. Le Guirriec[88], E.P. Le Quilleuc[138], M. LeBlanc[7], T. LeCompte[6], F. Ledroit-Guillon[58], C.A. Lee[27], G.R. Lee[34a], S.C. Lee[153], L. Lee[59], B. Lefebvre[90], G. Lefebvre[83], M. Lefebvre[172], F. Legger[102], C. Leggett[16], G. Lehmann Miotto[32], X. Lei[7], W.A. Leight[45], M.A.L. Leite[26d], R. Leitner[131], D. Lellouch[175], B. Lemmer[57], K.J.C. Leney[81], T. Lenz[23], B. Lenzi[32], R. Leone[7], S. Leone[126a], C. Leonidopoulos[49], G. Lerner[151], C. Leroy[97], R. Les[161], A.A.J. Lesage[138], C.G. Lester[30], M. Levchenko[125], J. Levêque[5], D. Levin[92], L.J. Levinson[175], M. Levy[19], D. Lewis[79], B. Li[36a,w], H. Li[150], L. Li[36c], Q. Li[35a,35d], Q. Li[36a], S. Li[48], X. Li[36c], Y. Li[143], Z. Liang[35a], B. Liberti[135a], A. Liblong[161], K. Lie[62c], A. Limosani[152], C.Y. Lin[30], K. Lin[93], S.C. Lin[182], T.H. Lin[86], R.A. Linck[64], B.E. Lindquist[150], A.E. Lionti[52], E. Lipeles[124], A. Lipniacka[15], M. Lisovyi[60b], T.M. Liss[169,ah], A. Lister[171], A.M. Litke[139], B. Liu[67], H. Liu[92], H. Liu[27], J.K.K. Liu[122], J. Liu[36b], J.B. Liu[36a], K. Liu[88], L. Liu[169], M. Liu[36a], Y.L. Liu[36a], Y. Liu[36a], M. Livan[123a,123b], A. Lleres[58], J. Llorente Merino[35a], S.L. Lloyd[79], C.Y. Lo[62b], F. Lo Sterzo[43], E.M. Lobodzinska[45], P. Loch[7], F.K. Loebinger[87], A. Loesle[51], K.M. Loew[25], T. Lohse[17], K. Lohwasser[141], M. Lokajicek[129], B.A. Long[24], J.D. Long[169], R.E. Long[75], L. Longo[76a,76b], K.A. Looper[113], J.A. Lopez[34b], I. Lopez Paz[13], A. Lopez Solis[83], J. Lorenz[102], N. Lorenzo Martinez[5], M. Losada[21], P.J. Lösel[102], X. Lou[35a], A. Lounis[119], J. Love[6], P.A. Love[75], H. Lu[62a], N. Lu[92], Y.J. Lu[63], H.J. Lubatti[140], C. Luci[134a,134b], A. Lucotte[58], C. Luedtke[51], F. Luehring[64], W. Lukas[65], L. Luminari[134a], B. Lund-Jensen[149], M.S. Lutz[89], P.M. Luzi[83], D. Lynn[27], R. Lysak[129], E. Lytken[84], F. Lyu[35a], V. Lyubushkin[68], H. Ma[27], L.L. Ma[36b], Y. Ma[36b], G. Maccarrone[50], A. Macchiolo[103], C.M. Macdonald[141], B. Maček[78], J. Machado Miguens[124,128b], D. Madaffari[170], R. Madar[37], W.F. Mader[47], A. Madsen[45], N. Madysa[47], J. Maeda[70], S. Maeland[15], T. Maeno[27], A.S. Maevskiy[101], V. Magerl[51], C. Maiani[119], C. Maidantchik[26a], T. Maier[102], A. Maio[128a,128b,128d], O. Majersky[146a], S. Majewski[118], Y. Makida[69], N. Makovec[119], B. Malaescu[83], Pa. Malecki[42], V.P. Maleev[125], F. Malek[58], U. Mallik[66], D. Malon[6], C. Malone[30], S. Maltezos[10], S. Malyukov[32], J. Mamuzic[170], G. Mancini[50], I. Mandić[78], J. Maneira[128a,128b], L. Manhaes de Andrade Filho[26b], J. Manjarres Ramos[47], K.H. Mankinen[84], A. Mann[102], A. Manousos[32], B. Mansoulie[138], J.D. Mansour[35a], R. Mantifel[90], M. Mantoani[57], S. Manzoni[94a,94b], L. Mapelli[32], G. Marceca[29], L. March[52], L. Marchese[122], G. Marchiori[83], M. Marcisovsky[129], C.A. Marin Tobon[32], M. Marjanovic[37], D.E. Marley[92], F. Marroquim[26a], S.P. Marsden[87], Z. Marshall[16], M.U.F Martensson[168], S. Marti-Garcia[170], C.B. Martin[113], T.A. Martin[173], V.J. Martin[49], B. Martin dit Latour[15], M. Martinez[13,v], V.I. Martinez Outschoorn[169], S. Martin-Haugh[133], V.S. Martoiu[28b], A.C. Martyniuk[81],

A. Marzin[32], L. Masetti[86], T. Mashimo[157], R. Mashinistov[98], J. Masik[87], A.L. Maslennikov[111,c], L.H. Mason[91], L. Massa[135a,135b], P. Mastrandrea[5], A. Mastroberardino[40a,40b], T. Masubuchi[157], P. Mättig[178], J. Maurer[28b], S.J. Maxfield[77], D.A. Maximov[111,c], R. Mazini[153], I. Maznas[156], S.M. Mazza[94a,94b], N.C. Mc Fadden[107], G. Mc Goldrick[161], S.P. Mc Kee[92], A. McCarn[92], R.L. McCarthy[150], T.G. McCarthy[103], L.I. McClymont[81], E.F. McDonald[91], J.A. Mcfayden[32], G. Mchedlidze[57], S.J. McMahon[133], P.C. McNamara[91], C.J. McNicol[173], R.A. McPherson[172,o], S. Meehan[140], T.J. Megy[51], S. Mehlhase[102], A. Mehta[77], T. Meideck[58], K. Meier[60a], B. Meirose[44], D. Melini[170,ai], B.R. Mellado Garcia[147c], J.D. Mellenthin[57], M. Melo[146a], F. Meloni[18], A. Melzer[23], S.B. Menary[87], L. Meng[77], X.T. Meng[92], A. Mengarelli[22a,22b], S. Menke[103], E. Meoni[40a,40b], S. Mergelmeyer[17], C. Merlassino[18], P. Mermod[52], L. Merola[106a,106b], C. Meroni[94a], F.S. Merritt[33], A. Messina[134a,134b], J. Metcalfe[6], A.S. Mete[166], C. Meyer[124], J-P. Meyer[138], J. Meyer[109], H. Meyer Zu Theenhausen[60a], F. Miano[151], R.P. Middleton[133], S. Miglioranzi[53a,53b], L. Mijović[49], G. Mikenberg[175], M. Mikestikova[129], M. Mikuž[78], M. Milesi[91], A. Milic[161], D.A. Millar[79], D.W. Miller[33], C. Mills[49], A. Milov[175], D.A. Milstead[148a,148b], A.A. Minaenko[132], Y. Minami[157], I.A. Minashvili[54b], A.I. Mincer[112], B. Mindur[41a], M. Mineev[68], Y. Minegishi[157], Y. Ming[176], L.M. Mir[13], A. Mirto[76a,76b], K.P. Mistry[124], T. Mitani[174], J. Mitrevski[102], V.A. Mitsou[170], A. Miucci[18], P.S. Miyagawa[141], A. Mizukami[69], J.U. Mjörnmark[84], T. Mkrtchyan[180], M. Mlynarikova[131], T. Moa[148a,148b], K. Mochizuki[97], P. Mogg[51], S. Mohapatra[38], S. Molander[148a,148b], R. Moles-Valls[23], M.C. Mondragon[93], K. Mönig[45], J. Monk[39], E. Monnier[88], A. Montalbano[150], J. Montejo Berlingen[32], F. Monticelli[74], S. Monzani[94a], R.W. Moore[3], N. Morange[119], D. Moreno[21], M. Moreno Llácer[32], P. Morettini[53a], M. Morgenstern[109], S. Morgenstern[32], D. Mori[144], T. Mori[157], M. Morii[59], M. Morinaga[174], V. Morisbak[121], A.K. Morley[32], G. Mornacchi[32], J.D. Morris[79], L. Morvaj[150], P. Moschovakos[10], M. Mosidze[54b], H.J. Moss[141], J. Moss[145,aj], K. Motohashi[159], R. Mount[145], E. Mountricha[27], E.J.W. Moyse[89], S. Muanza[88], F. Mueller[103], J. Mueller[127], R.S.P. Mueller[102], D. Muenstermann[75], P. Mullen[56], G.A. Mullier[18], F.J. Munoz Sanchez[87], W.J. Murray[173,133], H. Musheghyan[32], M. Muškinja[78], C. Mwewa[147a], A.G. Myagkov[132,ak], M. Myska[130], B.P. Nachman[16], O. Nackenhorst[46], K. Nagai[122], R. Nagai[69,af], K. Nagano[69], Y. Nagasaka[61], K. Nagata[164], M. Nagel[51], E. Nagy[88], A.M. Nairz[32], Y. Nakahama[105], K. Nakamura[69], T. Nakamura[157], I. Nakano[114], R.F. Naranjo Garcia[45], R. Narayan[11], D.I. Narrias Villar[60a], I. Naryshkin[125], T. Naumann[45], G. Navarro[21], R. Nayyar[7], H.A. Neal[92], P.Yu. Nechaeva[98], T.J. Neep[138], A. Negri[123a,123b], M. Negrini[22a], S. Nektarijevic[108], C. Nellist[57], A. Nelson[166], M.E. Nelson[122], S. Nemecek[129], P. Nemethy[112], M. Nessi[32,al], M.S. Neubauer[169], M. Neumann[178], P.R. Newman[19], T.Y. Ng[62c], Y.S. Ng[17], T. Nguyen Manh[97], R.B. Nickerson[122], R. Nicolaidou[138], J. Nielsen[139], N. Nikiforou[11], V. Nikolaenko[132,ak], I. Nikolic-Audit[83], K. Nikolopoulos[19], P. Nilsson[27], Y. Ninomiya[69], A. Nisati[134a], N. Nishu[36c], R. Nisius[103], I. Nitsche[46], T. Nitta[174], T. Nobe[157], Y. Noguchi[71], M. Nomachi[120], I. Nomidis[31], M.A. Nomura[27], T. Nooney[79], M. Nordberg[32], N. Norjoharuddeen[122], O. Novgorodova[47], M. Nozaki[69], L. Nozka[117], K. Ntekas[166], E. Nurse[81], F. Nuti[91], K. O'connor[25], D.C. O'Neil[144], A.A. O'Rourke[45], V. O'Shea[56], F.G. Oakham[31,d], H. Oberlack[103], T. Obermann[23], J. Ocariz[83], A. Ochi[70], I. Ochoa[38], J.P. Ochoa-Ricoux[34a], S. Oda[73], S. Odaka[69], A. Oh[87], S.H. Oh[48], C.C. Ohm[149], H. Ohman[168], H. Oide[53a,53b], H. Okawa[164], Y. Okumura[157], T. Okuyama[69], A. Olariu[28b], L.F. Oleiro Seabra[128a], S.A. Olivares Pino[34a], D. Oliveira Damazio[27], M.J.R. Olsson[33], A. Olszewski[42], J. Olszowska[42], A. Onofre[128a,128e], K. Onogi[105], P.U.E. Onyisi[11,ab], H. Oppen[121], M.J. Oreglia[33], Y. Oren[155], D. Orestano[136a,136b], E.C. Orgill[87], N. Orlando[62b], R.S. Orr[161], B. Osculati[53a,53b,*], R. Ospanov[36a], G. Otero y Garzon[29], H. Otono[73], M. Ouchrif[137d], F. Ould-Saada[121], A. Ouraou[138], K.P. Oussoren[109],

Q. Ouyang[35a], M. Owen[56], R.E. Owen[19], V.E. Ozcan[20a], N. Ozturk[8], K. Pachal[144], A. Pacheco Pages[13], L. Pacheco Rodriguez[138], C. Padilla Aranda[13], S. Pagan Griso[16], M. Paganini[179], F. Paige[27], G. Palacino[64], S. Palazzo[40a,40b], S. Palestini[32], M. Palka[41b], D. Pallin[37], E.St. Panagiotopoulou[10], I. Panagoulias[10], C.E. Pandini[52], J.G. Panduro Vazquez[80], P. Pani[32], S. Panitkin[27], D. Pantea[28b], L. Paolozzi[52], Th.D. Papadopoulou[10], K. Papageorgiou[9,s], A. Paramonov[6], D. Paredes Hernandez[179], A.J. Parker[75], M.A. Parker[30], K.A. Parker[45], F. Parodi[53a,53b], J.A. Parsons[38], U. Parzefall[51], V.R. Pascuzzi[161], J.M. Pasner[139], E. Pasqualucci[134a], S. Passaggio[53a], Fr. Pastore[80], S. Pataraia[86], J.R. Pater[87], T. Pauly[32], B. Pearson[103], S. Pedraza Lopez[170], R. Pedro[128a,128b], S.V. Peleganchuk[111,c], O. Penc[129], C. Peng[35a,35d], H. Peng[36a], J. Penwell[64], B.S. Peralva[26b], M.M. Perego[138], D.V. Perepelitsa[27], F. Peri[17], L. Perini[94a,94b], H. Pernegger[32], S. Perrella[106a,106b], R. Peschke[45], V.D. Peshekhonov[68,*], K. Peters[45], R.F.Y. Peters[87], B.A. Petersen[32], T.C. Petersen[39], E. Petit[58], A. Petridis[1], C. Petridou[156], P. Petroff[119], E. Petrolo[134a], M. Petrov[122], F. Petrucci[136a,136b], N.E. Pettersson[89], A. Peyaud[138], R. Pezoa[34b], F.H. Phillips[93], P.W. Phillips[133], G. Piacquadio[150], E. Pianori[173], A. Picazio[89], M.A. Pickering[122], R. Piegaia[29], J.E. Pilcher[33], A.D. Pilkington[87], M. Pinamonti[135a,135b], J.L. Pinfold[3], H. Pirumov[45], M. Pitt[175], L. Plazak[146a], M.-A. Pleier[27], V. Pleskot[86], E. Plotnikova[68], D. Pluth[67], P. Podberezko[111], R. Poettgen[84], R. Poggi[123a,123b], L. Poggioli[119], I. Pogrebnyak[93], D. Pohl[23], I. Pokharel[57], G. Polesello[123a], A. Poley[45], A. Policicchio[40a,40b], R. Polifka[32], A. Polini[22a], C.S. Pollard[56], V. Polychronakos[27], K. Pommès[32], D. Ponomarenko[100], L. Pontecorvo[134a], G.A. Popeneciu[28d], D.M. Portillo Quintero[83], S. Pospisil[130], K. Potamianos[45], I.N. Potrap[68], C.J. Potter[30], H. Potti[11], T. Poulsen[84], J. Poveda[32], M.E. Pozo Astigarraga[32], P. Pralavorio[88], A. Pranko[16], S. Prell[67], D. Price[87], M. Primavera[76a], S. Prince[90], N. Proklova[100], K. Prokofiev[62c], F. Prokoshin[34b], S. Protopopescu[27], J. Proudfoot[6], M. Przybycien[41a], A. Puri[169], P. Puzo[119], J. Qian[92], Y. Qin[87], A. Quadt[57], M. Queitsch-Maitland[45], D. Quilty[56], S. Raddum[121], V. Radeka[27], V. Radescu[122], S.K. Radhakrishnan[150], P. Radloff[118], P. Rados[91], F. Ragusa[94a,94b], G. Rahal[181], J.A. Raine[87], S. Rajagopalan[27], T. Rashid[119], S. Raspopov[5], M.G. Ratti[94a,94b], D.M. Rauch[45], F. Rauscher[102], S. Rave[86], I. Ravinovich[175], J.H. Rawling[87], M. Raymond[32], A.L. Read[121], N.P. Readioff[58], M. Reale[76a,76b], D.M. Rebuzzi[123a,123b], A. Redelbach[177], G. Redlinger[27], R. Reece[139], R.G. Reed[147c], K. Reeves[44], L. Rehnisch[17], J. Reichert[124], A. Reiss[86], C. Rembser[32], H. Ren[35a,35d], M. Rescigno[134a], S. Resconi[94a], E.D. Resseguie[124], S. Rettie[171], E. Reynolds[19], O.L. Rezanova[111,c], P. Reznicek[131], R. Rezvani[97], R. Richter[103], S. Richter[81], E. Richter-Was[41b], O. Ricken[23], M. Ridel[83], P. Rieck[103], C.J. Riegel[178], J. Rieger[57], O. Rifki[115], M. Rijssenbeek[150], A. Rimoldi[123a,123b], M. Rimoldi[18], L. Rinaldi[22a], G. Ripellino[149], B. Ristić[32], E. Ritsch[32], I. Riu[13], F. Rizatdinova[116], E. Rizvi[79], C. Rizzi[13], R.T. Roberts[87], S.H. Robertson[90,o], A. Robichaud-Veronneau[90], D. Robinson[30], J.E.M. Robinson[45], A. Robson[56], E. Rocco[86], C. Roda[126a,126b], Y. Rodina[88,am], S. Rodriguez Bosca[170], A. Rodriguez Perez[13], D. Rodriguez Rodriguez[170], S. Roe[32], C.S. Rogan[59], O. Røhne[121], J. Roloff[59], A. Romaniouk[100], M. Romano[22a,22b], S.M. Romano Saez[37], E. Romero Adam[170], N. Rompotis[77], M. Ronzani[51], L. Roos[83], S. Rosati[134a], K. Rosbach[51], P. Rose[139], N.-A. Rosien[57], E. Rossi[106a,106b], L.P. Rossi[53a], J.H.N. Rosten[30], R. Rosten[140], M. Rotaru[28b], J. Rothberg[140], D. Rousseau[119], D. Roy[147c], A. Rozanov[88], Y. Rozen[154], X. Ruan[147c], F. Rubbo[145], F. Rühr[51], A. Ruiz-Martinez[31], Z. Rurikova[51], N.A. Rusakovich[68], H.L. Russell[90], J.P. Rutherfoord[7], N. Ruthmann[32], E.M. Rüttinger[45], Y.F. Ryabov[125], M. Rybar[169], G. Rybkin[119], S. Ryu[6], A. Ryzhov[132], G.F. Rzehorz[57], A.F. Saavedra[152], G. Sabato[109], S. Sacerdoti[29], H.F-W. Sadrozinski[139], R. Sadykov[68], F. Safai Tehrani[134a], P. Saha[110], M. Sahinsoy[60a], M. Saimpert[45], M. Saito[157], T. Saito[157], H. Sakamoto[157], Y. Sakurai[174], G. Salamanna[136a,136b], J.E. Salazar Loyola[34b], D. Salek[109], P.H. Sales De Bruin[168], D. Salihagic[103], A. Salnikov[145], J. Salt[170], D. Salvatore[40a,40b],

F. Salvatore[151], A. Salvucci[62a,62b,62c], A. Salzburger[32], D. Sammel[51], D. Sampsonidis[156], D. Sampsonidou[156], J. Sánchez[170], A. Sanchez Pineda[167a,167c], H. Sandaker[121], R.L. Sandbach[79], C.O. Sander[45], M. Sandhoff[178], C. Sandoval[21], D.P.C. Sankey[133], M. Sannino[53a,53b], Y. Sano[105], A. Sansoni[50], C. Santoni[37], H. Santos[128a], I. Santoyo Castillo[151], A. Sapronov[68], J.G. Saraiva[128a,128d], O. Sasaki[69], K. Sato[164], E. Sauvan[5], G. Savage[80], P. Savard[161,d], N. Savic[103], C. Sawyer[133], L. Sawyer[82,u], C. Sbarra[22a], A. Sbrizzi[22a,22b], T. Scanlon[81], D.A. Scannicchio[166], J. Schaarschmidt[140], P. Schacht[103], B.M. Schachtner[102], D. Schaefer[33], L. Schaefer[124], J. Schaeffer[86], S. Schaepe[32], U. Schäfer[86], A.C. Schaffer[119], D. Schaile[102], R.D. Schamberger[150], V.A. Schegelsky[125], D. Scheirich[131], F. Schenck[17], M. Schernau[166], C. Schiavi[53a,53b], S. Schier[139], L.K. Schildgen[23], C. Schillo[51], M. Schioppa[40a,40b], S. Schlenker[32], K.R. Schmidt-Sommerfeld[103], K. Schmieden[32], C. Schmitt[86], S. Schmitt[45], S. Schmitz[86], U. Schnoor[51], L. Schoeffel[138], A. Schoening[60b], B.D. Schoenrock[93], E. Schopf[23], M. Schott[86], J.F.P. Schouwenberg[108], J. Schovancova[32], S. Schramm[52], N. Schuh[86], A. Schulte[86], M.J. Schultens[23], H.-C. Schultz-Coulon[60a], M. Schumacher[51], B.A. Schumm[139], Ph. Schune[138], A. Schwartzman[145], T.A. Schwarz[92], H. Schweiger[87], Ph. Schwemling[138], R. Schwienhorst[93], J. Schwindling[138], A. Sciandra[23], G. Sciolla[25], M. Scornajenghi[40a,40b], F. Scuri[126a], F. Scutti[91], J. Searcy[92], P. Seema[23], S.C. Seidel[107], A. Seiden[139], J.M. Seixas[26a], G. Sekhniaidze[106a], K. Sekhon[92], S.J. Sekula[43], N. Semprini-Cesari[22a,22b], S. Senkin[37], C. Serfon[121], L. Serin[119], L. Serkin[167a,167b], M. Sessa[136a,136b], R. Seuster[172], H. Severini[115], T. Šfiligoj[78], F. Sforza[165], A. Sfyrla[52], E. Shabalina[57], N.W. Shaikh[148a,148b], L.Y. Shan[35a], R. Shang[169], J.T. Shank[24], M. Shapiro[16], P.B. Shatalov[99], K. Shaw[167a,167b], S.M. Shaw[87], A. Shcherbakova[148a,148b], C.Y. Shehu[151], Y. Shen[115], N. Sherafati[31], A.D. Sherman[24], P. Sherwood[81], L. Shi[153,an], S. Shimizu[70], C.O. Shimmin[179], M. Shimojima[104], I.P.J. Shipsey[122], S. Shirabe[73], M. Shiyakova[68,ao], J. Shlomi[175], A. Shmeleva[98], D. Shoaleh Saadi[97], M.J. Shochet[33], S. Shojaii[94a,94b], D.R. Shope[115], S. Shrestha[113], E. Shulga[100], M.A. Shupe[7], P. Sicho[129], A.M. Sickles[169], P.E. Sidebo[149], E. Sideras Haddad[147c], O. Sidiropoulou[177], A. Sidoti[22a,22b], F. Siegert[47], Dj. Sijacki[14], J. Silva[128a,128d], S.B. Silverstein[148a], V. Simak[130], L. Simic[68], S. Simion[119], E. Simioni[86], B. Simmons[81], M. Simon[86], P. Sinervo[161], N.B. Sinev[118], M. Sioli[22a,22b], G. Siragusa[177], I. Siral[92], S.Yu. Sivoklokov[101], J. Sjölin[148a,148b], M.B. Skinner[75], P. Skubic[115], M. Slater[19], T. Slavicek[130], M. Slawinska[42], K. Sliwa[165], R. Slovak[131], V. Smakhtin[175], B.H. Smart[5], J. Smiesko[146a], N. Smirnov[100], S.Yu. Smirnov[100], Y. Smirnov[100], L.N. Smirnova[101,ap], O. Smirnova[84], J.W. Smith[57], M.N.K. Smith[38], R.W. Smith[38], M. Smizanska[75], K. Smolek[130], A.A. Snesarev[98], I.M. Snyder[118], S. Snyder[27], R. Sobie[172,o], F. Socher[47], A. Soffer[155], A. Søgaard[49], D.A. Soh[153], G. Sokhrannyi[78], C.A. Solans Sanchez[32], M. Solar[130], E.Yu. Soldatov[100], U. Soldevila[170], A.A. Solodkov[132], A. Soloshenko[68], O.V. Solovyanov[132], V. Solovyev[125], P. Sommer[141], H. Son[165], A. Sopczak[130], D. Sosa[60b], C.L. Sotiropoulou[126a,126b], S. Sottocornola[123a,123b], R. Soualah[167a,167c], A.M. Soukharev[111,c], D. South[45], B.C. Sowden[80], S. Spagnolo[76a,76b], M. Spalla[126a,126b], M. Spangenberg[173], F. Spanò[80], D. Sperlich[17], F. Spettel[103], T.M. Spieker[60a], R. Spighi[22a], G. Spigo[32], L.A. Spiller[91], M. Spousta[131], R.D. St. Denis[56,*], A. Stabile[94a,94b], R. Stamen[60a], S. Stamm[17], E. Stanecka[42], R.W. Stanek[6], C. Stanescu[136a], M.M. Stanitzki[45], B.S. Stapf[109], S. Stapnes[121], E.A. Starchenko[132], G.H. Stark[33], J. Stark[58], S.H Stark[39], P. Staroba[129], P. Starovoitov[60a], S. Stärz[32], R. Staszewski[42], M. Stegler[45], P. Steinberg[27], B. Stelzer[144], H.J. Stelzer[32], O. Stelzer-Chilton[163a], H. Stenzel[55], T.J. Stevenson[79], G.A. Stewart[56], M.C. Stockton[118], M. Stoebe[90], G. Stoicea[28b], P. Stolte[57], S. Stonjek[103], A.R. Stradling[8], A. Straessner[47], M.E. Stramaglia[18], J. Strandberg[149], S. Strandberg[148a,148b], M. Strauss[115], P. Strizenec[146b], R. Ströhmer[177], D.M. Strom[118], R. Stroynowski[43], A. Strubig[49], S.A. Stucci[27], B. Stugu[15], N.A. Styles[45], D. Su[145], J. Su[127], S. Suchek[60a], Y. Sugaya[120],

M. Suk[130], V.V. Sulin[98], DMS Sultan[162a,162b], S. Sultansoy[4c], T. Sumida[71], S. Sun[59], X. Sun[3], K. Suruliz[151], C.J.E. Suster[152], M.R. Sutton[151], S. Suzuki[69], M. Svatos[129], M. Swiatlowski[33], S.P. Swift[2], I. Sykora[146a], T. Sykora[131], D. Ta[51], K. Tackmann[45], J. Taenzer[155], A. Taffard[166], R. Tafirout[163a], E. Tahirovic[79], N. Taiblum[155], H. Takai[27], R. Takashima[72], E.H. Takasugi[103], K. Takeda[70], T. Takeshita[142], Y. Takubo[69], M. Talby[88], A.A. Talyshev[111,c], J. Tanaka[157], M. Tanaka[159], R. Tanaka[119], R. Tanioka[70], B.B. Tannenwald[113], S. Tapia Araya[34b], S. Tapprogge[86], S. Tarem[154], G.F. Tartarelli[94a], P. Tas[131], M. Tasevsky[129], T. Tashiro[71], E. Tassi[40a,40b], A. Tavares Delgado[128a,128b], Y. Tayalati[137e], A.C. Taylor[107], A.J. Taylor[49], G.N. Taylor[91], P.T.E. Taylor[91], W. Taylor[163b], P. Teixeira-Dias[80], D. Temple[144], H. Ten Kate[32], P.K. Teng[153], J.J. Teoh[120], F. Tepel[178], S. Terada[69], K. Terashi[157], J. Terron[85], S. Terzo[13], M. Testa[50], R.J. Teuscher[161,o], S.J. Thais[179], T. Theveneaux-Pelzer[88], F. Thiele[39], J.P. Thomas[19], J. Thomas-Wilsker[80], P.D. Thompson[19], A.S. Thompson[56], L.A. Thomsen[179], E. Thomson[124], Y. Tian[38], M.J. Tibbetts[16], R.E. Ticse Torres[57], V.O. Tikhomirov[98,aq], Yu.A. Tikhonov[111,c], S. Timoshenko[100], P. Tipton[179], S. Tisserant[88], K. Todome[159], S. Todorova-Nova[5], S. Todt[47], J. Tojo[73], S. Tokár[146a], K. Tokushuku[69], E. Tolley[113], L. Tomlinson[87], M. Tomoto[105], L. Tompkins[145,ar], K. Toms[107], B. Tong[59], P. Tornambe[51], E. Torrence[118], H. Torres[47], E. Torró Pastor[140], J. Toth[88,as], F. Touchard[88], D.R. Tovey[141], C.J. Treado[112], T. Trefzger[177], F. Tresoldi[151], A. Tricoli[27], I.M. Trigger[163a], S. Trincaz-Duvoid[83], M.F. Tripiana[13], W. Trischuk[161], B. Trocmé[58], A. Trofymov[45], C. Troncon[94a], M. Trovatelli[172], L. Truong[147b], M. Trzebinski[42], A. Trzupek[42], K.W. Tsang[62a], J.C-L. Tseng[122], P.V. Tsiareshka[95], N. Tsirintanis[9], S. Tsiskaridze[13], V. Tsiskaridze[51], E.G. Tskhadadze[54a], I.I. Tsukerman[99], V. Tsulaia[16], S. Tsuno[69], D. Tsybychev[150], Y. Tu[62b], A. Tudorache[28b], V. Tudorache[28b], T.T. Tulbure[28a], A.N. Tuna[59], S. Turchikhin[68], D. Turgeman[175], I. Turk Cakir[4b,at], R. Turra[94a], P.M. Tuts[38], G. Ucchielli[22a,22b], I. Ueda[69], M. Ughetto[148a,148b], F. Ukegawa[164], G. Unal[32], A. Undrus[27], G. Unel[166], F.C. Ungaro[91], Y. Unno[69], K. Uno[157], J. Urban[146b], P. Urquijo[91], P. Urrejola[86], G. Usai[8], J. Usui[69], L. Vacavant[88], V. Vacek[130], B. Vachon[90], K.O.H. Vadla[121], A. Vaidya[81], C. Valderanis[102], E. Valdes Santurio[148a,148b], M. Valente[52], S. Valentinetti[22a,22b], A. Valero[170], L. Valéry[13], A. Vallier[5], J.A. Valls Ferrer[170], W. Van Den Wollenberg[109], H. van der Graaf[109], P. van Gemmeren[6], J. Van Nieuwkoop[144], I. van Vulpen[109], M.C. van Woerden[109], M. Vanadia[135a,135b], W. Vandelli[32], A. Vaniachine[160], P. Vankov[109], G. Vardanyan[180], R. Vari[134a], E.W. Varnes[7], C. Varni[53a,53b], T. Varol[43], D. Varouchas[119], A. Vartapetian[8], K.E. Varvell[152], J.G. Vasquez[179], G.A. Vasquez[34b], F. Vazeille[37], D. Vazquez Furelos[13], T. Vazquez Schroeder[90], J. Veatch[57], V. Veeraraghavan[7], L.M. Veloce[161], F. Veloso[128a,128c], S. Veneziano[134a], A. Ventura[76a,76b], M. Venturi[172], N. Venturi[32], V. Vercesi[123a], M. Verducci[136a,136b], W. Verkerke[109], A.T. Vermeulen[109], J.C. Vermeulen[109], M.C. Vetterli[144,d], N. Viaux Maira[34b], O. Viazlo[84], I. Vichou[169,*], T. Vickey[141], O.E. Vickey Boeriu[141], G.H.A. Viehhauser[122], S. Viel[16], L. Vigani[122], M. Villa[22a,22b], M. Villaplana Perez[94a,94b], E. Vilucchi[50], M.G. Vincter[31], V.B. Vinogradov[68], A. Vishwakarma[45], C. Vittori[22a,22b], I. Vivarelli[151], S. Vlachos[10], M. Vogel[178], P. Vokac[130], G. Volpi[13], S.E. von Buddenbrock[147c], H. von der Schmitt[103], E. von Toerne[23], V. Vorobel[131], K. Vorobev[100], M. Vos[170], R. Voss[32], J.H. Vossebeld[77], N. Vranjes[14], M. Vranjes Milosavljevic[14], V. Vrba[130], M. Vreeswijk[109], R. Vuillermet[32], I. Vukotic[33], P. Wagner[23], W. Wagner[178], J. Wagner-Kuhr[102], H. Wahlberg[74], S. Wahrmund[47], K. Wakamiya[70], J. Walder[75], R. Walker[102], W. Walkowiak[143], V. Wallangen[148a,148b], A.M. Wang[59], C. Wang[36b,au], F. Wang[176], H. Wang[16], H. Wang[3], J. Wang[45], J. Wang[152], Q. Wang[115], R.-J. Wang[83], R. Wang[6], S.M. Wang[153], T. Wang[38], W. Wang[153,av], W. Wang[36a,aw], Z. Wang[36c], C. Wanotayaroj[45], A. Warburton[90], C.P. Ward[30], D.R. Wardrope[81], A. Washbrook[49], P.M. Watkins[19], A.T. Watson[19], M.F. Watson[19], G. Watts[140],

S. Watts[87], B.M. Waugh[81], A.F. Webb[11], S. Webb[86], M.S. Weber[18], S.M. Weber[60a], S.A. Weber[31], J.S. Webster[6], A.R. Weidberg[122], B. Weinert[64], J. Weingarten[57], M. Weirich[86], C. Weiser[51], P.S. Wells[32], T. Wenaus[27], T. Wengler[32], S. Wenig[32], N. Wermes[23], M.D. Werner[67], P. Werner[32], M. Wessels[60a], T.D. Weston[18], K. Whalen[118], N.L. Whallon[140], A.M. Wharton[75], A.S. White[92], A. White[8], M.J. White[1], R. White[34b], D. Whiteson[166], B.W. Whitmore[75], F.J. Wickens[133], W. Wiedenmann[176], M. Wielers[133], C. Wiglesworth[39], L.A.M. Wiik-Fuchs[51], A. Wildauer[103], F. Wilk[87], H.G. Wilkens[32], H.H. Williams[124], S. Williams[109], C. Willis[93], S. Willocq[89], J.A. Wilson[19], I. Wingerter-Seez[5], E. Winkels[151], F. Winklmeier[118], O.J. Winston[151], B.T. Winter[23], M. Wittgen[145], M. Wobisch[82,u], A. Wolf[86], T.M.H. Wolf[109], R. Wolff[88], M.W. Wolter[42], H. Wolters[128a,128c], V.W.S. Wong[171], N.L. Woods[139], S.D. Worm[19], B.K. Wosiek[42], J. Wotschack[32], K.W. Wozniak[42], M. Wu[33], S.L. Wu[176], X. Wu[52], Y. Wu[92], T.R. Wyatt[87], B.M. Wynne[49], S. Xella[39], Z. Xi[92], L. Xia[35c], D. Xu[35a], L. Xu[27], T. Xu[138], W. Xu[92], B. Yabsley[152], S. Yacoob[147a], K. Yajima[120], D. Yamaguchi[159], Y. Yamaguchi[159], A. Yamamoto[69], S. Yamamoto[157], T. Yamanaka[157], F. Yamane[70], M. Yamatani[157], T. Yamazaki[157], Y. Yamazaki[70], Z. Yan[24], H. Yang[36c], H. Yang[16], Y. Yang[153], Z. Yang[15], W-M. Yao[16], Y.C. Yap[45], Y. Yasu[69], E. Yatsenko[5], K.H. Yau Wong[23], J. Ye[43], S. Ye[27], I. Yeletskikh[68], E. Yigitbasi[24], E. Yildirim[86], K. Yorita[174], K. Yoshihara[124], C. Young[145], C.J.S. Young[32], J. Yu[8], J. Yu[67], S.P.Y. Yuen[23], I. Yusuff[30,ax], B. Zabinski[42], G. Zacharis[10], R. Zaidan[13], A.M. Zaitsev[132,ak], N. Zakharchuk[45], J. Zalieckas[15], A. Zaman[150], S. Zambito[59], D. Zanzi[32], C. Zeitnitz[178], G. Zemaityte[122], J.C. Zeng[169], Q. Zeng[145], O. Zenin[132], T. Ženiš[146a], D. Zerwas[119], D. Zhang[36b], D. Zhang[92], F. Zhang[176], G. Zhang[36a,aw], H. Zhang[119], J. Zhang[6], L. Zhang[51], L. Zhang[36a], M. Zhang[169], P. Zhang[35b], R. Zhang[23], R. Zhang[36a,au], X. Zhang[36b], Y. Zhang[35a,35d], Z. Zhang[119], X. Zhao[43], Y. Zhao[36b,x], Z. Zhao[36a], A. Zhemchugov[68], B. Zhou[92], C. Zhou[176], L. Zhou[43], M. Zhou[35a,35d], M. Zhou[150], N. Zhou[36c], Y. Zhou[7], C.G. Zhu[36b], H. Zhu[35a], J. Zhu[92], Y. Zhu[36a], X. Zhuang[35a], K. Zhukov[98], A. Zibell[177], D. Zieminska[64], N.I. Zimine[68], S. Zimmermann[51], Z. Zinonos[103], M. Zinser[86], M. Ziolkowski[143], L. Živković[14], G. Zobernig[176], A. Zoccoli[22a,22b], R. Zou[33], M. zur Nedden[17], L. Zwalinski[32].

[1] Department of Physics, University of Adelaide, Adelaide, Australia
[2] Physics Department, SUNY Albany, Albany NY, United States of America
[3] Department of Physics, University of Alberta, Edmonton AB, Canada
[4] [(a)] Department of Physics, Ankara University, Ankara; [(b)] Istanbul Aydin University, Istanbul; [(c)] Division of Physics, TOBB University of Economics and Technology, Ankara, Turkey
[5] LAPP, CNRS/IN2P3 and Université Savoie Mont Blanc, Annecy-le-Vieux, France
[6] High Energy Physics Division, Argonne National Laboratory, Argonne IL, United States of America
[7] Department of Physics, University of Arizona, Tucson AZ, United States of America
[8] Department of Physics, The University of Texas at Arlington, Arlington TX, United States of America
[9] Physics Department, National and Kapodistrian University of Athens, Athens, Greece
[10] Physics Department, National Technical University of Athens, Zografou, Greece
[11] Department of Physics, The University of Texas at Austin, Austin TX, United States of America
[12] Institute of Physics, Azerbaijan Academy of Sciences, Baku, Azerbaijan
[13] Institut de Física d'Altes Energies (IFAE), The Barcelona Institute of Science and Technology, Barcelona, Spain
[14] Institute of Physics, University of Belgrade, Belgrade, Serbia
[15] Department for Physics and Technology, University of Bergen, Bergen, Norway
[16] Physics Division, Lawrence Berkeley National Laboratory and University of California, Berkeley CA,

United States of America
[17] Department of Physics, Humboldt University, Berlin, Germany
[18] Albert Einstein Center for Fundamental Physics and Laboratory for High Energy Physics, University of Bern, Bern, Switzerland
[19] School of Physics and Astronomy, University of Birmingham, Birmingham, United Kingdom
[20] [(a)] Department of Physics, Bogazici University, Istanbul; [(b)] Department of Physics Engineering, Gaziantep University, Gaziantep; [(d)] Istanbul Bilgi University, Faculty of Engineering and Natural Sciences, Istanbul; [(e)] Bahcesehir University, Faculty of Engineering and Natural Sciences, Istanbul, Turkey
[21] Centro de Investigaciones, Universidad Antonio Narino, Bogota, Colombia
[22] [(a)] INFN Sezione di Bologna; [(b)] Dipartimento di Fisica e Astronomia, Università di Bologna, Bologna, Italy
[23] Physikalisches Institut, University of Bonn, Bonn, Germany
[24] Department of Physics, Boston University, Boston MA, United States of America
[25] Department of Physics, Brandeis University, Waltham MA, United States of America
[26] [(a)] Universidade Federal do Rio De Janeiro COPPE/EE/IF, Rio de Janeiro; [(b)] Electrical Circuits Department, Federal University of Juiz de Fora (UFJF), Juiz de Fora; [(c)] Federal University of Sao Joao del Rei (UFSJ), Sao Joao del Rei; [(d)] Instituto de Fisica, Universidade de Sao Paulo, Sao Paulo, Brazil
[27] Physics Department, Brookhaven National Laboratory, Upton NY, United States of America
[28] [(a)] Transilvania University of Brasov, Brasov; [(b)] Horia Hulubei National Institute of Physics and Nuclear Engineering, Bucharest; [(c)] Department of Physics, Alexandru Ioan Cuza University of Iasi, Iasi; [(d)] National Institute for Research and Development of Isotopic and Molecular Technologies, Physics Department, Cluj Napoca; [(e)] University Politehnica Bucharest, Bucharest; [(f)] West University in Timisoara, Timisoara, Romania
[29] Departamento de Física, Universidad de Buenos Aires, Buenos Aires, Argentina
[30] Cavendish Laboratory, University of Cambridge, Cambridge, United Kingdom
[31] Department of Physics, Carleton University, Ottawa ON, Canada
[32] CERN, Geneva, Switzerland
[33] Enrico Fermi Institute, University of Chicago, Chicago IL, United States of America
[34] [(a)] Departamento de Física, Pontificia Universidad Católica de Chile, Santiago; [(b)] Departamento de Física, Universidad Técnica Federico Santa María, Valparaíso, Chile
[35] [(a)] Institute of High Energy Physics, Chinese Academy of Sciences, Beijing; [(b)] Department of Physics, Nanjing University, Jiangsu; [(c)] Physics Department, Tsinghua University, Beijing 100084; [(d)] University of Chinese Academy of Science (UCAS), Beijing, China
[36] [(a)] Department of Modern Physics and State Key Laboratory of Particle Detection and Electronics, University of Science and Technology of China, Anhui; [(b)] School of Physics, Shandong University, Shandong; [(c)] Department of Physics and Astronomy, Key Laboratory for Particle Physics, Astrophysics and Cosmology, Ministry of Education; Shanghai Key Laboratory for Particle Physics and Cosmology, Shanghai Jiao Tong University, Tsung-Dao Lee Institute, China
[37] Université Clermont Auvergne, CNRS/IN2P3, LPC, Clermont-Ferrand, France
[38] Nevis Laboratory, Columbia University, Irvington NY, United States of America
[39] Niels Bohr Institute, University of Copenhagen, Kobenhavn, Denmark
[40] [(a)] INFN Gruppo Collegato di Cosenza, Laboratori Nazionali di Frascati; [(b)] Dipartimento di Fisica, Università della Calabria, Rende, Italy

[41] [(a)] AGH University of Science and Technology, Faculty of Physics and Applied Computer Science, Krakow; [(b)] Marian Smoluchowski Institute of Physics, Jagiellonian University, Krakow, Poland
[42] Institute of Nuclear Physics Polish Academy of Sciences, Krakow, Poland
[43] Physics Department, Southern Methodist University, Dallas TX, United States of America
[44] Physics Department, University of Texas at Dallas, Richardson TX, United States of America
[45] DESY, Hamburg and Zeuthen, Germany
[46] Lehrstuhl für Experimentelle Physik IV, Technische Universität Dortmund, Dortmund, Germany
[47] Institut für Kern- und Teilchenphysik, Technische Universität Dresden, Dresden, Germany
[48] Department of Physics, Duke University, Durham NC, United States of America
[49] SUPA - School of Physics and Astronomy, University of Edinburgh, Edinburgh, United Kingdom
[50] INFN e Laboratori Nazionali di Frascati, Frascati, Italy
[51] Fakultät für Mathematik und Physik, Albert-Ludwigs-Universität, Freiburg, Germany
[52] Departement de Physique Nucleaire et Corpusculaire, Université de Genève, Geneva, Switzerland
[53] [(a)] INFN Sezione di Genova; [(b)] Dipartimento di Fisica, Università di Genova, Genova, Italy
[54] [(a)] E. Andronikashvili Institute of Physics, Iv. Javakhishvili Tbilisi State University, Tbilisi; [(b)] High Energy Physics Institute, Tbilisi State University, Tbilisi, Georgia
[55] II Physikalisches Institut, Justus-Liebig-Universität Giessen, Giessen, Germany
[56] SUPA - School of Physics and Astronomy, University of Glasgow, Glasgow, United Kingdom
[57] II Physikalisches Institut, Georg-August-Universität, Göttingen, Germany
[58] Laboratoire de Physique Subatomique et de Cosmologie, Université Grenoble-Alpes, CNRS/IN2P3, Grenoble, France
[59] Laboratory for Particle Physics and Cosmology, Harvard University, Cambridge MA, United States of America
[60] [(a)] Kirchhoff-Institut für Physik, Ruprecht-Karls-Universität Heidelberg, Heidelberg; [(b)] Physikalisches Institut, Ruprecht-Karls-Universität Heidelberg, Heidelberg, Germany
[61] Faculty of Applied Information Science, Hiroshima Institute of Technology, Hiroshima, Japan
[62] [(a)] Department of Physics, The Chinese University of Hong Kong, Shatin, N.T., Hong Kong; [(b)] Department of Physics, The University of Hong Kong, Hong Kong; [(c)] Department of Physics and Institute for Advanced Study, The Hong Kong University of Science and Technology, Clear Water Bay, Kowloon, Hong Kong, China
[63] Department of Physics, National Tsing Hua University, Taiwan, Taiwan
[64] Department of Physics, Indiana University, Bloomington IN, United States of America
[65] Institut für Astro- und Teilchenphysik, Leopold-Franzens-Universität, Innsbruck, Austria
[66] University of Iowa, Iowa City IA, United States of America
[67] Department of Physics and Astronomy, Iowa State University, Ames IA, United States of America
[68] Joint Institute for Nuclear Research, JINR Dubna, Dubna, Russia
[69] KEK, High Energy Accelerator Research Organization, Tsukuba, Japan
[70] Graduate School of Science, Kobe University, Kobe, Japan
[71] Faculty of Science, Kyoto University, Kyoto, Japan
[72] Kyoto University of Education, Kyoto, Japan
[73] Research Center for Advanced Particle Physics and Department of Physics, Kyushu University, Fukuoka, Japan
[74] Instituto de Física La Plata, Universidad Nacional de La Plata and CONICET, La Plata, Argentina
[75] Physics Department, Lancaster University, Lancaster, United Kingdom

[76] [(a)] INFN Sezione di Lecce; [(b)] Dipartimento di Matematica e Fisica, Università del Salento, Lecce, Italy
[77] Oliver Lodge Laboratory, University of Liverpool, Liverpool, United Kingdom
[78] Department of Experimental Particle Physics, Jožef Stefan Institute and Department of Physics, University of Ljubljana, Ljubljana, Slovenia
[79] School of Physics and Astronomy, Queen Mary University of London, London, United Kingdom
[80] Department of Physics, Royal Holloway University of London, Surrey, United Kingdom
[81] Department of Physics and Astronomy, University College London, London, United Kingdom
[82] Louisiana Tech University, Ruston LA, United States of America
[83] Laboratoire de Physique Nucléaire et de Hautes Energies, UPMC and Université Paris-Diderot and CNRS/IN2P3, Paris, France
[84] Fysiska institutionen, Lunds universitet, Lund, Sweden
[85] Departamento de Fisica Teorica C-15, Universidad Autonoma de Madrid, Madrid, Spain
[86] Institut für Physik, Universität Mainz, Mainz, Germany
[87] School of Physics and Astronomy, University of Manchester, Manchester, United Kingdom
[88] CPPM, Aix-Marseille Université and CNRS/IN2P3, Marseille, France
[89] Department of Physics, University of Massachusetts, Amherst MA, United States of America
[90] Department of Physics, McGill University, Montreal QC, Canada
[91] School of Physics, University of Melbourne, Victoria, Australia
[92] Department of Physics, The University of Michigan, Ann Arbor MI, United States of America
[93] Department of Physics and Astronomy, Michigan State University, East Lansing MI, United States of America
[94] [(a)] INFN Sezione di Milano; [(b)] Dipartimento di Fisica, Università di Milano, Milano, Italy
[95] B.I. Stepanov Institute of Physics, National Academy of Sciences of Belarus, Minsk, Republic of Belarus
[96] Research Institute for Nuclear Problems of Byelorussian State University, Minsk, Republic of Belarus
[97] Group of Particle Physics, University of Montreal, Montreal QC, Canada
[98] P.N. Lebedev Physical Institute of the Russian Academy of Sciences, Moscow, Russia
[99] Institute for Theoretical and Experimental Physics (ITEP), Moscow, Russia
[100] National Research Nuclear University MEPhI, Moscow, Russia
[101] D.V. Skobeltsyn Institute of Nuclear Physics, M.V. Lomonosov Moscow State University, Moscow, Russia
[102] Fakultät für Physik, Ludwig-Maximilians-Universität München, München, Germany
[103] Max-Planck-Institut für Physik (Werner-Heisenberg-Institut), München, Germany
[104] Nagasaki Institute of Applied Science, Nagasaki, Japan
[105] Graduate School of Science and Kobayashi-Maskawa Institute, Nagoya University, Nagoya, Japan
[106] [(a)] INFN Sezione di Napoli; [(b)] Dipartimento di Fisica, Università di Napoli, Napoli, Italy
[107] Department of Physics and Astronomy, University of New Mexico, Albuquerque NM, United States of America
[108] Institute for Mathematics, Astrophysics and Particle Physics, Radboud University Nijmegen/Nikhef, Nijmegen, Netherlands
[109] Nikhef National Institute for Subatomic Physics and University of Amsterdam, Amsterdam, Netherlands
[110] Department of Physics, Northern Illinois University, DeKalb IL, United States of America

[111] Budker Institute of Nuclear Physics, SB RAS, Novosibirsk, Russia
[112] Department of Physics, New York University, New York NY, United States of America
[113] Ohio State University, Columbus OH, United States of America
[114] Faculty of Science, Okayama University, Okayama, Japan
[115] Homer L. Dodge Department of Physics and Astronomy, University of Oklahoma, Norman OK, United States of America
[116] Department of Physics, Oklahoma State University, Stillwater OK, United States of America
[117] Palacký University, RCPTM, Olomouc, Czech Republic
[118] Center for High Energy Physics, University of Oregon, Eugene OR, United States of America
[119] LAL, Univ. Paris-Sud, CNRS/IN2P3, Université Paris-Saclay, Orsay, France
[120] Graduate School of Science, Osaka University, Osaka, Japan
[121] Department of Physics, University of Oslo, Oslo, Norway
[122] Department of Physics, Oxford University, Oxford, United Kingdom
[123] [(a)] INFN Sezione di Pavia; [(b)] Dipartimento di Fisica, Università di Pavia, Pavia, Italy
[124] Department of Physics, University of Pennsylvania, Philadelphia PA, United States of America
[125] National Research Centre "Kurchatov Institute" B.P.Konstantinov Petersburg Nuclear Physics Institute, St. Petersburg, Russia
[126] [(a)] INFN Sezione di Pisa; [(b)] Dipartimento di Fisica E. Fermi, Università di Pisa, Pisa, Italy
[127] Department of Physics and Astronomy, University of Pittsburgh, Pittsburgh PA, United States of America
[128] [(a)] Laboratório de Instrumentação e Física Experimental de Partículas - LIP, Lisboa; [(b)] Faculdade de Ciências, Universidade de Lisboa, Lisboa; [(c)] Department of Physics, University of Coimbra, Coimbra; [(d)] Centro de Física Nuclear da Universidade de Lisboa, Lisboa; [(e)] Departamento de Fisica, Universidade do Minho, Braga; [(f)] Departamento de Fisica Teorica y del Cosmos, Universidad de Granada, Granada; [(g)] Dep Fisica and CEFITEC of Faculdade de Ciencias e Tecnologia, Universidade Nova de Lisboa, Caparica, Portugal
[129] Institute of Physics, Academy of Sciences of the Czech Republic, Praha, Czech Republic
[130] Czech Technical University in Prague, Praha, Czech Republic
[131] Charles University, Faculty of Mathematics and Physics, Prague, Czech Republic
[132] State Research Center Institute for High Energy Physics (Protvino), NRC KI, Russia
[133] Particle Physics Department, Rutherford Appleton Laboratory, Didcot, United Kingdom
[134] [(a)] INFN Sezione di Roma; [(b)] Dipartimento di Fisica, Sapienza Università di Roma, Roma, Italy
[135] [(a)] INFN Sezione di Roma Tor Vergata; [(b)] Dipartimento di Fisica, Università di Roma Tor Vergata, Roma, Italy
[136] [(a)] INFN Sezione di Roma Tre; [(b)] Dipartimento di Matematica e Fisica, Università Roma Tre, Roma, Italy
[137] [(a)] Faculté des Sciences Ain Chock, Réseau Universitaire de Physique des Hautes Energies - Université Hassan II, Casablanca; [(b)] Centre National de l'Energie des Sciences Techniques Nucleaires, Rabat; [(c)] Faculté des Sciences Semlalia, Université Cadi Ayyad, LPHEA-Marrakech; [(d)] Faculté des Sciences, Université Mohamed Premier and LPTPM, Oujda; [(e)] Faculté des sciences, Université Mohammed V, Rabat, Morocco
[138] DSM/IRFU (Institut de Recherches sur les Lois Fondamentales de l'Univers), CEA Saclay (Commissariat à l'Energie Atomique et aux Energies Alternatives), Gif-sur-Yvette, France
[139] Santa Cruz Institute for Particle Physics, University of California Santa Cruz, Santa Cruz CA, United

States of America
[140] Department of Physics, University of Washington, Seattle WA, United States of America
[141] Department of Physics and Astronomy, University of Sheffield, Sheffield, United Kingdom
[142] Department of Physics, Shinshu University, Nagano, Japan
[143] Department Physik, Universität Siegen, Siegen, Germany
[144] Department of Physics, Simon Fraser University, Burnaby BC, Canada
[145] SLAC National Accelerator Laboratory, Stanford CA, United States of America
[146] [(a)] Faculty of Mathematics, Physics & Informatics, Comenius University, Bratislava; [(b)] Department of Subnuclear Physics, Institute of Experimental Physics of the Slovak Academy of Sciences, Kosice, Slovak Republic
[147] [(a)] Department of Physics, University of Cape Town, Cape Town; [(b)] Department of Physics, University of Johannesburg, Johannesburg; [(c)] School of Physics, University of the Witwatersrand, Johannesburg, South Africa
[148] [(a)] Department of Physics, Stockholm University; [(b)] The Oskar Klein Centre, Stockholm, Sweden
[149] Physics Department, Royal Institute of Technology, Stockholm, Sweden
[150] Departments of Physics & Astronomy and Chemistry, Stony Brook University, Stony Brook NY, United States of America
[151] Department of Physics and Astronomy, University of Sussex, Brighton, United Kingdom
[152] School of Physics, University of Sydney, Sydney, Australia
[153] Institute of Physics, Academia Sinica, Taipei, Taiwan
[154] Department of Physics, Technion: Israel Institute of Technology, Haifa, Israel
[155] Raymond and Beverly Sackler School of Physics and Astronomy, Tel Aviv University, Tel Aviv, Israel
[156] Department of Physics, Aristotle University of Thessaloniki, Thessaloniki, Greece
[157] International Center for Elementary Particle Physics and Department of Physics, The University of Tokyo, Tokyo, Japan
[158] Graduate School of Science and Technology, Tokyo Metropolitan University, Tokyo, Japan
[159] Department of Physics, Tokyo Institute of Technology, Tokyo, Japan
[160] Tomsk State University, Tomsk, Russia
[161] Department of Physics, University of Toronto, Toronto ON, Canada
[162] [(a)] INFN-TIFPA; [(b)] University of Trento, Trento, Italy
[163] [(a)] TRIUMF, Vancouver BC; [(b)] Department of Physics and Astronomy, York University, Toronto ON, Canada
[164] Faculty of Pure and Applied Sciences, and Center for Integrated Research in Fundamental Science and Engineering, University of Tsukuba, Tsukuba, Japan
[165] Department of Physics and Astronomy, Tufts University, Medford MA, United States of America
[166] Department of Physics and Astronomy, University of California Irvine, Irvine CA, United States of America
[167] [(a)] INFN Gruppo Collegato di Udine, Sezione di Trieste, Udine; [(b)] ICTP, Trieste; [(c)] Dipartimento di Chimica, Fisica e Ambiente, Università di Udine, Udine, Italy
[168] Department of Physics and Astronomy, University of Uppsala, Uppsala, Sweden
[169] Department of Physics, University of Illinois, Urbana IL, United States of America
[170] Instituto de Fisica Corpuscular (IFIC), Centro Mixto Universidad de Valencia - CSIC, Spain
[171] Department of Physics, University of British Columbia, Vancouver BC, Canada
[172] Department of Physics and Astronomy, University of Victoria, Victoria BC, Canada

[173] Department of Physics, University of Warwick, Coventry, United Kingdom
[174] Waseda University, Tokyo, Japan
[175] Department of Particle Physics, The Weizmann Institute of Science, Rehovot, Israel
[176] Department of Physics, University of Wisconsin, Madison WI, United States of America
[177] Fakultät für Physik und Astronomie, Julius-Maximilians-Universität, Würzburg, Germany
[178] Fakultät für Mathematik und Naturwissenschaften, Fachgruppe Physik, Bergische Universität Wuppertal, Wuppertal, Germany
[179] Department of Physics, Yale University, New Haven CT, United States of America
[180] Yerevan Physics Institute, Yerevan, Armenia
[181] Centre de Calcul de l'Institut National de Physique Nucléaire et de Physique des Particules (IN2P3), Villeurbanne, France
[182] Academia Sinica Grid Computing, Institute of Physics, Academia Sinica, Taipei, Taiwan
[a] Also at Department of Physics, King's College London, London, United Kingdom
[b] Also at Institute of Physics, Azerbaijan Academy of Sciences, Baku, Azerbaijan
[c] Also at Novosibirsk State University, Novosibirsk, Russia
[d] Also at TRIUMF, Vancouver BC, Canada
[e] Also at Department of Physics & Astronomy, University of Louisville, Louisville, KY, United States of America
[f] Also at Physics Department, An-Najah National University, Nablus, Palestine
[g] Also at Department of Physics, California State University, Fresno CA, United States of America
[h] Also at Department of Physics, University of Fribourg, Fribourg, Switzerland
[i] Also at II Physikalisches Institut, Georg-August-Universität, Göttingen, Germany
[j] Also at Departament de Fisica de la Universitat Autonoma de Barcelona, Barcelona, Spain
[k] Also at Departamento de Fisica e Astronomia, Faculdade de Ciencias, Universidade do Porto, Portugal
[l] Also at Tomsk State University, Tomsk, and Moscow Institute of Physics and Technology State University, Dolgoprudny, Russia
[m] Also at The Collaborative Innovation Center of Quantum Matter (CICQM), Beijing, China
[n] Also at Universita di Napoli Parthenope, Napoli, Italy
[o] Also at Institute of Particle Physics (IPP), Canada
[p] Also at Horia Hulubei National Institute of Physics and Nuclear Engineering, Bucharest, Romania
[q] Also at Department of Physics, St. Petersburg State Polytechnical University, St. Petersburg, Russia
[r] Also at Borough of Manhattan Community College, City University of New York, New York City, United States of America
[s] Also at Department of Financial and Management Engineering, University of the Aegean, Chios, Greece
[t] Also at Centre for High Performance Computing, CSIR Campus, Rosebank, Cape Town, South Africa
[u] Also at Louisiana Tech University, Ruston LA, United States of America
[v] Also at Institucio Catalana de Recerca i Estudis Avancats, ICREA, Barcelona, Spain
[w] Also at Department of Physics, The University of Michigan, Ann Arbor MI, United States of America
[x] Also at LAL, Univ. Paris-Sud, CNRS/IN2P3, Université Paris-Saclay, Orsay, France
[y] Also at Graduate School of Science, Osaka University, Osaka, Japan
[z] Also at Fakultät für Mathematik und Physik, Albert-Ludwigs-Universität, Freiburg, Germany
[aa] Also at Institute for Mathematics, Astrophysics and Particle Physics, Radboud University Nijmegen/Nikhef, Nijmegen, Netherlands
[ab] Also at Department of Physics, The University of Texas at Austin, Austin TX, United States of America

[ac] Also at Institute of Theoretical Physics, Ilia State University, Tbilisi, Georgia
[ad] Also at CERN, Geneva, Switzerland
[ae] Also at Georgian Technical University (GTU),Tbilisi, Georgia
[af] Also at Ochadai Academic Production, Ochanomizu University, Tokyo, Japan
[ag] Also at Manhattan College, New York NY, United States of America
[ah] Also at The City College of New York, New York NY, United States of America
[ai] Also at Departamento de Fisica Teorica y del Cosmos, Universidad de Granada, Granada, Portugal
[aj] Also at Department of Physics, California State University, Sacramento CA, United States of America
[ak] Also at Moscow Institute of Physics and Technology State University, Dolgoprudny, Russia
[al] Also at Departement de Physique Nucleaire et Corpusculaire, Université de Genève, Geneva, Switzerland
[am] Also at Institut de Física d'Altes Energies (IFAE), The Barcelona Institute of Science and Technology, Barcelona, Spain
[an] Also at School of Physics, Sun Yat-sen University, Guangzhou, China
[ao] Also at Institute for Nuclear Research and Nuclear Energy (INRNE) of the Bulgarian Academy of Sciences, Sofia, Bulgaria
[ap] Also at Faculty of Physics, M.V.Lomonosov Moscow State University, Moscow, Russia
[aq] Also at National Research Nuclear University MEPhI, Moscow, Russia
[ar] Also at Department of Physics, Stanford University, Stanford CA, United States of America
[as] Also at Institute for Particle and Nuclear Physics, Wigner Research Centre for Physics, Budapest, Hungary
[at] Also at Giresun University, Faculty of Engineering, Turkey
[au] Also at CPPM, Aix-Marseille Université and CNRS/IN2P3, Marseille, France
[av] Also at Department of Physics, Nanjing University, Jiangsu, China
[aw] Also at Institute of Physics, Academia Sinica, Taipei, Taiwan
[ax] Also at University of Malaya, Department of Physics, Kuala Lumpur, Malaysia
[*] Deceased